Optimal integration of compressed air energy storage system for off-grid communities

Mahdieh Adib

A Thesis
in
The Department
of
Building, Civil, and Environmental Engineering

Presented in Partial Fulfillment of the Requirements
for the Degree of Master of Applied Science (Building Engineering) at
Concordia University
Montreal, Quebec, Canada

May 2023

CONCORDIA UNIVERSITY

School of Graduate Studies

This is to certify that the thesis prepared

By: **Mahdieh Adib**

Entitled: **Optimal integration of compressed air energy storage system for off-grid communities**

and submitted in partial fulfillment of the requirements for the degree of

Master of Applied Science (Building Engineering)

complies with the regulations of the University and meets the accepted standards with respect to originality and quality.

Signed by the final Examining Committee:

_____ Chair

Dr. Ursula Eicker

_____ Examiner

Dr. Ursula Eicker

_____ Examiner

Dr. Mohamed Ouf

_____ C o - Supervisor

Dr. Fariborz Haghighat

_____ C o - Supervisor

Dr. Fuzhan Nasiri

Approved by _____

Dr. Shahin Karimidorabati, Graduate Program Director

May 30, 2023 _____

Dr. Mourad Debbabi, Dean Faculty of Engineering and Computer Science

ABSTRACT

Optimal integration of compressed air energy storage system for off-grid communities

Mahdieh Adib

The integration of compressed air energy storage (CAES) and wind energy offers an attractive energy solution for remote areas with limited access to reliable and affordable energy sources. This thesis presents a design approach for an energy system comprising wind turbines, CAES, and diesel generators to satisfy the electricity demand in remote communities. This thesis proposes a bi-level programming (BLP) approach enabling the simultaneous optimization of the size and operation of the system while considering the interaction between them. Detailed mechanical design and configuration of the CAES system are considered, including the number and size of compressors and turbines, valves, recuperator operating conditions, etc. In contrast with conventional CAES systems, operating once a day for peak shaving, the proposed CAES system aims to mitigate wind fluctuations. Therefore, its operation is different from conventional CAES systems, and it would operate under partial load conditions most of the time, and as a result, the system's off-design modeling is also considered. The findings of this thesis indicate that the proposed system is a promising, cost-effective, reliable energy solution for remote areas, significantly decreasing the average daily total cost and CO_2 emissions by 69% and 76%, respectively. Additionally, by studying the system's performance under both design and off-design conditions, it is concluded that considering the off-design conditions is critical to ensure a more realistic performance of the system as the system is less likely to utilize the CAES in low charging and discharging opportunities.

Acknowledgments

I would like to express my sincere appreciation to my esteemed supervisors, Professor Haghighat, and Professor Nasiri, for their invaluable guidance, support, and unwavering commitment to my academic and professional development. Their expertise, wisdom, and constructive feedback have been instrumental in shaping my research's direction, scope, and quality.

I am deeply grateful to my parents and brother, whose unconditional love, encouragement, and unwavering support have been the cornerstone of my achievements. Their unwavering faith in my abilities and their continuous sacrifices have been the driving force behind my accomplishments.

Finally, I would like to extend my heartfelt thanks to my friends, whose unwavering support, understanding, and motivation have been invaluable during the arduous journey of my research. Finally, I would like to express my appreciation to all those who have contributed to this thesis in one way or another.

The research presented in this thesis received financial support from the India-Canada Centre for Innovative Multidisciplinary Partnerships to Accelerate Community Transformation and Sustainability (IC-IMPACTS). This organization is committed to fostering scientific partnerships between Canada and India, to promote sustainable and transformative solutions for communities.

Table of contents

List of figures

List of tables

List of abbreviations

Abbreviation	Stands for
A-CAES	Adiabatic compressed air energy storage
ANN	Artificial neural network
BLP	Bi-level programming
CAES	Compressed air energy storage system
CCHP	Combined cooling heating and power
CRF	Capital recovery factor
D-CAES	Diabatic CAES
EES	Energy storage system
FESS	Flywheel energy storage system
GHG	Greenhouse gas emission
HTES	High thermal energy storage
I-CAES	Iso thermal compressed air energy storage
ORC	Organic ranking cycle
NGCC	Natural gas combined cycle
PCM	Phase change material
PHS	Pumped hydro storage
PSO	Particle swarm optimization
SOC	State of charge
TES	Thermal energy storage

List of symbols

Symbol	Description
a	Fuel consumption characteristics
b	Fuel consumption characteristics
$c_{cur,WT}$	Cost coefficient of wind and curtailment [$/kWh]
$c_{cur,demand}$	Cost coefficient of demand curtailment [$/kWh]
c_{em}	Emission cost coefficient [$/kg]
c_f	Fuel cost coefficient [$/l]
$c_{inv,AC}$	Investment costs per unit of power of air compressor [$/kW]
$c_{inv,AT}$	Investment costs per unit of power of air turbine [$/kW]
$c_{inv,\tan k}$	Investment cost per unit of volume for the air reservoir [$/m^3]
$c_{inv,DG}$	Investment cost per unit of installed diesel generators [$/unit]
$c_{inv,WT}$	Investment cost per unit of installed wind turbines [$/unit]
$c_{op,AC}$	Operation cost coefficient of the air compressor [$/kWh]
$c_{op,AT}$	Operation cost coefficient of the air turbine [$/kWh]
$c_{p,air}$	Specific heat capacity of air [kJ/kg.K]
$c_{p,oil}$	Specific heat capacity of oil [kJ/kg.K]
$C_{cur,WT}$	Wind curtailment costs [$]
$C_{cur,demand}$	Demand curtailment costs [$]
C_{inv}	Total investment cost [$]
$C_{total,op}$	Total operation cost [$]
$C_{em,dg}$	Emission cost [$]
C_{op}	Operation cost of CAES and diesel generator [$]
$C_{op,CAES}$	Operation cost of CAES [$]
$C_{op,dg}$	Operation cost of diesel generator [$]
$\dot{E}x$	Exergy rate [MW]
$\dot{E}x_D$	Exergy destruction rate [MW]
h_x	Specific enthalpy at point x [kJ/kg]
H	Height [m]
K	Ratio of specific heats [-]
m	Mass [kg]
$\dot{m}_x$	Mass flow rate at point x [kg/s]
N_x	Number of components x
N_d	Number of days

N_y	Number of years
P_x	Electricity [kW]
p	Pressure at point x
q	Diesel generator fuel consumption [l]
$\dot{Q}$	Heat transfer [MW]
r_{AC}	Air compressor pressure ratio
r_{AT}	Air turbine pressure ratio
R_{up}	Ramp up limit [kW]
R_{down}	Ramp-down limit [kW]
s_x	Specific entropy at point x [kJ/kg.K]
t	Time [h]
T	Temperature [K]
u_x	Status indicator for component x
v	Velocity [m/s]
V_{CAES}	Volume of the CAES tank [m^3]
$\dot{W}$	Power consumption/generation [MW]
α	wind shear exponent power-law
β	Emission rate [g/l]
ρ	Density [kg/m^3]
η	efficiency [%]
0	Dead condition
AC	Air compressor
AT	Air turbine
ci	Cut in speed
co	Cut out speed
ch	Charging
D	Destruction
dch	Discharging
Dg	Diesel generator
in	Inlet
i	Charging states
j	Discharging states
out	Outlet
Q	Heat
r	Rated speed
$\mathrm{Re}c$	Recuperator
$\mathrm{Re}g$	Pressure-regulating valve
S	Isentropic
tot	Total
W	Power
WT	Wind turbine

Chapter 1 : Introduction

1.1 Background

While renewable energy is poised to make significant contributions to the global electricity production in grid-connected areas, remote communities still rely on diesel-fired systems for their power supply, posing economic, environmental, and social challenges. Many of these remote areas have abundant renewable resources, such as wind energy, but the intermittent nature of wind power makes it unreliable. The reliability of the energy system is crucial for these communities as they are not connected to the national grid [1]. Integrating energy storage systems (ESS) with renewable sources is a crucial step towards increasing the penetration of renewables in these communities and ensuring a reliable energy system [2]. Compressed air energy storage (CAES), among various energy storage systems, has emerged as a highly promising solution in recent years due to its numerous advantages and versatile range of applications [3]. The literature highlights that the integration of CAES with wind energy is a crucial implementation scenario, particularly in remote areas to meet the energy demand, thereby minimizing the cost of grid connection and decreasing dependence on diesel fuels [4]. This application of CAES stands in contrast to the typical implementation of the two working CAES systems, which operate once a day to achieve peak shaving. In the case of integration with wind energy for remote communities, CAES must operate more frequently and mainly in partial load conditions, which can impact the system's performance since CAES is a mechanical system [5]. Thus, the design and operation of CAES is markedly different from that of other energy storage systems, such as batteries, which can be easily manufactured and arranged to accommodate various capacities [6]. Hence, there is an imperative for additional research on the design and scheduling for integrating CAES with wind energy systems, particularly for remote communities with more profound comprehension of the mechanical aspects of CAES.

1.2 Problem statement

The current state of research on the design and scheduling of CAES systems is limited by oversimplified assumptions of their mechanical operation. Studies primarily focus on determining the capacities of the main components such as compressors, turbines, and air reservoir, while disregarding the nuances of mechanical operation. They treat CAES as a simple electricity-in, electricity-out system, overlooking the detailed mechanical design aspects of the

system. While the overall capacity and efficiency of CAES are important considerations, a comprehensive understanding of the mechanical components and their performance characteristics is critical to ensure the safe and reliable operation of the system. For example, the design of the compressor and expander, which are essential components of a CAES system, needs to consider factors such as the compression ratio, temperature rise, and the type of working fluid used for heat recovery, to achieve optimal efficiency and performance. Similarly, the design of the air storage vessel, valves, and recuperator needs to be considered for a safe and reliable operation of the system over its expected lifespan. The other case in point is the effect of partial load conditions when the application of CAES is smoothing out the wind output power.

In conclusion, the simplistic approach of previous studies fails to account for critical factors such as off-design conditions, temperature and pressure fluctuations, and the impact of important components like recuperators in the design and scheduling of the system. Consequently, there is a pressing need for further research to explore a more comprehensive approach to the design and operation of CAES systems that considers the complex mechanical processes involved.

1.3 Research objectives

This thesis proposes a comprehensive design and scheduling approach for integrating CAES with wind energy to meet the power needs of a remote community with a deeper understanding of mechanical aspect of CAES. The proposed approach includes bi-level programming for both design and scheduling of the system, considering both the technical and economic considerations. Achieving this objective could be done through:

(1) Detailed time dependent Mechanical modeling of CAES Operation:

The thesis proposes a detailed mechanical modeling of the CAES system, including all the required components such as valves, recuperators, and heat recovery system. The simulation results provide a detailed configuration of CAES that can meet the specific needs of the community.

(2) Modeling Off-Design Conditions of CAES:

The proposed design approach considers the off-design conditions of the system and studies the effect of partial load operation on both the design and scheduling of the system. This enables the system to operate efficiently and effectively under different operating conditions, providing reliable and cost-effective power supply to the community.

(3) Exergy Destruction Analysis of CAES:

The thesis conducts an exergy destruction analysis of the main components of the CAES system, enabling the identification of areas where improvements can be made to enhance the efficiency and performance of the system.

(4) Studying Economic and Environmental gains of the proposed system:

The proposed design approach investigates the economic and environmental gains of integrating CAES with wind energy in comparison to the current power system used in the community. This includes a detailed assessment of the capital and operating costs of the proposed system, as well as the environmental benefits such as reduced greenhouse gas emissions.

Overall, the proposed design approach provides a comprehensive and integrated framework for designing and scheduling a CAES system integrated with wind energy, enabling the provision of reliable and sustainable power supply to a remote community.

1.4 Organization of the thesis

This thesis is structured into six chapters, each focusing on a distinct aspect of the topic. The following is a brief overview of the remainder of the thesis:

- Chapter 2- Literature review: In this chapter, the theoretical foundations of the research are presented. It includes a detailed review of the relevant literature and theoretical frameworks.
- Chapter 3 - Methodology: This chapter describes the research design and methodology adopted for modeling different components and the optimization algorithm.
- Chapter 4 - Case study: This chapter presents the case study, energy source and demand data, and the design and economic parameters of each component.
- Chapter 5 - Results: This chapter presents the simulation results, which includes a detailed analysis of discussion of the findings, and interpretation of the results in light of the research objectives.
- Chapter 6 - Conclusions: In this chapter, the results and findings of the thesis are discussed in relation to the research questions and objectives. The chapter also provides a critical reflection on the limitations of the thesis and proposes areas for future research.

Chapter 2 : Literature review

Renewable energy technologies, and in particular wind energy, share in electricity generation is ever increasing [7]. As shown in Figure 2-1, the 2022 global wind energy council report indicates that the global wind power capacity has increased significantly in recent years from 24 GW in 2001 to 837 GW in 2021, saving more than 1.2 billion tons of CO2 emissions per year [8]. Although renewable energy generation increased in grid-connected areas, isolated communities' electricity production is relied on diesel generators [9]. Electricity providers come up against difficult issues with remote region power supply [10]. Lowering the reliance on diesel fuels in these communities is essential because of the environmental, economic, and social demerits of diesel-fired systems. Most of these off-grid communities are in locations with abundant wind energy that could supply their electricity demand [11].

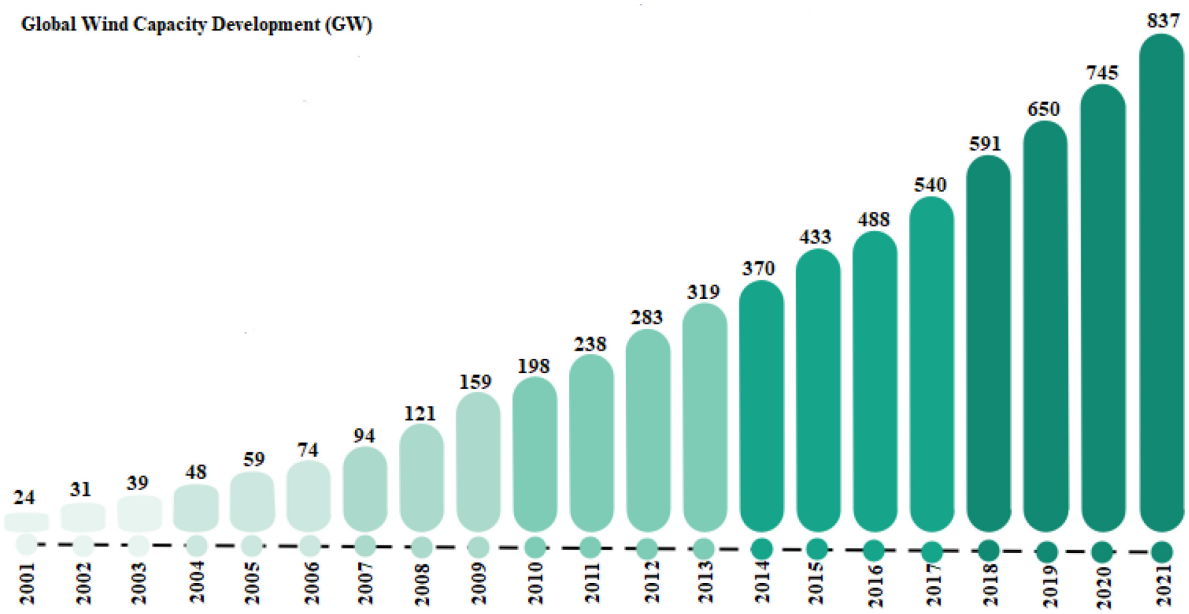

Figure 2-1: Global wind capacity development from 2001 to 2021.

2.1 Remote communities

Off-grid communities and remote communities are communities that are not presently connected to the North American electrical grid nor the piped natural gas network and are long-term (at least 5 years) or permanent settlements with more than 10 residences [12]. These off-grid/remote communities in Canada, over 280 communities (approximately 200 000 people), mainly rely on expensive diesel fried generation for electricity generation [13].

When diesel-fueled generators are properly maintained they are a stable and reliable

method of electricity production in remote communities. However, they are an extremely costly technology with unstable rates for that area, and their greenhouse gas emission results in air pollution, as well as soil pollution through diesel fuel spills and leakage [14]. Table 2-1 presents the main concerns brought up by diesel generation in remote communities in terms of environmental, social, and economic sustainability[12]. Regarding environmental issues, there would be a considerable amount of greenhouse emissions when burning diesel fuel also by the vehicles when transporting the fuel. On the other hand, there is a high risk of fuel spillage after long-distance transportation, also fuel leakage from tanks polluting soil and groundwater while stored. In terms of social concerns, in quiet places like these remote areas, diesel generators are noisy and disturbing. The emissions mentioned earlier could result in health problems for the community. As for the economic concerns, the cold climate contributes to the high demand for diesel, resulting in high energy expenditure. Also, transporting diesel to such areas is very costly. The other case in point is that the high cost of energy in these remote communities may result in the prevention of new businesses, restricting future economic opportunities.

Table 2-1: Diesel generation concerns in remote/off-grid communities [12].

Environmental Concerns	Social Concerns	Economic Concerns
Greenhouse gas emissions	The noise of the generators	High transportation cost
Fuel spillage during transportation	Blackouts of the generators	High energy expenditures due to high demand
Fuel tank leak during storage	Health problems from the emissions	Prevent new business because of high energy cost

Based on these demerits of using diesel-fired systems, to reduce the reliance on diesel fuel and diminish carbon emissions various remote communities are seeking opportunities like using renewable energy resources, hydro, or LNG, expanding electrical grids, and connecting to the North American grid to improve electricity reliability [15].

The other case in point is that Canada participated in the Paris Agreement and plans to lower the greenhouse gas (GHG) emissions (to reduce the global warming). By participating in this agreement countries are obliged to lower the GHG emissions by 30% below 2005 levels by 2030 and to control the average global temperature rise below 2 ℃ [16]. Correspondingly, the government of Canada developed the Pan-Canadian Framework on Clean Growth and Climate change (PCF) in 2017. The Government of Canada's Pan-Canadian Framework on Clean Growth and Climate change priorities powering remote communities. The framework aims to reduce greenhouse gas (GHG) emissions by assisting rural and remote areas in transitioning

away from diesel-fired power toward cleaner energy sources [17].

In this respect, one of the programs in federal funding programs, aiming to decrease the dependence on diesel fuel in Canada's rural and remote communities with encouraging sustainable energy solutions, is the Clean Energy for Rural and Remote Communities program. Another funding program related to remote areas is the Energy Innovation Program that aims to accelerate clean energy technology research and development (R&D) related to exploring reducing diesel consumption in northern and remote areas, and applying renewable and smart grid storage systems, etc. [16]. Accordingly, the details of two funding programs related to developing clean energy plants in off-grid/remote communities are listed in Table 2-2.

Table 2-2: Funding programs related to reducing the reliance on diesel fuel in remote communities of Canada [16]

Fund	Dept	Year	Amount (millions)	Fund Status
Clean Energy for Rural and Remote Communities	NRCAN	2018-2024	$220	Variable
Energy Innovation	NRCAN	Ongoing	$52.9/year	Continuous Intake

Most of the off-grid/remote communities of Canada can take advantage of the renewable energy sources and whether it is properly managed, could help contribute to the communities' sustainable development. Employing renewable energy sources for power generation would result in various merits like energy security, reduction of environmental impacts, health benefits, acting as a price hedge against higher diesel prices. The four renewable energy alternatives for diesel generators in off-grid communities are small hydro, biomass, wind, and solar energy [12].

As illustrated in The Atlas of Canada - Remote Communities Energy Database[11] most of these communities' locations have good wind resources. Taking advantage of these wind resources would result in local power generation in these communities, with no fuel transportation to these areas. In this respect, Hooshangi [18] carried out a feasibility study of a wind-diesel system for remote communities in northern Quebec and stated that storage systems are necessary alongside wind energy plants as a system with storage is more cost-effective, reliable, and reduces the amount of energy spillage significantly.

2.2 Energy storage systems

Renewable energy systems have the potential to significantly reduce carbon emissions in the environment as they do not produce any greenhouse gases or other pollutants. However, these systems rely on natural resources like sunlight, wind, water, and geothermal energy, which

are often unpredictable and dependent on weather conditions, seasons, and years. To address this issue, energy storage systems (ESS) can be employed so that renewable energy can be used consistently and in a controlled manner as required [19]. There are various types of ESSs based on the application needed, different types of energy storage system are shown in Figure 2-2.

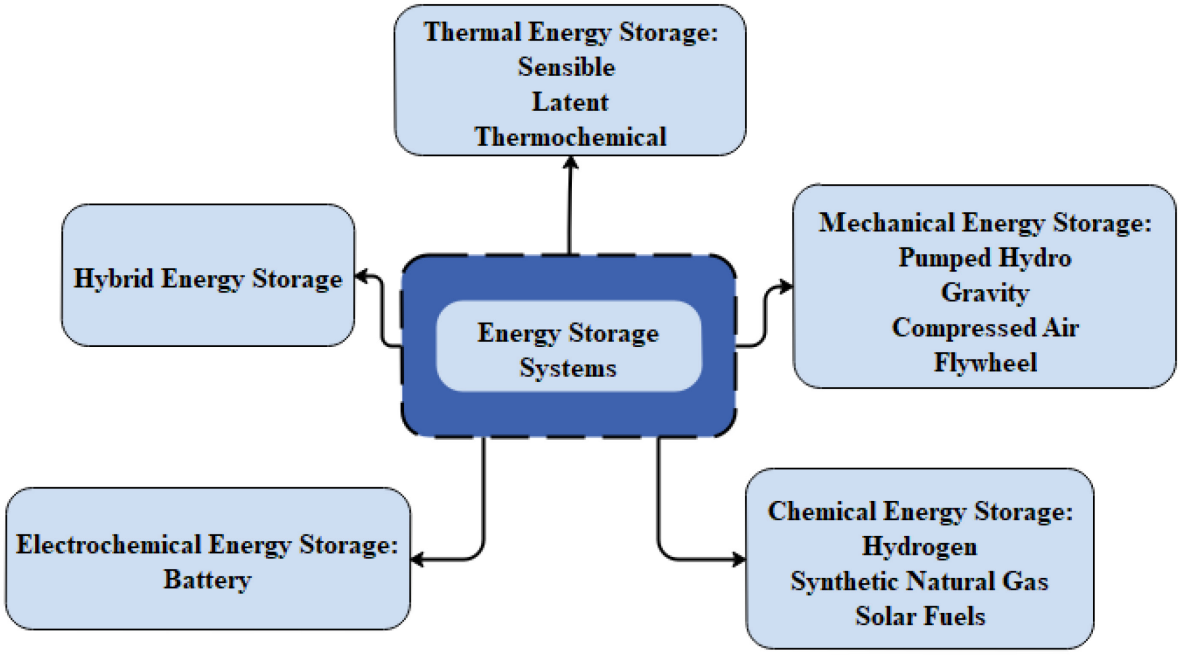

Figure 2-2: Different kind of energy storage system.

Electrochemical storage technologies such as batteries have matured as reliable options for small-scale energy storage, offering benefits such as high energy density. Nevertheless, these batteries are still subject to some significant drawbacks, including relatively short lifespans, high degradation costs, and limited operational durability [3]. Among various types of ESSs available today, like batteries, flywheels, pumped hydro, fuel cells, etc., there are only two plant-level ESSs options suitable for long-duration and large-scale storage; pumped hydro storage (PHS) and compressed air energy storage (CAES) [20]. PHS requires water as storage media which could be scarce in some jurisdictions while CAES uses air as storage media with no access restrictions as the compressed air could be stored in aboveground storages as well [21]. Lately, CAES technology is gaining momentum due to its large storage capacity, long service life, and relatively low cost and high economy of scale in comparison to other ESSs [22]. These benefits are mainly contributed to CAES being a mechanical system, which does not degrade like batteries ensuring a service life of 30 to 40 years [23].

2.3 Compressed air energy storage (CAES) system

In this section backgrounds about CAES are discussed including operational characteristics of CAES, classifications of CAES, and the basics of a wind-driven CAES system.

2.3.1 CAES operation

A CAES system operates like a conventional gas turbine, except that the compression and expansion processes occur independently and at different times [24]. A CAES system is typically comprised of a motor/generator, storage reservoir, compressor, expander, and auxiliary air heater. A simple illustration of a CAES system with an underground storage reservoir is shown in Figure 2-3 together with its main components. The CAES operation starts by compressing air using electricity from renewable sources or off-peak electricity storing the air with high pressure in a vessel, tank, or underground carven (charging process) [25]. Later, during the discharging process (in peak hours or whenever electricity is required), the compressed air is released to operate a turbine, generating electricity. One of the key merits of CAES is that it can be implemented on a variety of scales. If the rating power of the CAES system is under 10 MW, it is considered small-scale. The system is considered a large-scale one if its rating power is over 50 MW [3]. Large-scale CAES systems [26] are appropriate for grid applications for the purpose of load shifting, whereas small-scale CAES systems [27] are mainly suitable to ensure an uninterrupted power supply, by integrating renewable energies, for applications in buildings or small communities [28]. Using an artificial tank for large-scale CAES storage proved not to be economically viable [29]. For a small-scale CAES system, on the other hand, compressed air could be feasibly stored in an over-ground storage [30]. Underground energy storage chambers could be in place of a salt carven, a depleted aquifer, a lined rock carven, or depleted gas reservoirs [31]. It is worth mentioning that the two commercial CAES plants use a salt carven as an air reservoir with a promising performance in meeting CAES cycling requirements, showing resilience to high injection and removal rates [32]. Overall, the compression process generates heat, while the expansion process makes the air cool unless heat is added. This could be achieved by heating the air in combustors using natural gas. The heated air then runs through one or more expanders to generate electricity by powering a motor/generator.

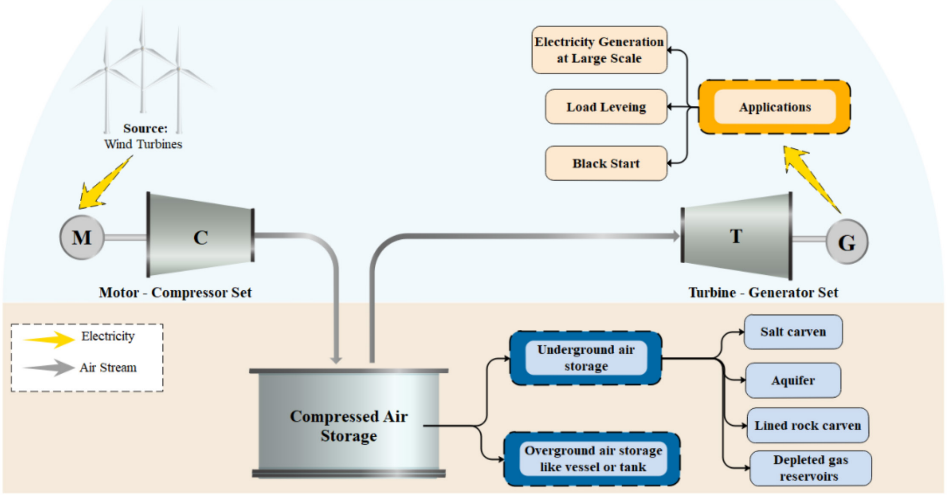

Figure 2-3: A schematic diagram of a CAES system.

2.3.2 CAES classifications

The classification of CAES systems is based on how they handle the waste heat during the charging process and how they provide heat during discharging process at the inlet of the turbine [33]. On that basis, Figure 2-4 illustrates a classification of CAES. If the waste heat is not recovered during the compression period and compressed air is heated with (external sources such as) fossil fuels, the system is called a diabatic compressed air energy storage system (D-CAES) [34]. This type of CAES system still uses fossil fuels, and thus, is not environmentally friendly [35]. Although several studies have been carried out to optimize D-CAES operation, its reliance on fossil fuels and the resulting CO_2 emissions are still the main demerits [36]. In case the heat generated during the charging process is stored and utilized to preheat the air before discharging, the system is considered an adiabatic compressed air energy storage (A-CAES) [37]. The third category is called isothermal compressed air energy storage (I-CAES) designed to minimize or prevent heat generation during the compression process [38], by ensuring a constant or near-constant temperature in both charging and discharging processes using a liquid piston or spray systems [39,40]. The majority of such CAES projects are in the research and development phase and those projects under construction for full-scale applications are either D-CAES or A-CAES [41]. Considering the disadvantage of D-CAES systems in having low efficiency and carbon emissions, and the I-CAES being still not practical for implementation, A-CAES has received growing attention in the past decade due to their higher efficiency and being emission-free [42].

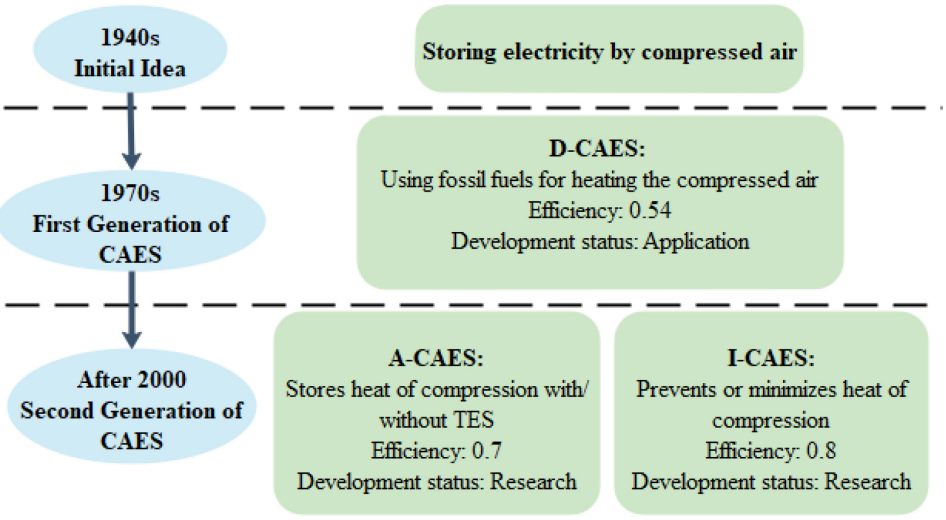

Figure 2-4: CAES system classification with its development timeline [38].

2.3.3 Wind-driven CAES systems

CAES as an energy storage system is well suited for a variety of services including peak shifting/shaving as well as facilitating integration with renewable energy systems [43]. CAES system is appropriate for ancillary services due to having a high ramp rate, the ability to operate consistently under partial load conditions, and very low or near zero greenhouse gas (GHG) emissions [44]. Hence, there is a growing interest in the integration of CAES and wind farms to create a fully dispatchable energy source minimizing the effects of wind energy intermittency [45]. In this regard, Mason et al. [46] compared the integration of wind farms with natural gas combined cycle (NGCC) and CAES, as a backup for tackling the intermittent nature of wind energy.

In the 1970s, two CAES systems started operations, the 290 MW Huntorf plant [47] and the 110 MW McIntosh plant [48], which were designed to store low-cost, off-peak electricity and generate electricity in peak hours. Later, changes in the market conditions lowered the interest in CAES systems. Now, with the uncertainties in natural gas markets due to geopolitical issues and considering a growing consensus towards CO_2 taxation to lower CO_2 emissions by 2050, Wind-CAES plants present themselves as a technological solution. It is worth mentioning that integration of CAES with renewables is more challenging compared to batteries as CAES is a multi-physical system (as a series of mechanical systems) subject to a lower efficiency due to losses at each stage. [49]. In addition, the rapid development of wind

turbine technologies has further improved the feasibility of CAES systems [5].

In summary, in the case of wind energy integration, to respond to wind intermittency, a CAES could adjust its input and output more frequently to shift between compression and expansion faster than its conventional peak-shaving applications aimed at storing energy at night and generating it at the peak hours. The sole existing CAES plant intended for balancing wind energy was located in Iowa which was terminated due to some geological issues in the plant site [50] caused mainly by the characteristics of aquifers in Iowa [37]. Accordingly, a deeper understanding of the effects of site conditions on the design and operation of the CAES system integrated with wind energy is required. There are also restrictions with respect to energy demand expectations that affect the sizing of CAES plants as oversizing of the plants could lead to having them stay idle for extended periods of time. For example, the Huntorf CAES plant was used daily for the first two years, but after 1995, it operates only between 50 to 60 times a year [51]. Considering Ontario grid data (both demand and supply data), Rouindej et al. [6] reported that a CAES system with one-tenth of the size typically proposed in the literature is enough for satisfying Ontario's elevated electricity demand in peak hours.

2.4 CAES literature classification

In this thesis, a comprehensive review of the literature is carried out to present state-of-the-art wind-driven CAES systems. Two keywords of "CAES" and "wind energy" are used for initial screening of the publications. Afterward, to highlight various aspects of wind-driven CAES systems, a third keyword was added, which was selected from a list of keywords that includes geological analysis, economic analysis, thermodynamic analysis, data-driven approach, design, operation, dynamic modeling, and off-design. Figure 2-5 illustrates a distribution of the identified literature, based on the year of publication. It can be seen from this figure, that out of nearly 120 papers identified, a relatively high number of studies were published in recent years considering the recent issues and priorities discussed above (with more than 60% of the publications being from 2018 and after).

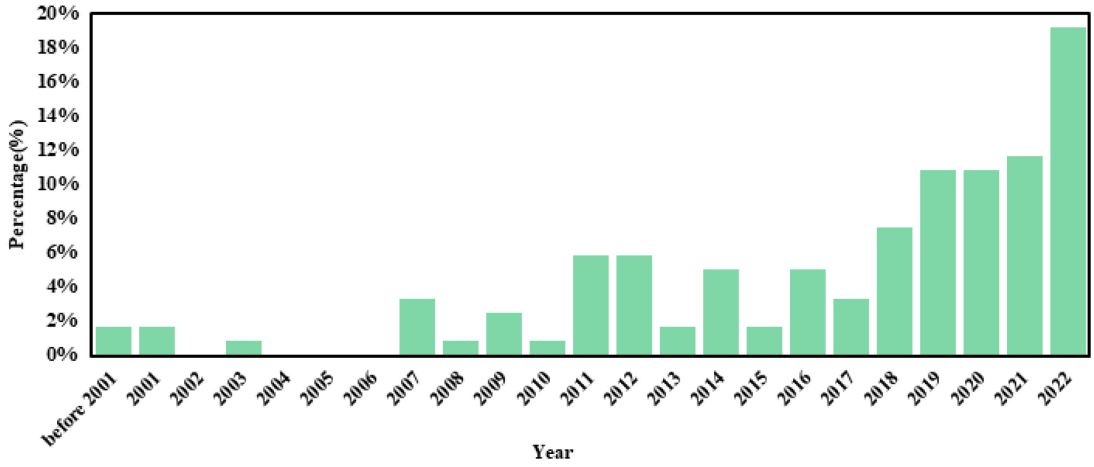

Figure 2-5: Distribution of identified CAES-related papers.

The identified articles are categorized into three categories namely i) feasibility analysis, ii) thermodynamic analysis, iii) system optimization. On that basis, the literature review is classified as presented in Figure 2-6 and is discussed in the following sections.

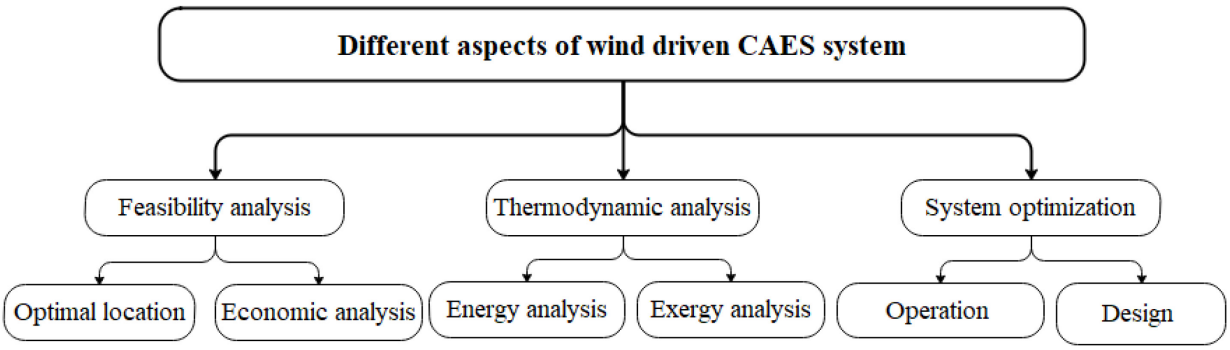

Figure 2-6: The classification of literature on wind-driven CAES.

2.4.1 CAES feasibility analysis

Some CAES projects were rescinded due to their economical and geological limitations. In this section, the focus will be on reviewing the articles addressing or analyzing the feasibility of the Wind/CAES plants from various aspects such as location and economic efficiency. As mentioned earlier, following the charging process, compressed air is stored under high-pressure [52]. Thus, finding a location with high wind potential and suitable geologies for CAES storage components is critical for wind-CAES integration. Using an artificial tank for large-scale CAES storage proved not to be economically viable [29]. For a small-scale CAES system, on the other hand, compressed air could be feasibly stored in an

over-ground storage [30]. Underground energy storage chambers could be in place of a salt carven, a depleted aquifer, a lined rock carven, or depleted gas reservoirs [31]. It is worth mentioning that the two commercial CAES plants use a salt carven as an air reservoir with a promising performance in meeting CAES cycling requirements, showing resilience to high injection and removal rates [32]. Table 2-3 provides a summary of the literature focusing on location analysis for wind energy integrated CAES plants. The literature points to the fact that identifying a suitable location with wind sources and underground air reservoirs is challenging. In this regard, Satkin et al. [53] developed a model to identify optimal locations for Wind-integrated CAES plants in Iran based on wind atlas data, salt dome location data (for storing compressed air), proximity to the electrical grid, proximity to gas transmission pipelines. He et al. [54] carried out a geological evaluation of alternative locations in the UK for large-scale CAES integrated with wind and solar energy maximizing carbon emissions reductions. King et al. [31] performed an investigation of the areas with renewable energy potentials that have locations suitable for CAES plants providing a comparison between cases in India and the UK. Tong et al. [55] conducted a feasibility study of available geologies for CAES in China investigating their potential to integrate wind energy considering government policies, energy demand, and electricity generation along with a cost and environmental effects analysis. Mason et al. [46] studied the locations with high wind potentials in the USA (with an above class four wind regime) that has available depleted aquifers, and domal and bedded salt cavern and their feasibility for generation of electricity from wind and storing it using CAES. Aghahosseini et al.[56] studied locations with suitable geological formations for CAES worldwide to identify locations with high potential. As Table 2 shows the literature is still limited regarding location analysis for wind-integrated CAES, especially in the case of underground caverns other than salt caverns.

Table 2-3: Literature in location analysis for wind integrated CAES.

Reference	Year	Location	Focus	Results
Succar et al. [5]	2008	US	Class 4 or higher wind sources. Aquifers, domal, and bedded salt caverns as an underground air reservoir.	Great potential from New Mexico to Arkansas.
Satkin et al. [53]	2014	Iran	Wind potential greater than 50 W/m^2. Salt domes for an air reservoir.	30 suitable locations were found.
Aghahosseini et al. [53]	2018	Worldwide	Salt deposits and aquifers for an air reservoir.	North and South America and Sub-Saharan Africa are the most promising locations.

He et al.[54]	2021	UK	Current wind generation locations. Mainly underground salt caverns for an air reservoir.	Up to 725 GWh ready-to-use capacity.
King et al.[31]	2021	India and UK	Wind distribution analysis Porous rock geologies, salt deposits, aquifers, and reservoirs.	Lack of salt deposits in India, only 1.05% of land areas are suitable for an air reservoir.
Tong et al.[55]	2021	China	Installed wind capacity Salt caverns and empty coal reserves for air storage.	Spatial mismatch between underground reservoirs and wind generation locations

Denholm et al. [57] conducted an economic feasibility analysis considering transmission costs in the case of co-locating wind farms and CAES. Mauch et al. [58] investigated the economic feasibility of wind-integrated CAES, considering its contributions to the day-ahead electricity markets. Fertig et al. [59] studied the economic benefits of implementing a Wind/CAES system in a wind farm in central Texas subject to scenarios on gas and electricity prices. Madlener et al. [60] investigated the economic feasibility of integrating CAES into a wind park in Germany. The authors compared three scenarios namely i) the wind park without CAES, ii) the wind park integrated with a centralized CAES, and iii) the wind park with a decentralized CAES. For the second and third scenarios, the authors compared the use of diabatic and adiabatic CAES. Their results indicated that a centralized diabatic CAES is the most cost-efficient option. Cleary et al. [61] studied the revenue loss due to wind curtailment in ALL-Island Ireland with and without CAES scenarios. Swider [62] employed a stochastic model to represent the electricity market in Germany and analyzed the impact of the increase in the amount of wind power generation on improving the feasibility of CAES. The literature highlights the fact that integration of CAES with renewable sources is more economically feasible when the electricity market is carbon-constrained or is subject to carbon taxes/incentives [63]. Considering the push from the governments towards the reduction of GHG emissions and increasing share of renewable energy sources in electricity generation, the literature needs to evolve further towards analyzing the impact of carbon policies on CAES adoption.

2.4.2 CAES thermodynamic analysis

CAES is a multi-physical mechanical system. In this sense, the literature presents several studies on thermodynamic analysis of CAES systems [64]. CAES could be designed such

that to operate either in constant volume (isochoric) [65] or constant pressure (isobaric) conditions [66]. The most common operating condition reported in the literature is the case of CEAS operating with a constant volume and either a varying pressure at the inlet of the turbine or a constant pressure by using a throttling valve. In this sense, as shown in Figure. 2-7, a CAES system can operate in three different modes. Succar et al. [5] compared these operational modes using thermodynamic analysis in the case of integration with wind energy.

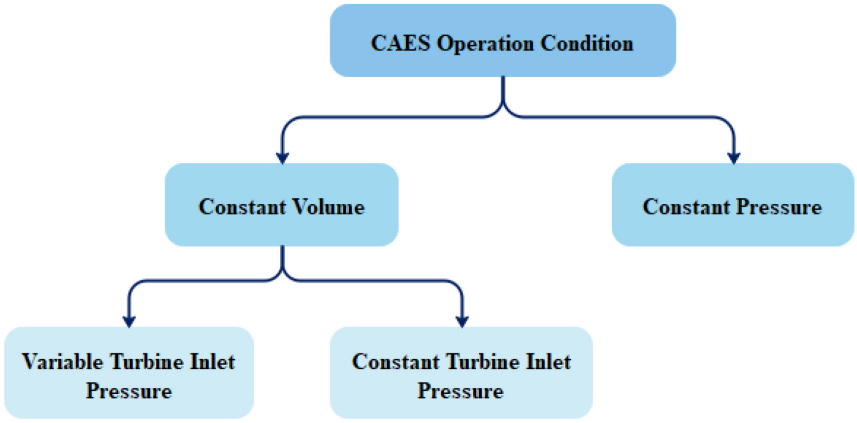

Figure. 2-7. CAES operating conditions based on volume-pressure scenarios.

In thermodynamic modeling of compressor and turbine, every component is usually defined with a control volume, with assumptions on either isentropic [67] or polytropic [68] efficiencies, with the former as the approach most reported in the literature. In doing so, thermodynamic studies are focusing on energy and exergy analysis of CAES systems based on the first and the second law of thermodynamics, respectively [69]. The aim of such studies is to increase the efficiency of the system and decrease exergy destruction [70]. Venkataramani & Velraj [71] performed energy and exergy analysis of the I-CAES system thereby considering the storage vessel being placed underwater to maintain a constant temperature.

In case of thermodynamic analysis of CAES system integrated with wind energy, Razmi et al. [72] investigated the integration of CAES system for two nearby wind farms in Iran, Kahak and Abhar, with a collective capacity of 162.5 MW, by carrying out a thermodynamic analysis with a parametric assessment of thermodynamic properties of CAES systems. Gorbani et al. [73] suggested a CAES system with thermal energy storage (TES) filled with phase change materials (PCM) to tackle wind fluctuation. Mohammadi et al. [74] studied the

integration of a Wind/CAES system with combined cooling, heating system, and power (CCHP). They carried out a thermodynamic analysis including energy and exergy analysis with sensitivity analysis of several thermodynamic properties (such as maximum-minimum pressure of the tank and inlet temperature of the turbine). With a fixed minimum pressure of air carven, increasing the maximum pressure of air carven would result in an increment in power consumption, outlet temperature, and exergy destruction of the compressors. Chen et al. [75] carried out a study on wind and solar potentials in China and proposed a CAES system integrated with wind, as an electricity source for compressors, and with solar, as a heat source for turbines with a thermal heat recovery system. They investigated the effect of change in several thermodynamic parameters such as ambient temperature, heat exchanger effectiveness, mass flow rate, total pressure ratio, and the number of compressors and turbines. Yang et al. [76] carried out a thermodynamic analysis on A-CAES integrated with wind energy while using a TES that is charged by both the waste heat during the compression process and the excess electricity generated by wind turbines.

In summary, the literature on thermodynamic analysis of CAES aims at improving its system efficiency and performance by introducing modifications at the component level and assigning a constant amount of wind power for compressor operation. As the integration of CAES with wind farms is faced with a challenge to mitigate the intermittent nature of wind energy, it has to be designed and analyzed thermodynamically considering the specific environment in which the integrated (Wind/CAES) is intended to operate requiring analysis and understanding of the environmental data. This aspect is mainly missing from the studies focusing on thermodynamic analysis of wind-CAES systems as summarized in Table 2-4.

2.4.3 CAES system optimization

Considering wind energy fluctuations, the operation of a Wind/CAES system is subject to uncertainties. Li et al. [77] developed a dynamic model of A-CAES with wind power generation for microgrid emergency backup. Their results show that for locations with high diesel prices and high wind potentials, implementing an A-CAES would yield better economic merits in comparison with diesel generators. Zhang et al. [78] studied the dynamic aspects of scroll compressor and expander operations in a small-scale Wind/CAES system and developed an experimentally validated model to optimize their performance using data collected on a specific day. Jin et al. [79] developed a dynamic modeling approach

representing the performance of a Wind/CAES system analyzing the impact of wind fluctuations. By minimizing the difference between real wind data and forecasted ones, the model was able to incorporate predictions of wind uncertainties more accurately. The results show that a CAES system can absorb wind power fluctuations effectively. Das et al. [80] proposed a system model for a CAES reservoir investigating inlet and outlet mass flow rates and interior pressure considering two scenarios of storing energy when wind power is more than its forecasts and discharging when wind power is less than its forecasts.

The above-mentioned studies concentrated on addressing the fluctuations of wind energy either by adopting a dynamic behavior for the components or by equipping the CAES with a predictive model that minimizes the mismatch between forecasted and real wind generation.

Besides the supply side uncertainties, there are demand side uncertainties that need to be incorporated in the designing and sizing of CAES systems. Marano et al. [81] employed dynamic programming for optimal management of a small-scale CAES plant integrated with a wind farm considering a single day predicted demand data combined with ANN-based forecasting approach for wind energy potentials. Abbaspour et al. [44] used wind data for a hypothetical day in which the wind profile is nearly equal to the annual average. They developed a short-term optimal operation and scheduling model to analyze the effect of CAES integration with wind energy alongside changes in demand. According to their results, a conventional gas-fired power system combined with wind and CAES system ensured a lower total cost in comparison with the same system without a CAES. Wang et al. [82] suggested an optimization model for the sizing of a CAES system when integrated with a wind farm. Zhang et al. [83] employed bi-level programming to plan a microgrid that includes a CAES system, solar panels, wind turbines, and diesel generators. Xu et al. [84] employed scenario-based bi-level programming for designing a hybrid system encompassing wind turbines CAES, and diesel generators to achieve an optimal demand response. The uncertainties, related to demand and wind power generation, are simulated through consideration of future corresponding scenarios. They also studied the effect of considering penalties for wind power curtailment and load loss, showing that a wind power curtailment is having a more remarkable effect on the total cost of the system. Several studies used stochastic programming for Wind-CAES system optimization [57],. In stochastic programming, a probability distribution for each uncertain parameter is summed or estimated

[86]. To avoid such a need to assume/estimate probability distributions, Bai et al. [87] employed a robust optimization model to incorporate the system uncertainties in CAES scheduling CAES.

The literature reviewed in this section mainly focuses on the system-level sizing of compressors and turbines without a thermodynamic analysis of design and operation parameters. Even though CAES, unlike batteries, is a complex mechanical system with various components requiring analysis of these mechanical components and parameters (and their thermodynamic behavior) such as pressure regulating valve, mass flow rates, heat recovery system, etc., these papers have treated a CAES as electricity-to-electricity (black-box) storage.

Table 2-4 summarizes the articles reported in the literature on thermodynamic analysis and system optimization for Wind/CAES systems. In this table, aspects related to wind and thermodynamic design and modeling are listed as related to the scale, technology, and operation type of the system. In this table, it is also indicated whether the studies have considered a real wind farm or a simulated one. In the case of a simulated wind farm, it is also investigated whether the number of wind turbines is given or is optimized alongside the capacities of CAES components. The last column of this table discusses if the article analyzes the economic and environmental gains of adopting CAES including GHG savings or smoothing wind energy output. These gains could present the merits of a Wind/CAES system in comparison with other power systems.

Table 2-4: Summary of literature on thermodynamic analysis and system optimization for wind/CAES .

Ref	Research category	Scale	Technology	Available or designed wind farm	Operation type	Wind input	Design and modeling focus	Economic and environmental gain analysis
[72]	Thermodynamic Steady state	Large-scale	A-CAES	Available wind farm.	Constant volume air reservoir and constant turbine inlet pressure	One wind profile is based on the average hourly wind speed of summer. Constant electricity input for compressors and variable input for high-temperature energy storage system	Complete energy and exergy analysis for all the components of the proposed system and parametric study.	---
[73]	Thermodynamic Steady state	Large-scale	A-CAES	A simulated wind farm assumed the number of wind turbines for their case study.	Constant volume air reservoir and constant turbine inlet pressure	Wind profile for a specific month (February 2019). Constant electricity input for compressors	Integrating a packed bed latent thermal energy storage, and comprehensive energy exergy and heat transfer analysis.	---
[74]	Thermodynamic Steady state	Small-scale	D-CAES	A simulated wind farm assumed the number of wind turbines for their case study.	Constant volume air reservoir and constant turbine inlet pressure	Constant CAES input is based on an average wind speed number.	Through thermodynamic analysis of CAES integrated with CCHP system, energy, and exergy.	---
[71]	Thermodynamic Steady state	Large-scale	A-CAES	---	Constant volume air reservoir and constant turbine inlet pressure	Site selection based on wind availability in China.	Integrated system with solar thermal heat recovery system, thermodynamic modeling of the proposed system and parametric study of key parameters.	---
[76]	Thermodynamic Steady state	Large-scale	A-CAES	---	Constant volume air reservoir and constant turbine inlet pressure	Constant share for compressors, the reluctant part of wind energy charges the	Thermodynamic and heat transfer modeling and parametric study.	---

					TES.			
[77]	Dynamic	Small-scale	A-CAES	Available wind farm.	Constant volume air reservoir and constant turbine inlet pressure	Wind speed data of a typical day for each season.	Dynamic modeling of the mechanical components.	Economic gain analysis based on CAES capital cost, operation, and maintenance cost fuel, and carbon emission cost.
[78]	Dynamic	Small-scale	A-CAES	One wind turbine.	Constant volume air reservoir	Wind speed data for a typical day.	Dynamic performance of the key mechanical components. Comparing the model with experimental results as well.	---
[79]	Dynamic	Small-scale	D-CAES	One wind turbine.	Constant volume air reservoir	Wind speed data for a typical day.	Dynamic modeling of the components and dynamic output power data.	---
[80]	Dynamic	Large-scale	D-CAES	Available wind site.	Constant volume air reservoir and constant turbine inlet pressure	Wind speed data for a year. Analyzing the mismatch between forecasted and real wind data.	Detailed dynamic model of the air reservoir, interior pressure, and mass flow rates. Introducing different CAES designs for the case.	Comprehensive economic analysis, CAES investment and operation cost, carbon tax wind curtailment lost etc.
[81]	Optimization	Small-scale	D-CAES	A simulated wind farm assumed the number of wind turbines for their case study.	Constant volume air reservoir and constant turbine inlet pressure	Wind speed data for a typical day. Wind speed forecasting by an artificial neural network.	Dynamic programming is applied, for finding optimum air reservoir pressure by minimizing cost and ensuring meeting demand	Analyzed the economic benefits and the reduction of CO2 for the proposed system.
[44]	Optimization	Large-scale	D-CAES	A simulated wind farm assumed the number of wind	---	10 minutes interval wind speed for a specific day. Hourly	Short-term optimal scheduling mixed-integer non-linear programming	Comparing two scenarios of profit maximization and

				turbines for their case study.		average is used for the study.	(MINLP). Only based on compressor turbine and air storage capacities.	cost minimization.
[82]	Optimization	Large-scale	D-CAES	Fixed installed wind power capacity.	---	Statistical analysis of the power requirements based on year data.	Economical optimization for deciding on the rated capacities of the components.	Analyzing the economic benefit of the system and reduction of coal consumption and CO2 emission analysis.
[83]	Optimization	Small-scale	A-CAES	Optimized the number of wind turbines.	Constant volume air reservoir and variable turbine inlet pressure	Wind speed data for typical days for each season.	Bi-level programming, sizing at the upper level, and operation at a lower level. Working only on the component capacities of the mechanical design.	Minimizing cost; operational and emission cost.
[84]	Optimization	Small-scale	A-CAES	Optimized the number of wind turbines.	Constant volume air reservoir and variable turbine inlet pressure	Data for four typical days for four seasons. Scenario generation with the Mont Carlo method.	Bi-level programming, sizing at the upper level, and operation at a lower level. Considering demand response. Deciding on component capacities, and the number of wind turbine and diesel generators.	Minimizing cost; operational and investment cost, wind curtailment penalty cost and emission cost.
[87]	Optimization	Small-scale	A-CAES	---	---	Wind prediction for a day.	Robust optimization, working only on the capacities of the main components.	Minimizing system operational costs.

Based on earlier research in design and scheduling, the energy system must follow a predetermined operation strategy to size the system or fixed capacities for the components for optimal scheduling. However, considering energy management (optimization of operation) in the initial design stage of a microgrid is vital, focusing on just operation or sizing, would lead to a suboptimal solution. [83]. Bi-level programming framework is ideal for such problems, providing interaction for the sizing and scheduling problems [88]. In bi-level programming studies, the upper layer (outer layer) decides on the capacities of each component and transfers it to the lower level (inner layer), then the lower level (inner layer) optimizes the operation strategy of the system based on the given capacities and sends the results to the upper layer (outer layer). In this regard, Xu et al. [84] proposed a scenario-based bi-level programming method for designing a stand-alone energy system containing wind turbines diesel generators, and a CAES system. They employed quantum particle swarm optimization (QPSO) for the outer layer and sequential quadratic programming for the inner layer. The demand response is considered in their model as well. Zhang et al. [83] employed a bi-level programming approach, with the genetic algorithm (GA) for the upper level and CPLEX solver for the lower level, planning a microgrid with, photovoltaic, wind turbine, diesel generators, and CAES. Yin et al. [89] proposed a model for co-optimization of the economy and reliability for integrated energy systems including CAES, with planning and scheduling level optimization, using bi-level programming. Li et al. [90] developed a multi-objective bi-level optimization model to reduce cost and enhance energy saving for an a wind-driven CAES system integrated with the CCHP system. Worth mentioning that, their case study demonstrates how the bi-level optimization method can be used to achieve the globally optimal solution, and optimizing one aspect at a time, sizing, or operation, would result in a suboptimal solution of the overall system. In the above-mentioned studies regarding bi-level programming, their CAES design is limited to the compressor and turbine capacities and volume. In detail, they did not propose a configuration for CAES and solved their design problem with a predefined number of compressors and turbines with a given outlet temperature after each heat recovery step and mostly considering a defined constant pressure for the air reservoir or a fixed volume design considered a pre-set maximum and minimum pressure for the air reservoir. However, for CAES as a mechanical system with various operating components defining only the capacities is not the case. Also, none of them considered off-design conditions in their design process, considering fixed isentropic efficiencies

even though a stand-alone microgrid would probably operate in part load conditions and this would affect the operating parameters at each time step.

2.5 Gap Analysis

In the light of the review of the relevant literature, it has become apparent that several gaps currently exist in the body of research pertaining to CAES:

(1) The majority of studies conducted on CAES have been focused on grid-connected systems, and the thermodynamic analyses studies are aimed solely at peak shaving applications.

(2) Studies that focus on the design and scheduling of CAES systems primarily concentrate on recommending compression, expansion, and air reservoir capacities, especially in BLP studies. However, since CAES is a complex mechanical system, a detailed configuration of all components, including valves, heat recovery systems, and recuperators, is necessary for a more comprehensive understanding of its operation.

(3) Design and scheduling studies often fail to account for the impact of off-design conditions, particularly in BLP studies. Neglecting off-design characteristics can be detrimental to the design and scheduling of such mechanical systems, especially in terms of addressing wind fluctuations in off-grid areas. It is essential to consider off-design conditions, as the operation of compressors and turbines can vary significantly under partial load conditions.

Considering the importance of linking the operational optimization of with the design stage of microgrids, this thesis is proposing a bi-level design approach for an energy system with a CAES system with wind turbines and diesel generators for a remote community. The optimization formulation is in a way that for the CAES system alongside the required compressor and turbine capacities the detailed mechanical configuration and operating conditions of all the required components, like valve recuperator, air reservoir, etc., would be presented at the end. Considering the mechanical parameters, the heat transfer fluid operating temperature for instance, in the design and scheduling optimization process would lead to a more realistic design. Also, due to the constant variation of input and output power, modeling the off-design conditions of the CAES system is vital for achieving a more accurate result and a better understanding of the performance of the CAES system for the application of integration with renewable energies. Eventually, the exergy destruction of the system and the economic and environmental gain in comparison to the current power system, merely diesel generators, is studied as well. Table 2-5 presents the contributions of this thesis in

comparison of related studies.

Table 2-5: Design and schedule papers with bi-level programming.

Ref	Algorithm	Objective	CAES Decision Variables	CAES configuration design	Off-design conditions
[84]	QPSO for the outer layer, sequential quadratic programming for the inner layer (MATLAB)	Economic optimization	Power capacity compressor turbine, volume air storage.	✖	✖
[83]	GA for the upper layer, CPLEX solver for the lower level (MATLAB)	Economic optimization	Power capacity compressor turbine, volume air storage.	✖	✖
[89]	PSO for the outer layer, Gurobi for the inner layer	optimization of economy and reliability	Power capacity compressor turbine, volume air storage.	✖	✖
[90]	Hybrid multi-objective genetic algorithm	Economic optimization	Power capacity compressor turbine, volume air storage.	✖	✖
Present Thesis	PSO for the outer layer, Gurobi for the inner layer (Python)	Economic optimization	Power capacity compressor turbine, volume air storage, Number of turbine and compressor, maximum and minimum pressure of air storage.	✓	✓

Chapter 3 : Methodology

3.1 Mathematical modeling

Figure 3-1 illustrates the schematic diagram of the CAES system integrated with wind turbines and diesel generators for satisfying the electricity demand of the remote community. The electricity demand of the case study is met through a combination of wind turbines, CAES systems, and diesel generators. The dispatch system and its controllers function as an energy management system, managing the generation and consumption of electricity and determining the output of the diesel generators and the behavior of the CAES system. When the wind turbines generate more electricity than is needed, the excess energy is stored in the CAES system. Conversely, when the wind turbines generate less electricity than is needed, the stored energy in the CAES system is discharged to cover the shortage. As for the CAES operation, The CAES charging process starts by compressing the ambient air through the compression train. After every compression stage, the air temperature rises; if this high-temperature air enters the next compressor, the system's power consumption would rise. Therefore, a heat recovery system is employed to lower the system's power consumption as much as possible using this waste heat in the expansion process. WD-350 oil is the heat transfer fluid (HTF) that circulates in heat exchangers absorbs the waste heat during the compression process and stores it in the hot oil tank. The compressed air is stored in the CAES tank at the end of the charging process. The discharging process starts by passing the air through the pressure regulating valve, lowering the compressed air pressure. This valve is employed to set the discharging pressure and benefit from the stored air in the CAES tank during the discharging period. Afterward, the air is first heated by a recuperator and then by hot oil, stored in the charging stage, ensuring an appropriate inlet temperature for the turbine. Eventually, the compressed air is expanded in the air turbines for power generation. As the outlet temperature of the last turbine is still high, a recuperator is employed to transfer this heat to the cold air exiting the pressure regulating valve.

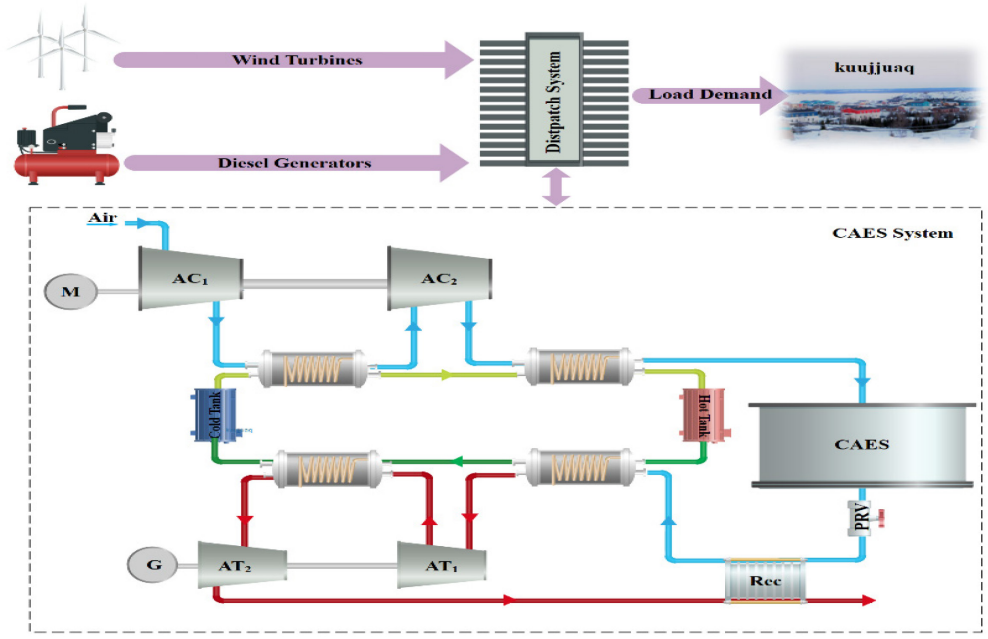

Figure 3-1: Schematic diagram of the proposed system.

3.1.1 Wind Turbines

For calculating the power generation of the wind turbines, first, the wind speed was calculated at wind turbine hub height based on the power-law equation [91]:

$$\alpha = \frac{\log_{10}(\frac{v_2}{v_1})}{\log_{10}(\frac{H_2}{H_1})} \tag{1}$$

which could also be represented as:

$$\frac{v_2}{v_1} = (\frac{H_2}{H_1})^{\alpha} \tag{2}$$

where α is the wind shear exponent power-law or power-law index and is equal to 0.3 [92], v_1 and v_2 are the wind speed at H_1 and H_2, respectively.

The wind turbine power output at different time steps is calculated below [93]:

$$P(t)_{wt} = \begin{cases} 0 & v(t) < v_{ci}, v(t) \geq v_{co} \\ P_{r,wt} \times \dfrac{v(t)^3 - v_{ci}^{\ 3}}{v_r^3 - v_{ci}^3} & v_{ci} \leq v(t) < v_r \\ P_{r,wt} & v_r \leq v(t) < v_{co} \end{cases} \quad (3)$$

where $P(t)_{wt}$ and $P_{r,wt}$ are the power generation of one wind turbine at each time step and the wind turbine rated output power, respectively. $v(t)$, v_{ci}, v_{co},and v_r are the wind speed at hub height at one-time step, wind turbine cut-in speed, wind turbine cut out speed, and the wind turbine rated speed, respectively. For a wind turbine, the cut-in speed is the speed that the wind turbine starts working with it. Afterward, as the wind speed increases the wind turbine power generation increases as well until the wind speed reaches the wind turbine-rated speed. When the wind speed is between the turbine-rated speed and cut-out speed, the wind turbine power output is constant and equal to the rated power of the wind turbine. The turbine stops working if the wind speed is higher than the cut-out speed.

3.1.2 Diesel generator:

The main portion of the operation cost for diesel generators is their fuel cost consumption, as in remote communities the fuel cost is significantly high. The amount of fuel consumption and its cost are calculated as below [94]:

$$q(t) = aP_{dg}(t) + bP_{dg,rated} \quad (4)$$

where q is the fuel consumption at the time t, a and b are the fuel consumption characteristics ,based on the linear equation between the fuel consumption and power rate.

Based on the hourly fuel consumption, the diesel generator's operation cost and the system's emission cost are calculated as below [83].

$$C_{op,Dg}(t) = c_f \times q(t) \quad (5)$$

$$C_{em,Dg}(t) = c_{em} \times \beta \times q(t) \quad (6)$$

where $C_{op,dg}$ and $C_{em,dg}$ are the diesel generator operation cost and CO_2 emission cost at the time t, respectively. c_f, c_{em}, and β are the cost of fuel, CO_2 emission rate, and emission cost, respectively.

3.1.3 CAES:

In this section, the energy and exergy analysis of all CAES components are described. Every component is defined as a control volume and is investigated by applying the first and second laws of thermodynamics. For simplicity, the following assumptions are made:

(1) The air is considered an ideal gas, with a constant specific heat capacity. [95].

(2) The pressure loss is assumed to be negligible in all pipes and heat exchangers [96].

(3) The compressed air at the CAES tank is stored at ambient temperature [97].

(4) Kinematic and potential energies are negligible in all components [98].

(5) The isentropic efficiency of the compressor and turbine is a function of the partial load [99].

(6) Throttling process of air is adiabatic [100].

Energy modeling is applied to describe each component's energy conversion. The energy balance equation for each component is based on the first law of thermodynamics and the mass balance equation [101]:

$$\sum \dot{m}_{out}(t) = \sum \dot{m}_{in}(t) \tag{7}$$

$$\dot{Q}(t) - \dot{W}(t) = \sum \dot{m}_{out}(t) h_{out}(t) - \sum \dot{m}_{in}(t) h_{in}(t) \tag{8}$$

3.1.3.1 Compressor train:

Initially, during the charging process, the ambient air enters the compressor train, therefore the inlet temperature and pressure of the first compressor are equal to the ambient temperature and pressure. As the air pressure increases in each compressor, the temperature increases as well, and the outlet temperature and pressure of each compressor could be calculated as below [102]:

$$T_{AC,i}^{out}(t) = T_{AC,i}^{in}(t)\left(1 + \frac{r_{AC}^{\frac{k-1}{k}} - 1}{\eta_{AC,s}(t)}\right) \tag{9}$$

$$p_{AC,i}^{out}(t) = p_{AC,i}^{in}(t) \times r_{AC} \tag{10}$$

where $T_{AC,i}^{out}(t)$ and $T_{AC,i}^{in}(t)$ are the output and input temperatures of each compressor, respectively. $p_{AC,i}^{out}(t)$ and $p_{AC,i}^{in}(t)$ are the output and input pressures of each compressor, respectively. r_{AC} is the compression ratio of each compressor, k is the ratio of specific heats,

and $\eta_{AC,s}$ is the isentropic efficiency of each compressor, which differs based on the input power in every time step and is calculated based on Figure 3-2, data provided in [103].

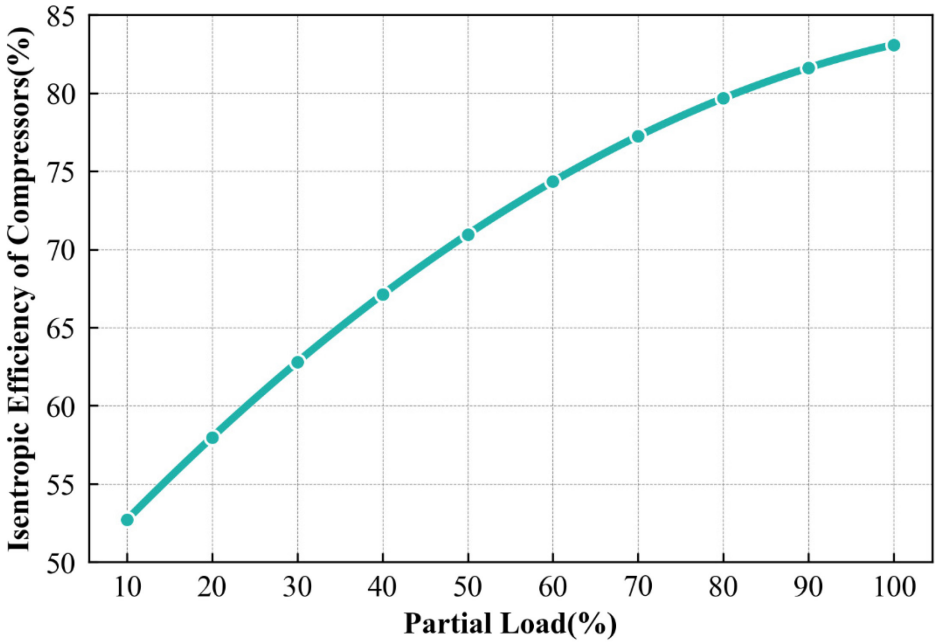

Figure 3-2: Variation of compressor isentropic efficiency with the partial load.

The air temperature after each heat recovery step is [104]:

$$T_{HEX,i}^{out}(t) = (1-\varepsilon)T_{AC,i}^{out}(t) + \varepsilon T_{oil,cold}(t) \qquad c_{p,air}\dot{m}_{ch}(t) \le c_{p,oil}\dot{m}_{oil}(t) \tag{11}$$

where $T_{HEX,i}^{out}$ is the output temperature of the heat exchangers which is the same as the input temperature of compressors, except for the first compressor that air enters the compressor at the ambient air conditions. ε is the effectiveness of the heat exchanges, $c_{p,air}$ and $c_{p,oil}$ is the specific heat capacity of air and oil. $\dot{m}_{ch}$ and $\dot{m}_{oil}$ are the air mass flow rate and the oil heat recovery loop mass flow rate.

Eventually, the compressor input power formulation based on the charging mass flow rate is as per below [70]:

$$P_{AC}(t) = \sum_{i=1}^{n} c_{p,air}\dot{m}_{ch}(t)[T_{AC,i}^{out}(t) - T_{AC,i}^{in}(t)] \tag{12}$$

where $P_{AC}(t)$ is the power consumption of the compressor train.

3.1.3.2 CAES tank:

After the charging stage, the air with high pressure is stored in the CAES tank with the ambient temperature. Throughout the discharging process, the compressed air leaving the CAES tank passes through the pressure regulating valve, and accordingly, its pressure is adjusted. Valves processes are considered isentropic, so the enthalpy is constant. The pressure and state of the charge CAES tank at each time step is calculated with [80]:

$$p_{\tan k}(t+1) = p_{\tan k}(t) + RT_{\tan k}\left(\frac{(\dot{m}_{ch}(t) - \dot{m}_{dch}(t)) \times \Delta t}{V_{CAES}}\right) \tag{13}$$

$$SOC_{CAES}(t) = \frac{p_{\tan k}(t) - p_{\min}}{p_{\max} - p_{\min}} \tag{14}$$

where $p_{\tan k}, T_{\tan k}$ and V_{CAES} are the pressure, temperature, and volume of the CAES tank. SOC_{CAES} is the state of charge of CAES at time t. $p_{\min}$ and $p_{\max}$ are the minimum and maximum pressure of the CAES tank, respectively.

3.1.3.3 Turbine train:

Mostly the air exhausting the last turbine is at a high temperature consequently, to recover this heat a recuperator is placed at the end of the cycle, utilizing this waste heat to preheat the air before the expansion process. After, the air passes through the receptor and first heat exchanger, its temperature rises, the air enters the turbine, and the outlet temperature and pressure of the turbines are calculated [105]:

$$T_{AT,j}^{out}(t) = T_{AT,j}^{in}(t) - \eta_{AT,s}(t) T_{AT,j}^{in}(t)\left(1 - (r_{AT})^{\frac{k-1}{k}}\right) \tag{15}$$

$$p_{AT,j}^{out}(t) = \frac{p_{AT,j}^{in}(t)}{r_{AT}} \tag{16}$$

where $T_{AT,j}^{out}(t)$ and $T_{AT,j}^{in}(t)$ are the output and input temperatures of each turbine, respectively. $p_{AT,j}^{out}(t)$ and $p_{AT,j}^{in}(t)$ are the output and input pressures of each turbine, respectively. r_{AT} is the expansion ratio of each turbine, and $\eta_{AT,s}$ is the isentropic efficiency of each turbine, which differs based on the input power at every time step and is calculated based on Figure 3-3, data provided in [103].

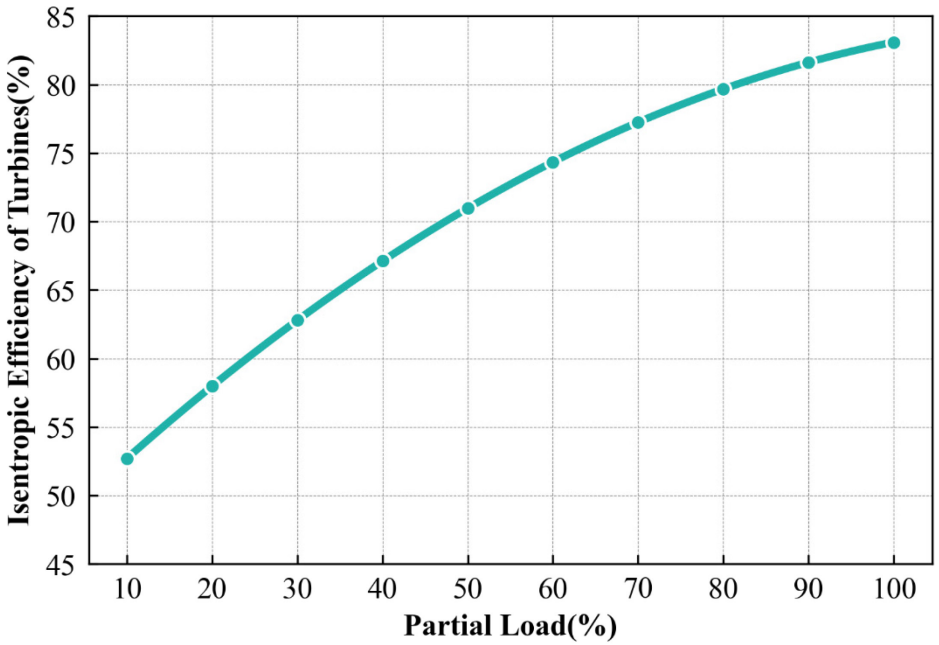

Figure 3-3: Variation of turbine isentropic efficiency with partial load.

The air temperature after each heat recovery step is [104]:

$$T_{HEX,j}^{out}(t) = (1-\varepsilon)T_{AT,j}^{out}(t) + \varepsilon T_{oil,cold}(t) \quad c_{p,air}\dot{m}_{dch}(t) \le c_{p,oil}\,\dot{m}_{oil}(t) \tag{17}$$

Eventually, the turbine output power formulation based on the discharging mass flow rate is as per below [106]:

$$P_{AT}(t) = \sum_{i=1}^{n} c_{p,air}\dot{m}_{dch}(t)(T_{AT,i}^{in}(t) - T_{AT,i}^{out}(t))] \tag{18}$$

where $P_{AT}(t)$ is the power generation of the turbine train.

3.1.3.4 Recuperator

Mostly the air exhausting the last turbine is at a high temperature consequently, to recover this heat a recuperator is placed at the end of the cycle, utilizing this waste heat to preheat the air before the expansion process and the energy balance equation for this component is given by [107]:

$$\dot{Q}_{\mathrm{Rec}}(t) = \dot{m}_{dch}(t)c_{p,air}(T_{rec,out}(t) - T_{rec,in}(t)) \tag{19}$$

where $T_{rec,in}(t)$ is the same as the outlet temperature of the last turbine which enters the recuperator at the end and $T_{rec,out}(t)$ is the outlet temperature of the recuperator at the last

stage of the cycle, which is the same as the air exiting to the ambient.

3.1.3.5 Exergy modelling of the CAES components

The exergy analysis is of prominent importance since it defines the quality of available energy and the irreversible losses of the system. The amount of exergy at each stream is given by [108]:

$$\dot{E}x_i = \dot{m}_i[(h_i - h_0) - T_0(s_i - s_0)] \tag{20}$$

where s is the specific entropy and subscript i refers to the state number and subscript 0 is related to the dead state conditions.

The exergy balancing equation and work and heating exergy transfer for each component is stated as below [109]:

$$\dot{E}x_Q + \sum \dot{E}x_{in} = \sum \dot{E}x_{out} + \dot{E}x_W + \dot{E}x_D \tag{21}$$

$$\dot{E}x_W = \dot{W} \tag{22}$$

$$\dot{E}x_Q = \dot{Q}(1 - \frac{T_0}{T_i}) \tag{23}$$

where $\dot{E}x_D$ is the amount of exergy destruction of every component and the total exergy destruction would be [110]:

$$\dot{E}x_{D,total} = \sum_{i=1}^{n} \dot{E}x_{D,i} \tag{24}$$

The exergy destruction formula of every component is presented in Table 3-1.

Table 3-1: Exergy destruction equations of the CAES system components [111–114].

Component	Exergy destruction rate equation
Air Compressor	$\dot{E}x_{D,AC} = (\dot{E}x_{in} - \dot{E}x_{out} + \dot{W}_{AC}).t_{ch}$
Air Turbine	$\dot{E}x_{D,AT} = (\dot{E}x_{in} - \dot{E}x_{out} - \dot{W}_{AT}).t_{dch}$
CAES Tank	$\dot{E}x_{D,CAES} = \dot{E}x_{in}.t_{ch} - \dot{E}x_{out}.t_{dch}$
Pressure-regulating valve	$\dot{E}x_{D.vavle} = (\dot{E}x_{in} - \dot{E}x_{out}).t_{dch}$
Recuperator	$\dot{E}x_{D,Rec} = (\dot{E}x_{air2,in} + \dot{E}x_{air1,in} - \dot{E}x_{air2,out} - \dot{E}x_{air1,out}).t_{dch}$

3.2 Problem formulation

Use of a BLP approach is proposed with the upper level optimizing the size of the components to minimize the total cost of the system and the lower level optimizing the operation strategy to minimize the operational cost. BLP enables the sizing and scheduling of the system at the same time where the sizing problem is a long-term decision, and the scheduling is a short-term decision [83]. In this problem, the upper optimization problem, i.e., sizing, is constrained by the lower optimization problem, i.e., scheduling. This is explained in detail in the following in sections 3.2.1, 3.2.2, and 3.3.2 To provide a clearer understanding of bi-level programming, Figure 3-4 presents a process chart that outlines the different stages of the proposed BLP.

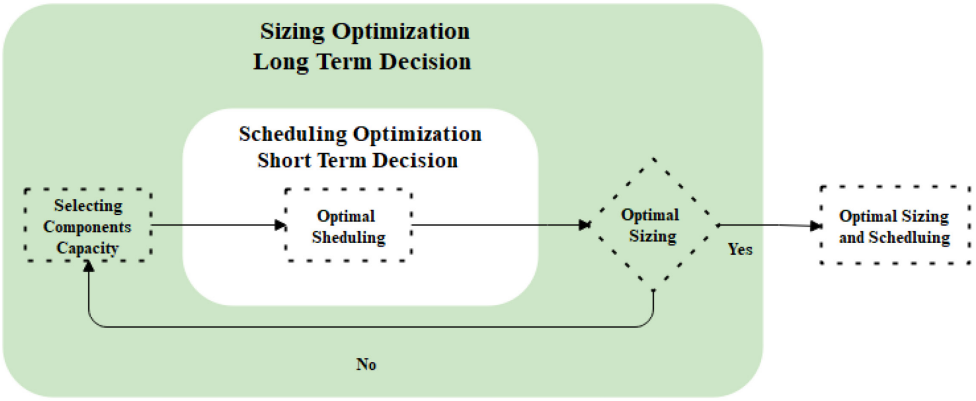

Figure 3-4: Bi-level programming process chart.

3.2.1 Upper-level optimization:

Given the unit capacity of wind turbines and diesel generators, the decision variables of the upper level and their upper and lower bounds are listed in Table 3-2:

Table 3-2: Decision variables of the upper level [84,98].

Variable	Lower bound-upper bound	Variable type
Number of wind turbines (N_{wt})	1-100	discrete
Number of diesel generators (N_{dg})	1-100	discrete
Air compressor nominal capacity (P_{AC})[kW]	1-2000	continuous
Air turbine nominal capacity (P_{AT})[kW]	1-2000	continuous
The volume of the compressed air reservoir (V_{CAES})[m^3]	1-3000	continuous
Number of air compressors (N_{AC})	1-5	discrete

Number of air turbines (N_{AT})	1-5	discrete
Maximum pressure (charging pressure) (p_{ch})[bar]	60-100	continuous
Minimum pressure (discharging pressure) (p_{dch})[bar]	30-55	continuous

The objective function of the upper level is to minimize the average daily cost [89]:

$$\min C_{daily,total} = C_{inv} + \frac{1}{N_d}\sum_{l=1}^{N_d} C_{total,op} \tag{25}$$

where C_{inv} and $C_{total,op}$ are the investment and operation costs of the system, respectively. In addition, N_d is the number of chosen days for the optimization identified based using a clustering approach. This will be explained further in the following sections 3.3.1 and 4.1. The operational cost of the system is based on the daily operation of the system and is calculated at the lower level. The investment cost is the sum of the investment cost of all components of the system which is formulated as [83]:

$$C_{inv} = \frac{1}{365}((c_{inv,AC}P_{ch,\max} + c_{inv,AT}P_{dch,\max} + c_{inv,\tan k}V_{CAES} + c_{inv,DG}N_{DG} + c_{inv,WT}N_{WT}) \times CRF) \tag{26}$$

$$CRF = \frac{r(1+r)^{N_y}}{(1+r)^{N_y} - 1} \tag{27}$$

where $c_{inv,AC}$, $c_{inv,AT}$ are investment costs per unit of power for the air compressor and air turbine, respectively. $c_{inv,\tan k}$ is the investment cost per unit of volume for the air reservoir volume. $c_{inv,DG}$ and $c_{inv,WT}$ are the investment cost per unit of installed diesel generators and wind turbines, respectively. CRF is the capital recovery factor of the project, and r and N_y the real interest rate and the service life, respectively.

3.2.2 Lower-level optimization:

The objective of the lower-level optimization is to minimize the daily operation cost consisting of the components' operation cost, emission cost, wind curtailment cost, and demand curtailment cost.

$$C_{total,op}(t) = C_{op}(t) + C_{em,DG}(t) + C_{cur,WT}(t) + C_{cur,demand}(t) \quad (28)$$

where $C_{op}(t)$ is the operation cost of the CAES system, the diesel generators and wind turbines at each time step.

$$C_{op}(t) = C_{op,Dg}(t) + C_{op,CAES}(t) + C_{op,WT}(t) \quad (29)$$

$$C_{op,CAES}(t) = c_{op,AC} \times P_{ch}(t) + c_{op,AT} \times P_{dch}(t) \quad (30)$$

where $C_{op,CAES}$ is the operation cost of CAES for each time step. $c_{op,AC}$ and $c_{op,AT}$ are the operation cost coefficient for the air compressor and air turbine, respectively. $P_{ch}(t)$ and $P_{dch}(t)$ are the charging and discharging power at the time t.

Also, in equation (28) $C_{cur,WT}(t)$ and $C_{cur,demand}(t)$ are the wind and demand curtailment costs, respectively. These costs are considered for reliability and lowering wind curtailment, and are calculated with the [89]:

$$C_{cur,WT}(t) = c_{cur,WT} \times P_{cur,WT}(t) \quad (31)$$

$$C_{cur,demand}(t) = c_{cur,demand} \times P_{cur,demand}(t) \quad (32)$$

where $c_{cur,demand}$ and $c_{cur,WT}$ are the cost coefficient for wind and demand curtailment for each time step.

The objective function of the lower level is subject to the following constraints:

The power balance constraint:

$$P_{demand}(t) + P_{ch,CAES}(t) + P_{cur,WT}(t) = P_{WT}(t) + P_{DG}(t) + P_{dch,CAES}(t) + P_{cur,demand}(t) \quad (33)$$

Wind turbine output limits:

$$0 \le P_{i,WT}(t) \le u_{i,WT}(t) \times P_{rated,WT} \quad \forall_i = 1,2,...,N_{WT} \tag{34}$$

where u_i is the unit status indicator that is a binary variable, 1 for the component is operating and 0 when the components are off.

Diesel generator output limits:

$$u_{i,DG}(t) \times P_{\min,DG} \le P_{i,DG}(t) \le u_{i,DG}(t) \times P_{\max,DG} \quad \forall_i = 1,2,...,N_{DG} \tag{35}$$

CAES input and output limits:

$$u_{AC}(t) \times P_{\min,AC} \le P_{ch}(t) \le u_{AC}(t) \times P_{\max,AC} \tag{36}$$

$$u_{AT}(t) \times P_{\min,AT} \le P_{dch}(t) \le u_{AT}(t) \times P_{\max,AT} \tag{37}$$

$$u_{AC}(t) + u_{AT}(t) \le 1 \tag{38}$$

3.3Solution algorithm

As shown in Figure 3-5 the optimization model works with the CAES off-design model and load and wind clusters.

3.3.1 Load and wind profile clustering

Clustering of load and wind profiles is employed to categorize the daily profiles[115]. K-means algorithm is employed for clustering the load and wind profiles [116]. Each data point has 48 attributes, with the first 24 attributes representing the hourly demand, and the second 24 attributes representing the hourly wind speed for a specific day. First, the load and wind data for each day are normalized. Then, the optimal number of clusters is defined using the elbow method [117]. Distortion metric is used for scoring each cluster number, computing the sum of square distances from each data point to the assigned center. Then, based on the specified number of clusters the load and wind profiles are grouped with the K-means algorithm. The

clustered data will be used as the input of the optimization algorithm instead of using the data for the whole year.

3.3.2 Linear regression for off-design conditions

Neglecting the off-design conditions of compressor and turbine, the relation between the mass flow rate and power rate would be linear all the time. However, considering off-design characteristics, this relation becomes non-linear. Using a mixed integer linear programming (MILP) approach, this equation needs to be converted to a linear equivalent. A linear regression model is thus used to represent each off-design curve. Accordingly, the mass flow rate in both charging and discharging can be calculated as follows:

$$\dot{m} = a \times P + b \tag{39}$$

where $\dot{m}$ is the charging or discharging mass flow rate, P is the compressor or turbine power. a and b are coefficient and the intercept of the regression model.

3.3.2 Optimization framework

Bi-level programming is employed in this thesis to design an energy system encompassing a wind turbine diesel generator and CAES system. The particle swarm optimization (PSO) algorithm is employed for the upper layer. PSO is popular because of its ease of implementation, ability to quickly reach a reasonable solution and robustness [118]. PSO has a very fast convergence speed and better results in comparison to GA [84]. The PSO learning process is based on a particle's own experience as well as the experience of the most successful particle. Each particle was assigned a random position in the n-dimensional space as a candidate solution. Each particle has a position and a velocity and moves through the search space by updating its position and velocity [119]. The pseudo-code of the PSO algorithm is demonstrated in Table 3-3.

Table 3-3: Pseudo code of the PSO algorithm [119].

Algorithm: Particle swarm optimization.
1. Setting t=1(number of iteration). Initialization of the particle position and velocities randomly.
2. Repeat:
a. Calculating the fitness value of each particle. Whether for each particle the fitness value is greater than the best fitness value found to do far, then update the particle's best position.

b. Defining the location of the particle with the highest fitness value and updating best global position if required.
c. Updating the velocity and position of each particle.
d. Setting t=t+1

Until stopping criteria are met.

Using a two-level optimization method, a set of parameters would be set in the upper level, therefore in the lower level they are constant, and the lower-level problem would be linear. The only nonlinearity left is related to the off-design formulation that in this thesis the related functions are linearized. Accordingly, the lower-level problem is a linear problem with continuous and binary variables (mixed integer linear programming (MILP)) and the Gurobi solver is applied for the lower-level optimization as a mature solver for MILP problems [120]. The proposed algorithm is modelled with Python and the flow chart of the optimization process is shown in Figure 3-5. As shown in this figure the optimization steps are as follows:

1) *Upper-level algorithm parameters:* Setting the number of particles (defining the swarm size) and the maximum number of iterations for the PSO algorithm.

2) *Upper-level particle population initialization:* Initialization of the particle position and velocities under the lower and upper bound constraints. The problem aims to find the vector $X = \{x_1, x_2, ..., x_n\}$ that minimizes the total daily cost, initially a random position is assumed for the location of every particle (X) in the search space. The search space is defined based on the lower and upper bands of the variables:

$$X_{lower} \leq X \leq X_{upper} \tag{40}$$

3) *Lower-level input:* The input data containing the hourly demand and wind speed data and the viables from the upper level are transmitted to the lower level.

4) *Lower-level optimization:* In the lower level, for each day the operation strategy is updated to find the minimum value for the operation cost, the total operation cost would be returned to the upper level after all days have been calculated.

5) *Upper-level total cost calculation:* based on the total operation cost at the lower level and investment cost at the upper level the total cost of the system is calculated.

6) *Upper-level total updating parameters:* Updating the particle positions, velocities, and individual and global optimal fitness. Particles update their velocity and position at iteration $t+1$ by the following equation:

$$V_i^{I+1} = w.V_i^I + c_1.r_1^t(X_{b_i}^t - X_i^t) + c_2.r_2^t(X_{gb}^t - X_i^t) \tag{41}$$

$$X_i^{I+1} = X_i^I + V_i^{I+1} \tag{42}$$

where V and X are the particles velocity and position at each iteration and W is the inertia weight. c_1 and c_2 are positive accelerating constants for individual and group learning (cognitive and social parameters), respectively. r_1 and r_2 are random numbers between 0 and 1. X_{b_i} and X_{gb} are the best position of the particle and the global best position. The suggested number for both c_1 and c_2 is 2 in the literature [121]. The inertia weight decreases from its maximum to its minimum value [119]:

$$w = w_{\max} - (w_{\max} - w_{\min})\frac{I}{I_{\max}} \tag{43}$$

where $I_{\max}$ is the maximum number of iterations and I is the number of iterations.

7) *Upper-level stopping criteria:* check whether the algorithm reached the maximum number of iterations. If not, the algorithm goes on.

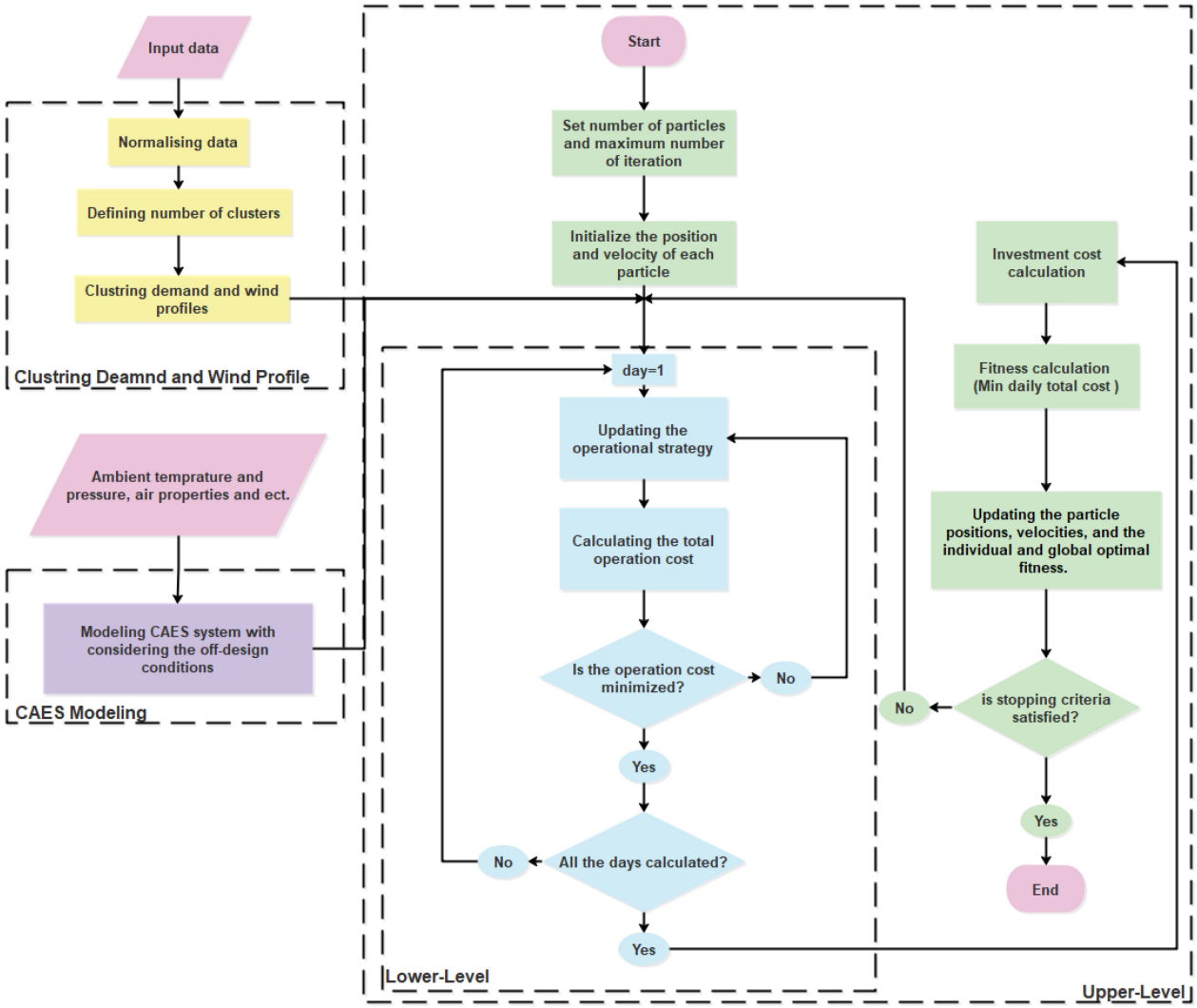

Figure 3-5: Flow chart of the optimization process.

Chapter 4 : Case study

Kuujjuaq a remote community in the Nunavik region of northern Canada is selected for this thesis. This isolated community is an interesting case for designing a CAES as these northern communities are merely dependent on diesel fuel for their electricity production and the delivery process is challenging [122]. Worth mentioning that connecting Kuujjuaq to Hydro Quebec's main grid would cost $750,000 per km or about $340 million [123]. That is why Canada is aiming to reduce the reliance on fossil fuels in these communities and reach zero-emission energy production [124]. In 2021, $7.1 million was invested for TUGLIQ Energy Co to support the third phase of the wind energy project in northern Quebec [125], also weather masts are going to be installed to collect the wind data in five communities in Nunavik with the highest wind speed, Kuujjuaq, Quaqtaq, Kangiqsujuaq, Salluit, and Puvirnituq. As Kuujjuaq is one of these locations it is chosen as a case study for a Wind-CAES, a promising pathway for augmenting the utilization of renewable energy sources in remote areas [1]. Detailed information on Kuujjuaq was gathered from The Atlas of Canada - Remote Communities Energy Database and is presented in Table 4-1[11].

Table 4-1: Remote community information [11].

Specification	Value
Community Name	Kuujjuaq
Province	QC - Canada
Latitude (°)	58.10006
Longitude (°)	-68.40612
Community classification	Indigenous
population	2754
Name of the service provider	Hydro-Quebec
Total fossil fuel generation capacity(kW)	6010
Annual fossil fuel generation (MWh/year)	20333
Total renewable energy generation(kW)	0

The hourly electricity demand data of Kuujjuaq for 2013 is used for this thesis. The meteorological information, temperature, pressure (for the compressor input), and hourly wind speed data are collected from the Kuujjuaq airport weather station [126].

Table 4-2 demonstrates the data description, containing the hourly demand data, hourly wind speed at 50-meters height, and the hourly wind power generation for one wind turbine.

Table 4-2: Data description before clustering.

	Demand (kW)	Wind Speed (m/s)	Wind Power (kW)
count	8760	8760	8760
mean	2256.00	5.90	126.14
std	382.82	4.14	109.85

min	1407.83	0	0
25%	1978.83	3.15	9.68
50%	2257.75	5.85	114.03
75%	2506.52	8.56	250
max	3322.50	25.23	250

4.1 Clustering demand and wind profiles:

In this part, the demand and wind clusters are demonstrated. Based on elbow method the optimal number of clusters is five, as shown in Figure 4-1. The data description after clustering is listed in Table 4-3. The number of days for each cluster is presented in Table 4-4.

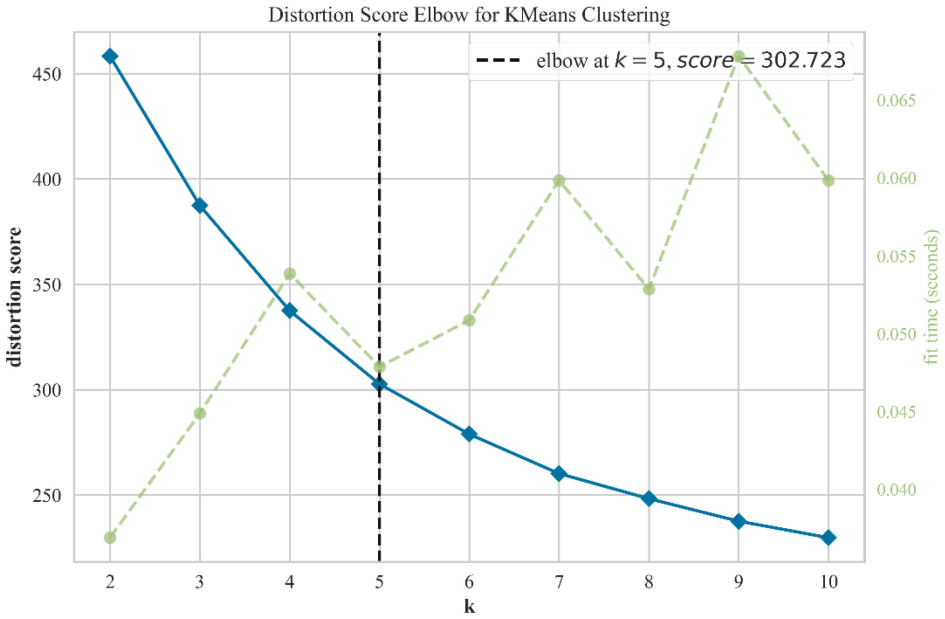

Figure 4-1: The distortion score based on the number of k (clusters).

Table 4-3: Data description after clustering.

	Demand (kW)	Wind Speed (m/s)	Wind Power (kW)
count	120	120	120
mean	2325.36	6.29	133.53
std	363.37	2.75	108.70
min	1553.77	2.09	0
25%	2080.81	3.79	24.03
50%	2318.20	5.69	105.42
75%	2592.60	8.92	250
max	3112.27	11.89	250

Table 4-4: Number of days allotted to each cluster.

Cluster number	Number of days
0	118
1	62
2	44
3	68
4	73

Figure 4-2 and Figure 4-3show the mean of each cluster for demand and wind speed, respectively.

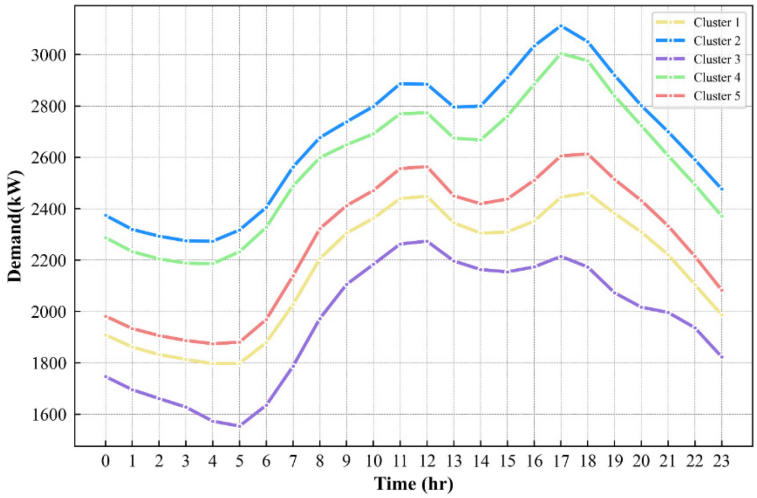

Figure 4-2: Demand clusters.

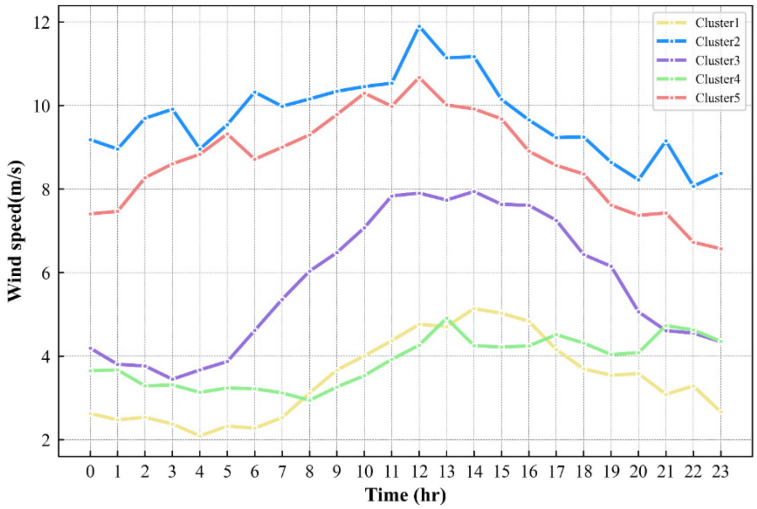

Figure 4-3: Wind clusters.

4.2 Technical and economic parameters

In this section, the technical and economical parameters are provided for the simulation. The design and economic parameters of wind turbines, diesel generators, and CAES system is listed in Table 4-5, Table 4-6, and Table 4-7, respectively.

Table 4-5: Design and economic parameters of the wind turbines [127,128].

Parameter	Value
Hub height (m)	50
Rated power generation (kW)	250
Cut-in speed (m/s)	2.5
Rated speed (m/s)	7.5

Cut-out speed (m/s)	25
Capital cost factor ($/unit)	375000
O&M cost factor ($/kWh)	0.0122
Wind curtailment cost factor ($/kWh)	0.1
Lifetime (years)	20

Table 4-6: Design and economic parameters of diesel generator [83,84,94]**.**

Parameter	Value
a	0.246
b	0.08415
Output Upper-Lower limit (kW)	10 – 150
Ramp up and down limit(kW)	30
Capital cost factor ($/kw)	210
Maintenance cost factor ($/kWh)	0.003
Emission cost factor ($/kg)	0.1
Disel cost ($/l)	2.5
CO_2 Emission rate (g/l)	2633.3

Table 4-7: Design and economic parameters of CAES [83,128–130].

Parameter	Value
Ambient Temperature(K)	267
Ambient Pressure (bar)	1.01
Specific heat capacity of air at constant pressure (kJ/kg.K)	1.1
Adiabatic exponent of air	1.4
The gas constant of air (kJ/kg.K)	0.287
Specific heat capacity of HTF (kJ/kg.K)	3
Effectiveness of heat exchangers	0.85
Air compressor capital cost factor ($/kW)	390
Air compressor O&M cost factor ($/kWh)	0.003
Air turbine capital cost factor ($/kW)	325
Air turbine O&M cost factor ($/kWh)	0.003
Air storage capital cost factor ($/$m^3$)	1000

Chapter 5 : Results and discussion

5.1 Validation

The CAES modeling results are validated with [100], which can be seen in Table 5-1. The design parameters of this reference were applied to the current modeling and as shown in this table the divergence between the present thesis and the reference is negligible, implying that the results are accurate and reliable.

Table 5-1: Validation of CAES thermodynamic modeling with ref [100].

Parameter	Current work	Reference	Deviation (%)
Outlet temperature of first compressor (K)	448.96	447.6	0.30%
Outlet pressure of first compressor (bar)	3.59	3.58	0.28%
Outlet temperature of second compressor (K)	493.55	490.9	0.54%
Outlet pressure of second compressor (bar)	12.77	12.69	0.63%
Outlet temperature of third compressor (K)	506.90	503.6	0.66%
Outlet pressure of third compressor (bar)	45	45	-
Outlet temperature of turbine (K)	690.59	692.4	0.26%
Outlet pressure of first turbine (bar)	1.01	1.01	-

5.2 Results

In this section, the results of the proposed method is presented. Figure 5-1 displays the variation of the average daily total cost during the optimization process, with a maximum iteration number of 120 with 60 particles. The figure provides a clear visualization of the rapid convergence of the PSO algorithm towards the optimal solution. This indicates the efficiency of our proposed method in achieving the desired cost reduction.

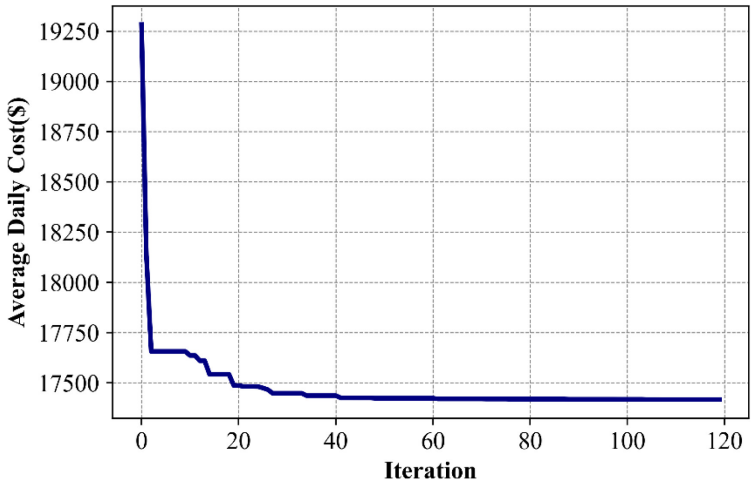

Figure 5-1: Variation of average daily cost during the optimization process.

In this section, the optimization results is presented in Table 5-2 and Table 5-3. Table 5-2 displays the optimum values for the decision variables, resulting in the minimum average total daily

cost. On the other hand, Table 5-3 presents the average total daily cost and the total daily CO2 emission of the proposed system for one year of data. The results show that the proposed system achieved an average total daily cost of 17,396.35$ and a total daily CO2 emission of 12611.15 kg. Furthermore, Table 5-3 also indicates that the proposed system outperforms the energy system operating solely with diesel generators, reducing the average daily total cost and the average daily CO2 emission by 69% and 76%, respectively. These findings highlight the effectiveness of the proposed system in achieving significant cost savings and reducing environmental impact.

Table 5-2: Optimization results.

Parameter	**Value**
Number of wind turbines	24
Number of diesel generators	20
Compressor capacity(kW)	712
Turbine capacity(kW)	956
Air storage volume (m^3)	2463
Number of air compressors	4
Number of air turbines	3
Air storage minimum pressure (bar)	38
Air storage minimum pressure (bar)	92

Table 5-3: Comparison of the proposed system with only diesel generators.

	Average daily total cost ($)	Average daily CO_2 emission (kg)
Diesel Generator	56328.72	53421.98
CAES, Wind, Diesel Generator	17396.35	12611.15
Reduction	69%	76%

To validate the robustness of the optimization algorithm, ten run attempts were conducted, and their outcomes are displayed in Figure 5-2, which shows the fitness values. These results demonstrate the consistency and stability of the optimization algorithm as the fitness values converge to a similar optimal value in each run attempt. Thus, it can be concluded that the proposed method is reliable and robust in achieving the optimal solution.

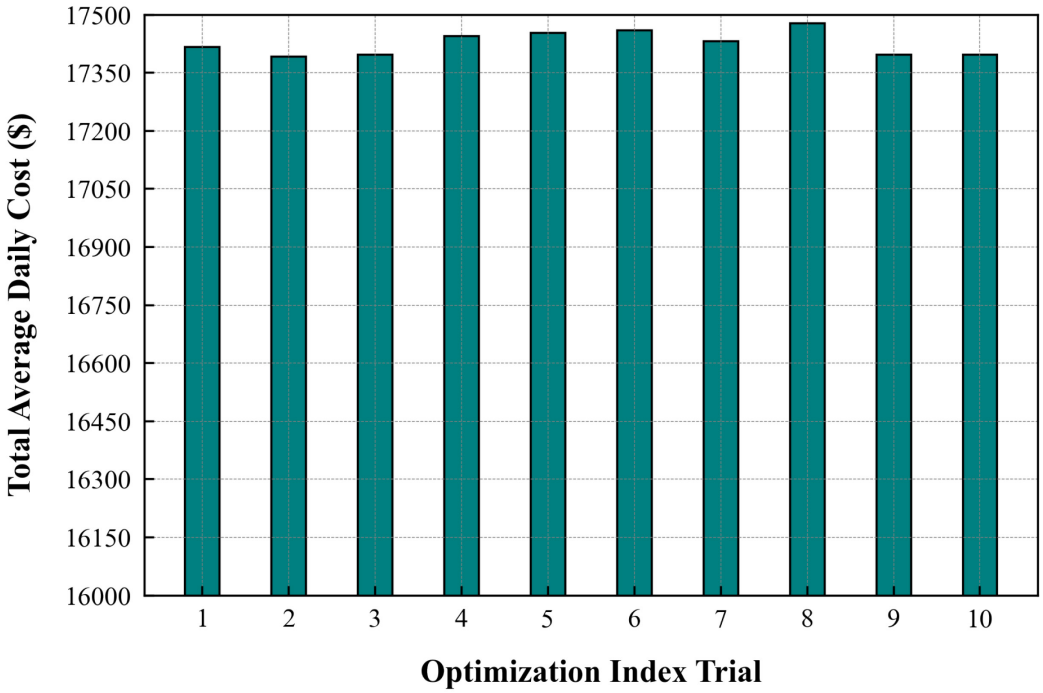

Figure 5-2: Fitness value of ten times of trial.

In Figure 5-3 the results of variations in demand curtailment are presented throughout the year based on different demand curtailment penalty costs. As depicted in this figure, due to a high diesel price in our case study, low demand curtailment penalty costs result in a high amount of demand curtailment throughout the year. It can be observed that when the demand curtailment penalty cost is set to 50 ($/kWh), the demand curtailment becomes constant and does not decrease further. Therefore, the demand curtailment penalty cost is assumed as 50 ($/kWh) in this thesis. These findings provide valuable insights for decision-makers to determine an optimal demand curtailment penalty cost ensuring a cost-effective and sustainable energy system.

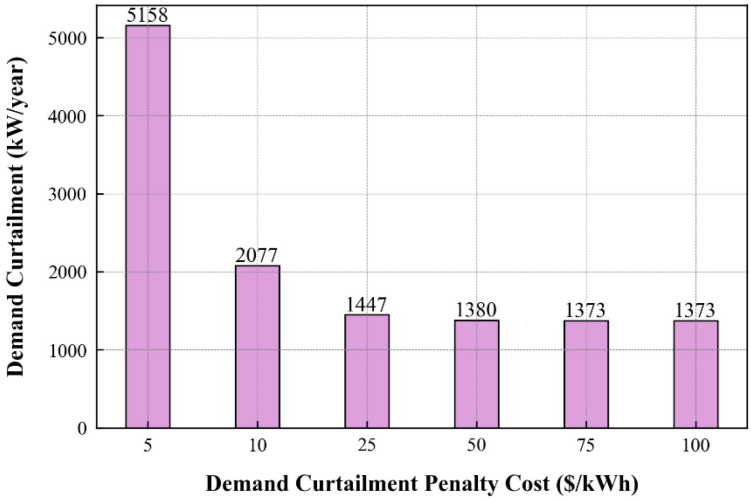

Figure 5-3: Variation of the demand curtailment for one year based on different demand curtailment penalty cost.

The scheduling results and pressure variation of the air reservoir during the day are shown in Figures 5-4 to 5-7 for four different days throughout the year. These figures demonstrate how the CAES system operates differently and how the air reservoir pressure changes based on the energy requirements of each specific day. By analyzing these figures, it can be observed that the flexibility and efficiency of the proposed CAES system in meeting the demand and regulating the air reservoir pressure according to the energy requirements of each day. This indicates the effectiveness of the proposed system in optimizing energy management and reducing costs while ensuring reliable and sustainable energy supply.

As per Figure 5-4, the CAES system is not fully charged on the day before, and since the beginning of the day up to hour 11, where there is no wind power available, the energy demand is satisfied with the diesel generator and the CAES system. Starting from hour 11, when wind energy becomes available, the CAES system begins to charge when the wind energy exceeds the energy demand and discharges when there is a mismatch between the wind energy and the demand. In Figure 5-5 frequent charging and discharging periods occur for one day, and the CAES system is fully charged at the beginning of the day. Additionally, we can see that although there is wind curtailment in some hours of the day, the CAES system discharges energy. This is because the wind curtailment cost is higher than the CAES operating cost in those specific hours. Hence, the system tries to lower the wind curtailment cost by discharging around 2200 kW of electricity, reducing the SOC of the CAES, as it is already fully charged at the beginning of the day, and charging around 2800 kW of electricity. Towards the end of the day, the wind power is not sufficient to meet the

energy demand, and therefore, the CAES system charges to its full capacity so that it has enough power to satisfy the demand at the end of the day. These results demonstrate the effectiveness of the proposed CAES system in optimizing energy management and reducing the reliance on fossil fuels while ensuring reliable and sustainable energy supply. As shown in Figure 5-6 shows that there are not significant pressure changes in the air reservoir on this day, as there is not much wind energy available, and the energy demand is mostly satisfied with the diesel generators. In Figure 5-7 it can be seen that the CAES system is at its minimum pressure at the beginning of the day and cannot discharge. As there is no wind energy available until the final hours of the day, the CAES system stays on standby, and almost the entire energy demand on this specific day is satisfied by diesel generators. However, towards the end of the day, there are some hours where the wind energy is higher than the energy demand, and the CAES system starts charging. These findings demonstrate the flexibility and efficiency of the proposed energy system in integrating different energy sources and meeting the energy demand based on the availability and variability of wind power. The proposed system optimizes energy management and reduces the reliance on fossil fuels, leading to cost savings and environmental benefits.

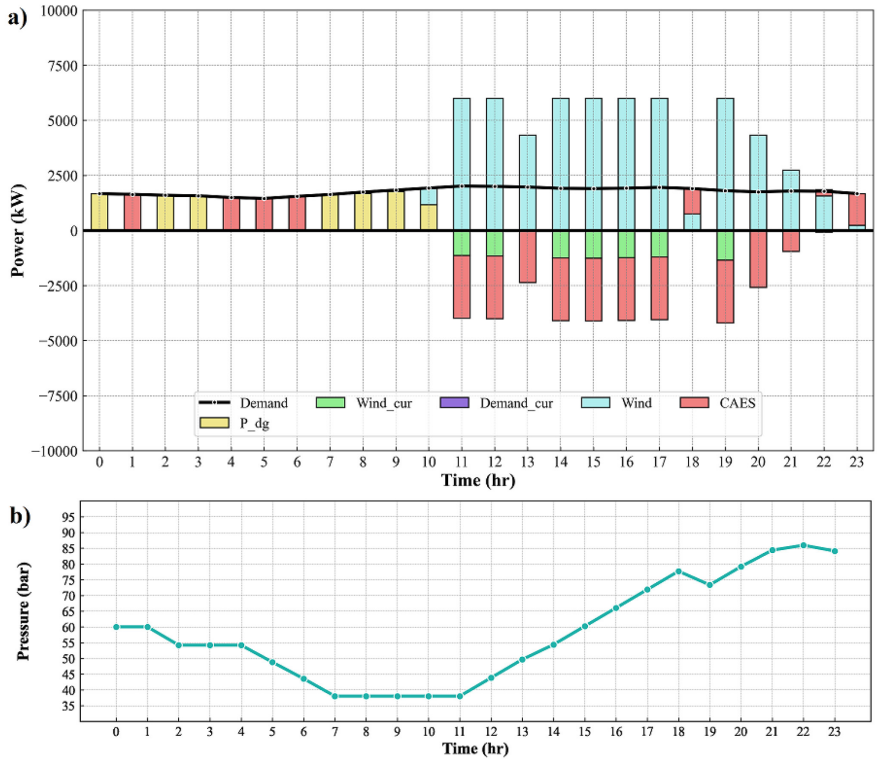

Figure 5-4: a) the scheduling result and b) the pressure variation of the air reservoir for day 201 of the dataset.

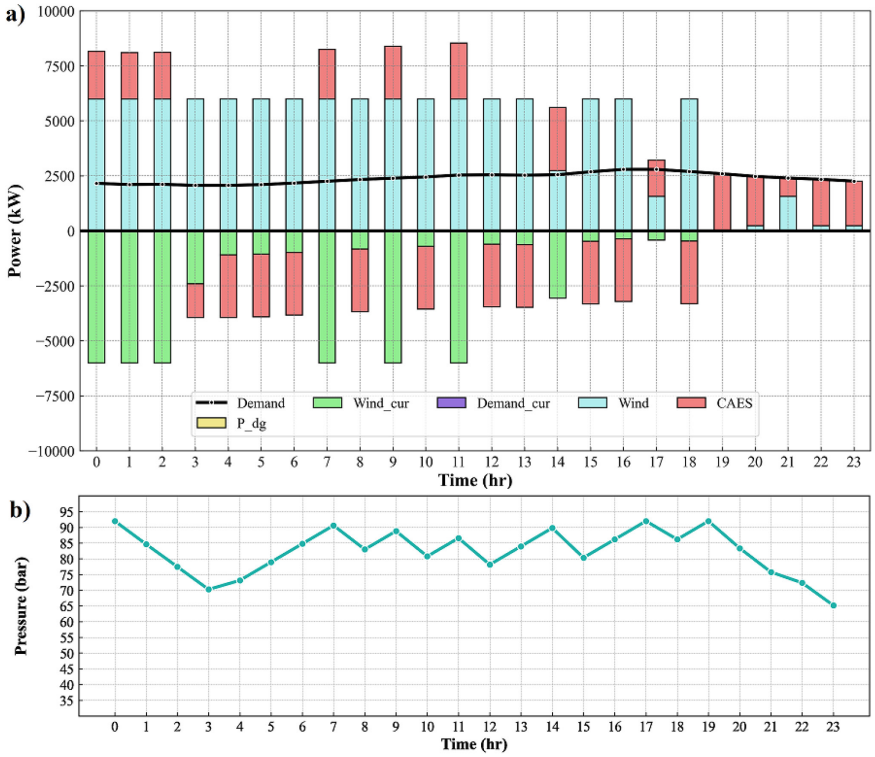

Figure 5-5: a) the scheduling result and b) the pressure variation of the air reservoir for day 2 of the dataset.

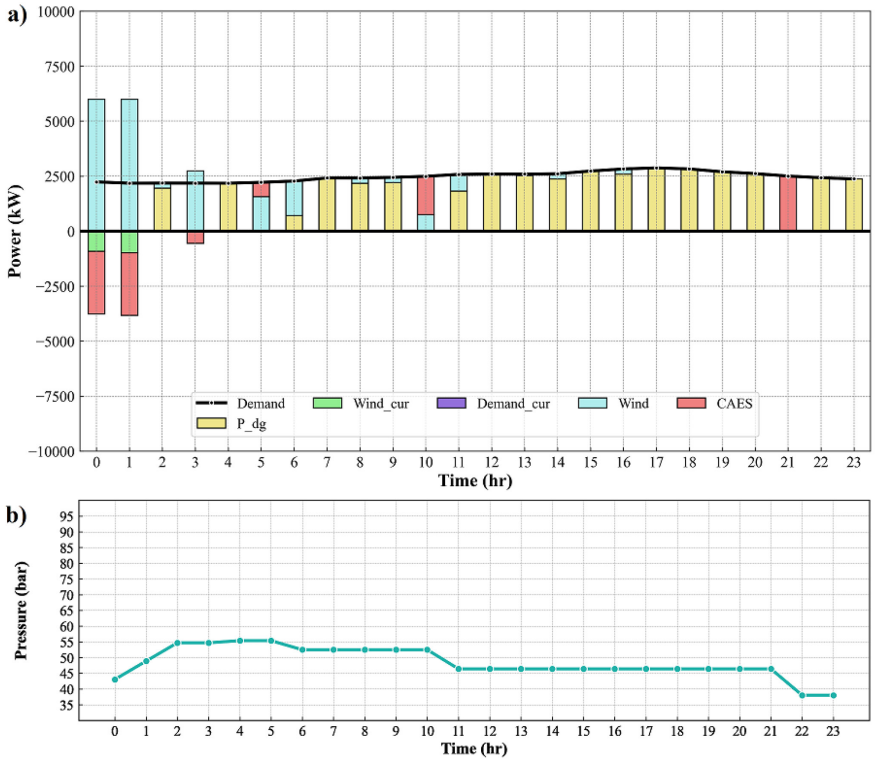

Figure 5-6: a) the scheduling result and b) the pressure variation of the air reservoir for day 4 of the dataset.

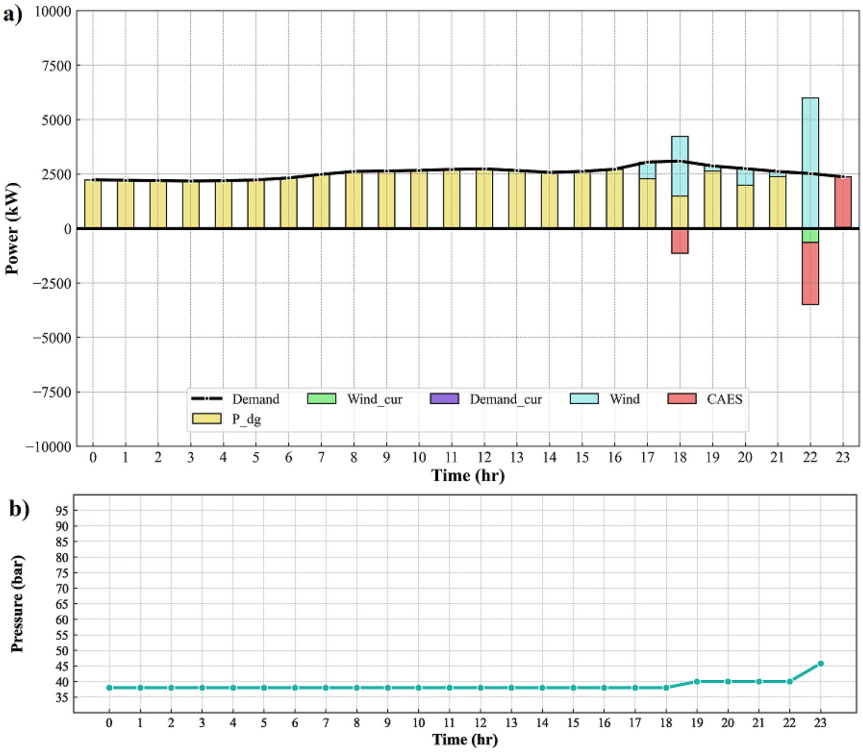

Figure 5-7: a) the scheduling result and b) the pressure variation of the air reservoir for day 56 of the dataset.

As mentioned earlier, the relationship between power and mass flow rate in both compressor and turbine is nonlinear due to partial load effects. Therefore, in each iteration, the equation is linearized based on CAES compressor and turbine in the upper level. The regression results for the compressor and turbine are shown in Figure 5-8 and Figure 5-9, respectively. These Figures provide valuable insights into the performance characteristics of the compressor and turbine and help optimize CAES system's overall efficiency. By understanding the relationship between power and mass flow rate, the optimization algorithm can better balance the energy supply and demand, minimizing the use of fossil fuels and maximizing the use of renewable energy sources. As shown in these figures, considering off-design conditions, for power rates less than the nominal capacity, higher mass flow rates are needed during discharging to provide the same amount of power output. On the other hand, in the charging process, less air is stored in the off-design conditions using the same amount of input power. Such investigations help better design and schedule the CAES system with respect to demand.

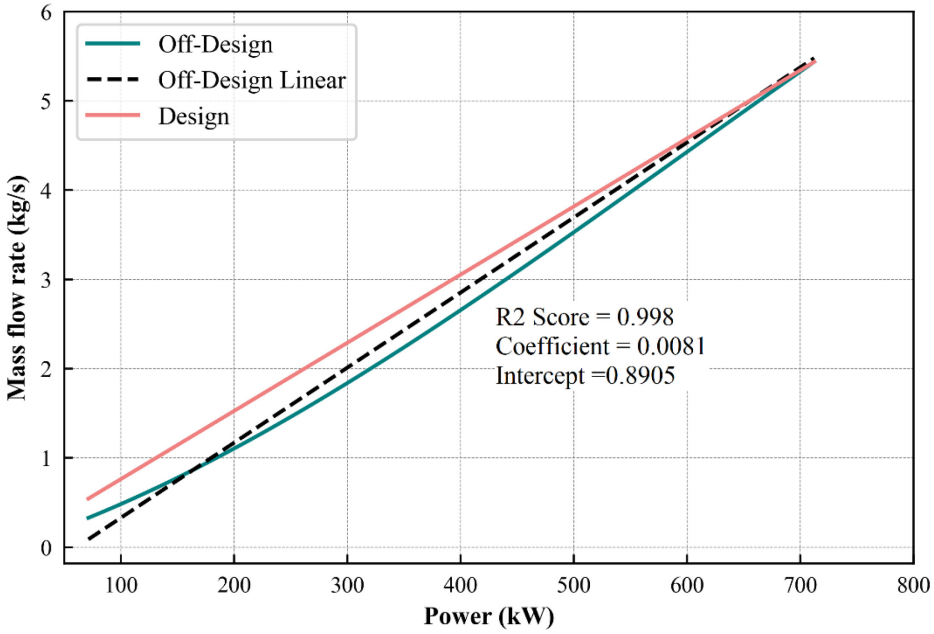

Figure 5-8: Variation of charging mass flow rate with compressor power.

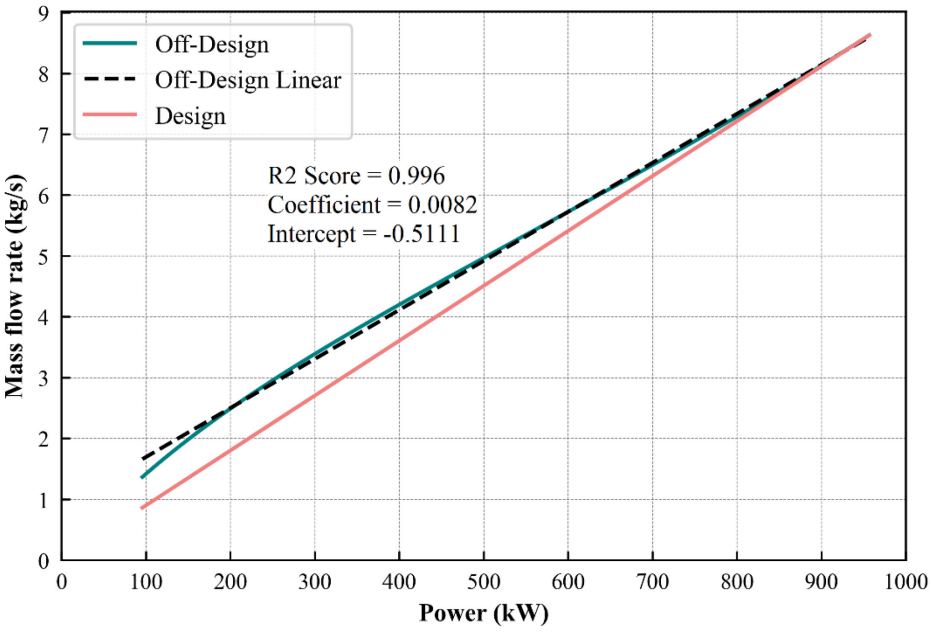

Figure 5-9: Variation of discharging mass flow rate with turbine power.

To better understand the performance of the designed CAES system, the thermodynamic properties of the system when it operates under full load condition are presented in Table 5-4. The effect of using a recuperator in the system can also be seen in the table, as the outlet temperature of the last turbine is still high at 361.76 K, entering the ambient air. This heat is recovered by the

recuperator and transferred to the compressed air stream before entering the first turbine, increasing the thermal efficiency of the system. Overall, the table shows that the designed CAES system has promising thermodynamic performance when operating at full load.

Table 5-4: Operating conditions of CAES system under full load conditions.

State	Temperature (K)	Pressure (bar)	State	Temperature (K)	Pressure (bar)
Inlet of first compressor	267	1.01	Outlet of valve	267	38
Outlet of first compressor	382.22	3.13	First outlet of recuperator	347.55	38
Inlet of second compressor	286.04	3.13	Inlet of first turbine	469.51	38
Outlet of second compressor	417.29	9.69	Outlet of first turbine	359.63	11.30
Inlet of third compressor	293.06	9.69	Inlet of second turbine	471.92	11.30
Outlet of third compressor	427.52	30	Outlet of second turbine	361.48	3.36
Inlet of fourth compressor	295.10	30	Inlet of the third turbine	472.29	3.36
Outlet of fourth compressor	430.29	92.92	Outlet of the third turbine	361.76	1.01
Inlet of the air reservoir	293.7	92.92	Second outlet of recuperator	281.21	1.01
Inlet of the valve	267	92.92			

Table 5-5 and Figure 5-10 provide a comprehensive overview of the exergy destruction in each component of the CAES system. It is evident from the results that the pressure regulating valve incurs the highest amount of exergy destruction, accounting for almost 50% of the total. This is primarily due to the significant pressure drop that occurs in this component. Furthermore, the turbines and compressors contribute 33% and 19% of the total exergy destruction, respectively. The exergy destruction associated with the recapture process is negligible compared to the other components, representing only 1.4% of the total exergy destruction. In summary, the analysis reveals that the pressure regulating valve is the primary source of exergy destruction in the CAES system. Therefore, optimizing the design and operation of this component could lead to significant improvements in the system's overall performance.

Table 5-5: Exergy destruction of CAES components.

Component	Exergy destruction (kW)
Compressors	346.91
Turbines	614.34
Pressure regulating valve	874.72
Recuperator	25.46

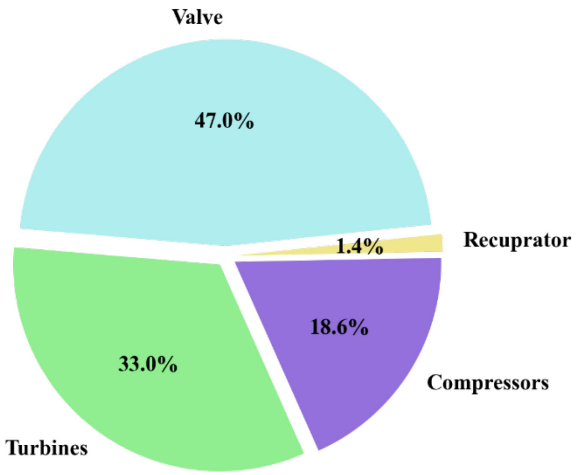

Figure 5-10: Exergy destruction share of the CAES components.

Table 5-6 provide a comparison of the scheduling results obtained by neglecting or considering the off-design conditions in the modeling of the CAES system. The analysis reveals that considering design conditions leads to lower average daily total cost, CO2 emissions, and demand curtailment. However, since the CAES system is designed to make wind energy dispatchable, it will mostly operate in partial load, off-design conditions. Therefore, relying solely on the design condition results may not be realistic. The optimization results depicted in Figure 5-11 demonstrating that when considering only design conditions CAES operates more than when the off-design conditions are considered. While design conditions may provide useful insights into the CAES system's performance, it is important to consider the system's behavior under off-design conditions as well for a realistic result.

Table 5-6: Result comparison of considering design or off-design conditions of CAES.

	Design condition	**Off-design conditions**
Average daily total cost ($)	16846.48	17396.35
Average daily CO_2 emissions (kg)	11882.33	12611.15
Demand curtailment throughout a year (kW)	1161.47	1380.97

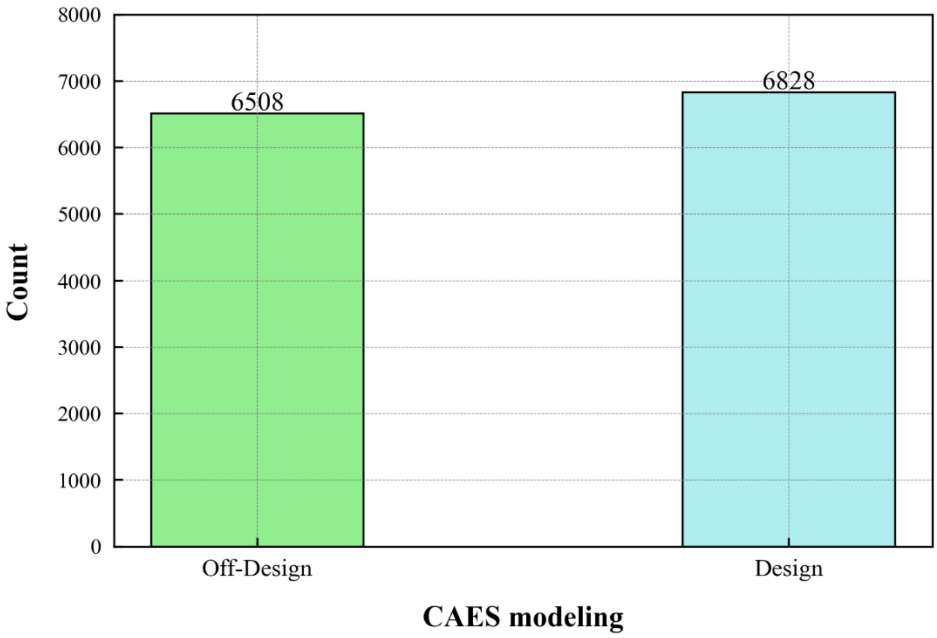

Figure 5-11: Compering the number of operating hours for design and off-design conditions.

Figure 5-12 illustrated the CAES operating power frequencies for design and off design conditions. It can be concluded from this figure that when moving towards low power requirements the CAES is less likely to operate when considering off-design conditions as it would not be efficient as the full load conditions. For instance, for the category of (-1000, -500) when considering off-design conditions the CAES system operates 227 hours, but when the off-design conditions are neglected, it would operate 291 hours in this power category. Figure 5-13 provides a comparison of the scheduling results obtained by considering and neglecting off-design conditions. As depicted in the figure, when off-design conditions are neglected, the CAES system operates in hour 2 and 3. However, when partial load conditions are taken into account, the CAES system does not operate during those hours, as it would not be efficient enough to meet the demand. the results indicate that neglecting off-design conditions can lead to overestimating the CAES system's operating hours. Therefore, it is crucial to consider the system's behavior under different operating conditions, especially in partial load scenarios, to ensure efficient and effective operation of the CAES system.

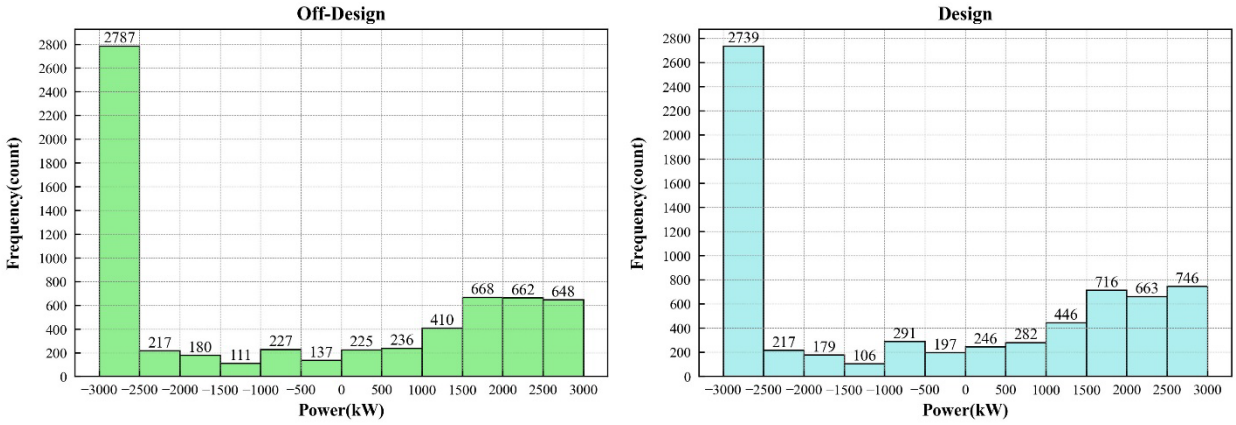

Figure 5-12: Power frequencies of CAES for off-design and design conditions.

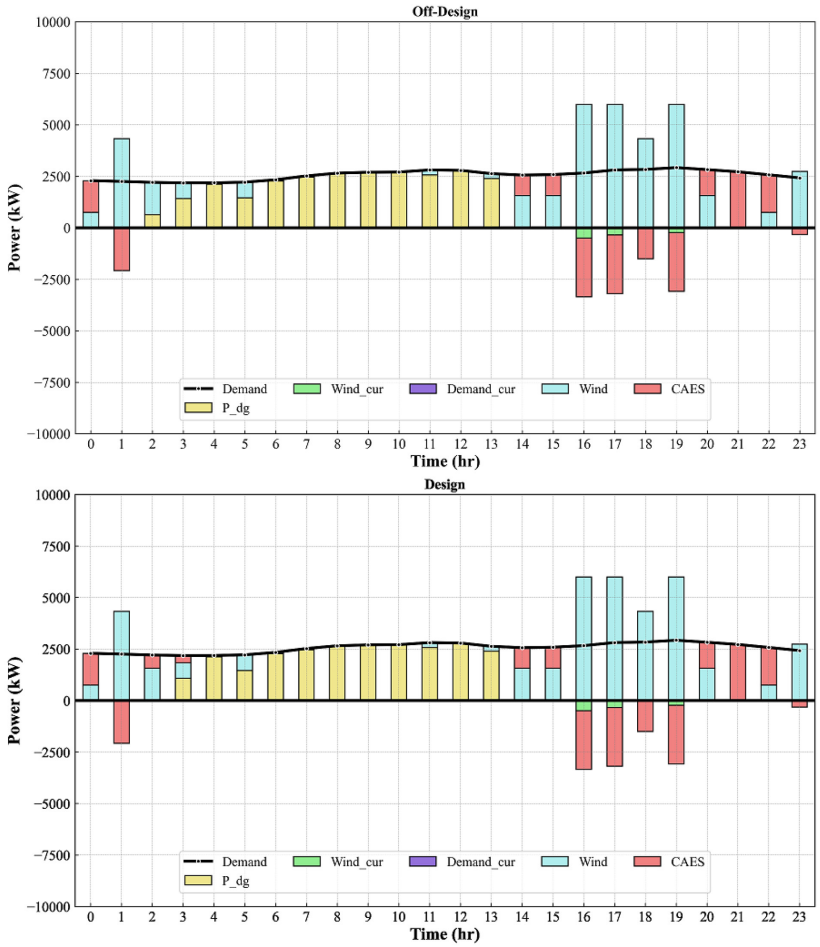

Figure 5-13: Comparison of the scheduling results for off-design and design conditions.

As shown earlier in Table 5-4 the recuperator plays a crucial role in enhancing the efficiency of the CAES system by recovering the heat from the high outlet temperature of the last turbine.

Figure 5-14 depicts the discharge power frequencies of the CAES system with and without the recuperator. The optimization results indicate that the system with recuperator discharges more frequently, typically by 24 hours, than the system without recuperator. It is worth noting that the outlet temperature is higher when the turbine operates at higher power rates, resulting in a larger amount of waste heat compared to lower power rates. As a result, the frequency difference between the two systems is more significant for power rates higher than 1500 kW. Overall, the recuperator plays a significant role in enhancing the efficiency of the CAES system by recovering waste heat, which would otherwise be lost. By taking advantage of this recovered heat, the system can operate more efficiently and discharge more frequently, making it more effective in meeting energy demands.

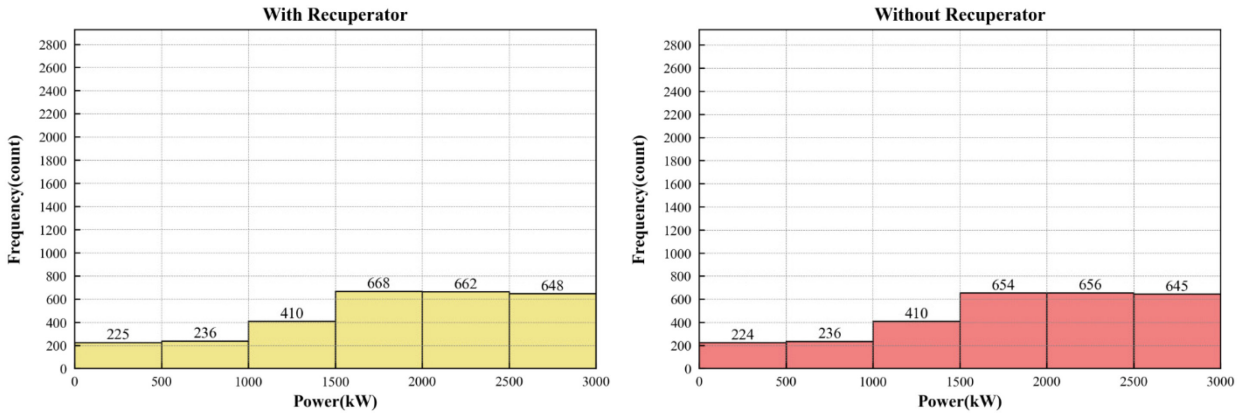

Figure 5-14: Discharge power frequencies of CAES with and without recuperator.

Figure 5-15 illustrates the effect of neglecting the off-design conditions in the design process on the operation of the system. Initially the system was designed based on the design conditions and the pressure variation throughout a year is shown in Figure 5-15. The operation results (Disel generation, wind generation, CAES charging and discharging etc. at each time step) were applied to CAES model while considering off-design conditions. As shown in this figure there would be myriads of violations in terms of minimum and maximum pressure. Because In reality, when the required power is lower than the nominal capacity of the CAES system, it operates in the off-design condition, which means it discharges more air to provide the same power as the design conditions. As the load rate decreases, the isentropic efficiency of the compressor and turbine drops, requiring the system to discharge more air to maintain the same power output and on the other hand the same amount of input power less air would be stored in the charging process. Therefore, neglecting off-design conditions during the design process could lead to pressure violations and unmet demand. In

this case study, neglecting off-design conditions resulted in 2280 hours of pressure violation, leading to significant demand curtailment. It is crucial to consider off-design conditions during the design process to ensure that the system operates efficiently and satisfies the energy demands without violating any pressure limits.

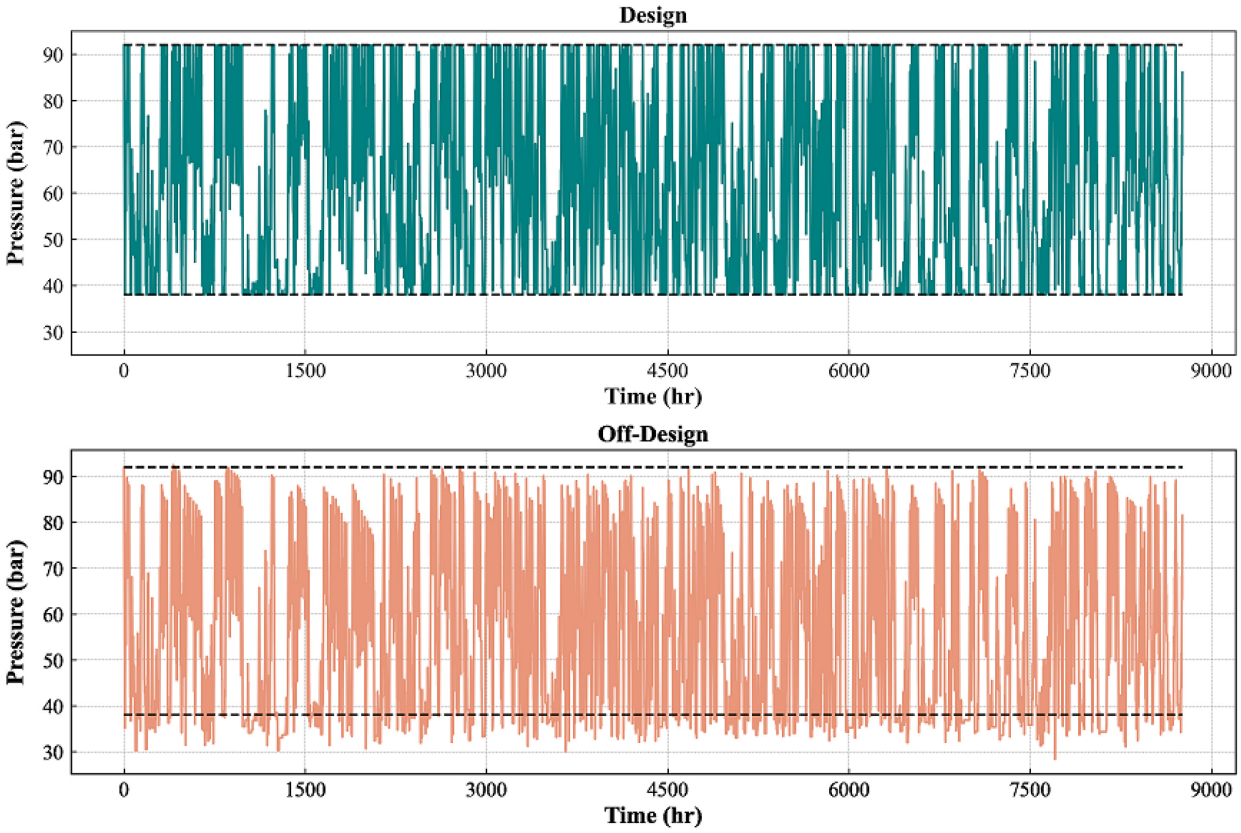

Figure 5-15: Effect of neglecting the off-design conditions in the design process on the operation of the system.

The results presented in Figure 5-16 demonstrate the impact of particle numbers and iteration numbers on the optimization process in the PSO algorithm. The figure clearly shows that as the number of particles increases, the convergence speed of the algorithm improves significantly. Moreover, increasing the particle numbers and iteration number results in a decrease in the minimum average daily cost, which drops from around 17600$ to approximately 17400$ as the particle numbers and iteration numbers increase.

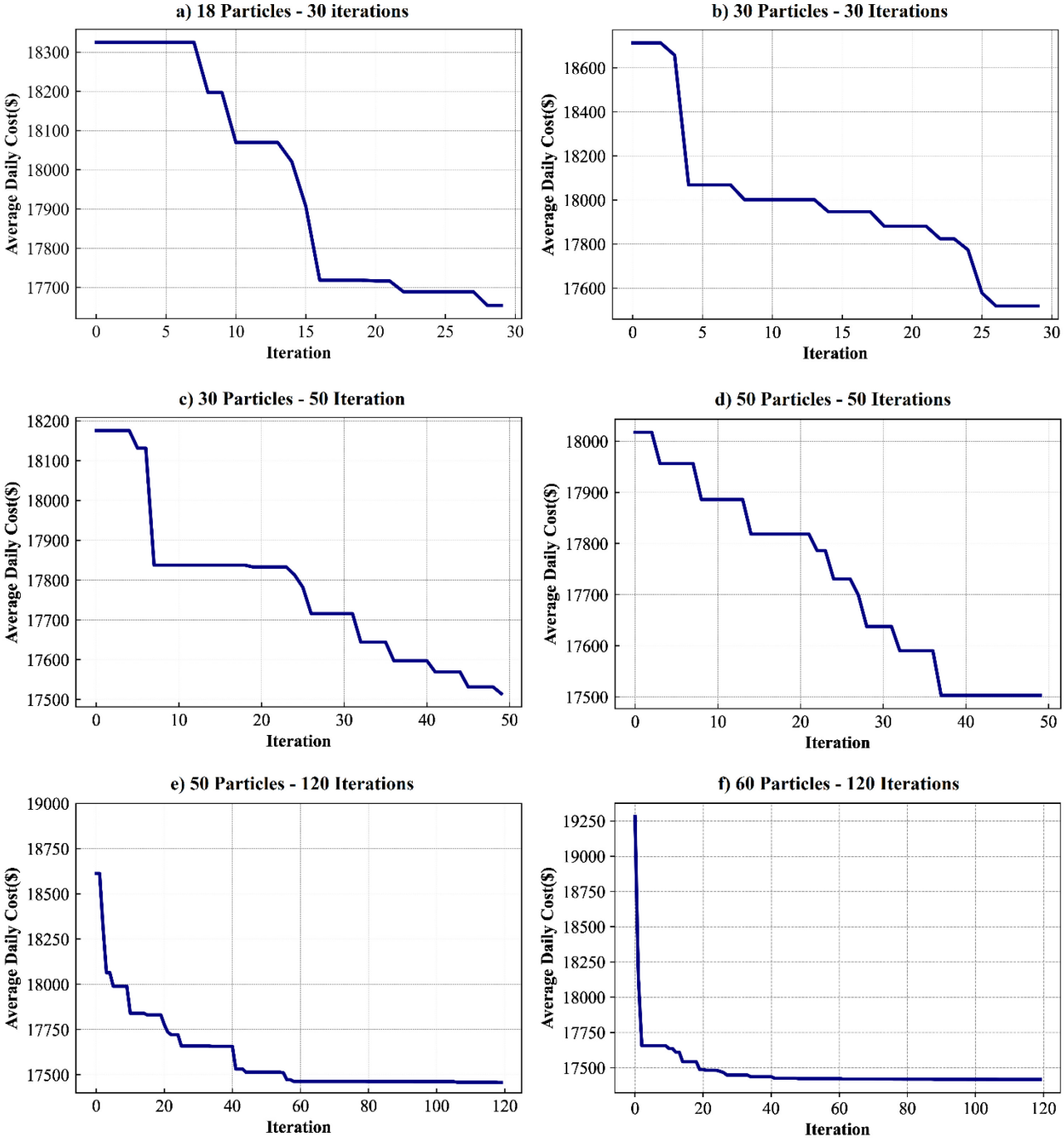

Figure 5-16: Optimization process for different particles and Iteration numbers.

Chapter 6 : Conclusions

6.1 Summary

In this thesis, a bi-level programming approach was proposed to design an energy system consisting of wind turbines, CAES, and diesel generators to meet the electricity demands of the remote community of Kuujjuaq in northern Quebec. The primary objective was to gain a deeper understanding of the mechanical modeling and performance of CAES during sizing and scheduling. A comprehensive mechanical model of the CAES system was developed, along with all necessary comments and considerations of off-design conditions when using bi-level programming for designing and scheduling. The findings indicated that the integration of CAES into the energy system reduced the reliance on diesel generators and decreased the overall operational costs. The bi-level programming approach allowed for the optimal sizing and scheduling of the energy system, resulting in a more reliable and sustainable energy supply. Overall, the thesis provided valuable insights into the application of CAES in remote communities and highlights its potential as a viable solution for meeting electricity demands in areas with limited access to traditional power sources.

6.2 Contributions

The main research contributions of this thesis can be categorized as:

(1) It was demonstrated that the utilization of an energy system incorporating wind turbines, CAES, and diesel generators in remote areas with ample wind resources could significantly decrease daily total cost and CO2 emissions compared to a system powered solely by diesel generators. The case study showed a remarkable 69% and 76% reduction in average daily total cost and CO2 emissions, respectively. The integration of CAES into the energy system allowed for efficient energy storage and utilization during periods of low wind generation, reducing the reliance on diesel generators and resulting in lower operational costs and emissions. This approach not only provides a more sustainable and environmentally friendly solution but also has economic benefits for remote communities that would otherwise face high energy costs due to reliance on diesel fuel. The thesis highlights the potential of integrating renewable energy sources, such as wind turbines, with energy storage technologies like CAES to improve the reliability, sustainability, and affordability of energy supply in remote areas while reducing environmental impacts.

(2) It was proved crucial to consider the off-design conditions of CAES during the design and scheduling phases to avoid obtaining unrealistic results. Neglecting partial load conditions in the design process, for example, can lead to lower daily total cost, CO2 emissions, and demand curtailment. However, this approach is flawed because it assumes that the system always operates at design efficiency, regardless of the power requirements. In reality, the efficiency of the compressor and turbine significantly decreases when operating below their maximum capacity. Neglecting the off-design conditions during design and scheduling can also result in increased unmet demand, reducing the reliability and performance of the energy system. This highlights the importance of accurately modeling the mechanical behavior of the CAES system, including off-design conditions, to optimize its performance and improve the overall energy system design. The thesis emphasizes the significance of considering off-design conditions in the design and scheduling of CAES systems. Neglecting these conditions can lead to unrealistic results, including lower daily total cost and CO2 emissions, increased unmet demand, and decreased overall system performance.

(3) Detailed mechanical modeling with consideration of all the required components led to a deeper understating of the design of CAES. For instance, modeling a recuperator would enhance the performance of the system as it recovers the heat from the outlet of the last turbine. Conducting an exergy analysis of the CAES system can provide insight into the system's energy losses and help identify opportunities for improvement. The analysis revealed that the valve is responsible for most of the exergy destruction in the system due to its significant pressure drop. This finding highlights the importance of selecting an appropriate valve design and optimizing its operating conditions to minimize energy losses. Detail mechanical modeling and considering all the required components can lead to a deeper understanding of the design of a mechanical system, ultimately resulting in a more efficient and effective system design.

6.3 Key assumptions and limitations

Below is a list of limitations identified as relate to the research presented in this thesis:

(1) The mechanical losses on the motor and generator side were not considered and these components are not simulated.

(2) The response time and the ramp-up and ramp-down limitations on compressor and turbine

were not considered.

(3) The investigation into the dynamic operation and temperature variability of thermal storage in the heat recovery system was not studied and the hot and cold tanks were considered at a constant temperature.

(4) All model parameters, including both cost and technical parameters, remain constant throughout the analysis and are obtained from the literature.

6.4 Future works

For future works the following avenues could be explored:

(1) Taking into account the response time of the CAES system as well as any losses that may occur on the motor and generator side. By carefully considering these factors, it is possible to gain a more complete understanding of the system's efficiency and effectiveness. This information can then be used to optimize the system's performance and identify opportunities for improvement, ultimately leading to a more reliable and cost-effective energy storage solution.

(2) It is also important to consider the dynamics of the CAES heat recovery system in the design and operation. This involves careful consideration of factors such as the heat transfer fluid, hot tank and cold tank design, and system control mechanisms. By optimizing these factors, it is possible to improve the overall efficiency and reliability of the CAES system, ultimately leading to a more sustainable and effective energy storage solution.

(3) In addition to minimizing costs, it is also important to consider other objectives such as improving the efficiency and reliability of the CAES system. By considering these additional objectives, it is possible to develop a more comprehensive and effective energy storage solution that not only minimizes costs but also maximizes performance, durability, and sustainability.

(4) Incorporating uncertainties in both demand and wind variables can improve the accuracy and reliability of design and scheduling. This will help to better account for variations and fluctuations in these parameters, resulting in more robust energy planning and management strategies.

(5) To enhance the robustness and reliability of the findings, it would be advantageous for future research to perform sensitivity analysis on the model assumptions, as well as the technical

and cost parameters used. This analysis would help evaluate the impact of variations or uncertainties in these factors on the overall results. By testing different scenarios and considering the range of potential values for these parameters, a more comprehensive understanding of the model's behavior and its implications can be gained.

References

[1] Beaugendre E, Lagrandeur J, Cheayb M, Poncet S. Integration of vortex tubes in a trigenerative compressed air energy storage system. Energy Convers Manag 2021;240. https://doi.org/10.1016/j.enconman.2021.114225.

[2] Hamilton J, Negnevitsky M, Wang X, Lyden S. High penetration renewable generation within Australian isolated and remote power systems. Energy 2019;168:684–92. https://doi.org/10.1016/j.energy.2018.11.118.

[3] Bazdar E, Sameti M, Nasiri F, Haghighat F. Compressed air energy storage in integrated energy systems: A review. Renewable and Sustainable Energy Reviews 2022;167:112701. https://doi.org/10.1016/j.rser.2022.112701.

[4] Bullough C, Gatzen C, Jakiel C, Koller M, Nowi A, Zunft S, et al. Advanced Adiabatic Compressed Air Energy Storage for the Integration of Wind Energy AA - CAES = Advanced Adiabatic - Compressed Air Energy Storage 2011:22–5.

[5] Succar S, Williams RH. NRC Staff Prefiled Hearing Exhibit NRC000040, Samir Succar & Robert H. Williams, Princeton University: Energy Systems Analysis Group, Compressed Air Energy Storage: Theory, Resources, and Applications for Wind Power (2008). 2008.

[6] Rouindej K, Samadani E, Fraser RA. A comprehensive data-driven study of electrical power grid and its implications for the design , performance , and operational requirements of adiabatic compressed air energy storage systems. Appl Energy 2020;257:113990. https://doi.org/10.1016/j.apenergy.2019.113990.

[7] Ai C, Zhang L, Gao W, Yang G, Wu D, Chen L, et al. A review of energy storage technologies in hydraulic wind turbines. Energy Convers Manag 2022;264:115584. https://doi.org/10.1016/j.enconman.2022.115584.

[8] Global Wind Report 2022 - Global Wind Energy Council n.d. https://gwec.net/global-wind-report-2022/ (accessed May 25, 2022).

[9] McCallum CS, Kumar N, Curry R, McBride K, Doran J. Renewable electricity generation for off grid remote communities; Life Cycle Assessment Study in Alaska, USA. Appl Energy 2021;299. https://doi.org/10.1016/j.apenergy.2021.117325.

[10] Fathi M, Mehrabipour A, Mahmoudi A, Mohd Zin AA bin, Ramli MAM. Optimum Hybrid Renewable Energy Systems Suitable For Remote Area. Smart Science 2019;7:147–59. https://doi.org/10.1080/23080477.2019.1600111.

[11] Remote Communities Energy Database | Natural Resources Canada n.d. https://atlas.gc.ca/rced-bdece/en/index.html (accessed January 11, 2022).

[12] of Canada G. Status of remote/off-grid communities in Canada. 2011.

[13] CER – Market Snapshot: Overcoming the challenges of powering Canada's off-grid communities n.d. https://www.cer-rec.gc.ca/en/data-analysis/energy-markets/market-snapshots/2018/market-snapshot-overcoming-challenges-powering-canadas-off-grid-communities.html (accessed January 24, 2022).

[14] Heerema D, Lovekin D. Power Shift in Remote Indigenous Communities A cross-Canada scan of diesel reduction and clean energy policies. Pembina Institute 2019.

[15] CER – Market Snapshot: Overcoming the challenges of powering Canada's off-grid communities n.d. https://www.cer-rec.gc.ca/en/data-analysis/energy-markets/market-snapshots/2018/market-snapshot-overcoming-challenges-powering-canadas-off-grid-communities.html (accessed January 2, 2022).

[16] Resources N. " Smart Grid (s)" у ЈП ЕПС -визија , циљеви и правци развоја- Дефиниције

термина Smart Grid (s) n.d.;1888:1–47.
[17] Pan-Canadian Framework on Clean Growth and Climate Change - Canada.ca n.d. https://www.canada.ca/en/services/environment/weather/climatechange/pan-canadian-framework.html (accessed January 3, 2022).
[18] Hooshangi HR. Feasibility study of wind-diesel hybrid power system for remote communities in north of Quebec. Journal for Advancement of Clean Energy 2014;1:84–95.
[19] Mitali J, Dhinakaran S, Mohamad AA. Energy storage systems: a review. Energy Storage and Saving 2022;1:166–216. https://doi.org/10.1016/j.enss.2022.07.002.
[20] Schoenung SM. SANDIA REPORT Characteristics and Technologies for Long-vs. Short-Term Energy Storage A Study by the DOE Energy Storage Systems Program. 2001.
[21] Xia T, Li Y, Zhang N, Kang C. Role of compressed air energy storage in urban integrated energy systems with increasing wind penetration. Renewable and Sustainable Energy Reviews 2022;160. https://doi.org/10.1016/j.rser.2022.112203.
[22] Tan X, Li Q, Wang H. Advances and trends of energy storage technology in Microgrid. International Journal of Electrical Power and Energy Systems 2013;44:179–91. https://doi.org/10.1016/j.ijepes.2012.07.015.
[23] Chen L, Zheng T, Mei S, Xue X, Liu B, Lu Q. Review and prospect of compressed air energy storage system. Journal of Modern Power Systems and Clean Energy 2016;4:529–41. https://doi.org/10.1007/S40565-016-0240-5.
[24] Luo X, Wang J, Dooner M, Clarke J, Krupke C. Overview of current development in compressed air energy storage technology. Energy Procedia, vol. 62, Elsevier Ltd; 2014, p. 603–11. https://doi.org/10.1016/j.egypro.2014.12.423.
[25] Alirahmi SM, Bashiri Mousavi S, Razmi AR, Ahmadi P. A comprehensive techno-economic analysis and multi-criteria optimization of a compressed air energy storage (CAES) hybridized with solar and desalination units. Energy Convers Manag 2021;236. https://doi.org/10.1016/j.enconman.2021.114053.
[26] Yu H, Engelkemier S, Gençer E. Process improvements and multi-objective optimization of compressed air energy storage (CAES) system. J Clean Prod 2022;335. https://doi.org/10.1016/j.jclepro.2021.130081.
[27] Cheayb M, Marin Gallego M, Tazerout M, Poncet S. A techno-economic analysis of small-scale trigenerative compressed air energy storage system. Energy 2022;239. https://doi.org/10.1016/j.energy.2021.121842.
[28] Olabi AG, Wilberforce T, Ramadan M, Abdelkareem MA, Alami AH. Compressed air energy storage systems: Components and operating parameters – A review. J Energy Storage 2020;34:102000. https://doi.org/10.1016/j.est.2020.102000.
[29] Zakeri B, Syri S. Electrical energy storage systems: A comparative life cycle cost analysis. Renewable and Sustainable Energy Reviews 2015;42:569–96. https://doi.org/10.1016/j.rser.2014.10.011.
[30] Ko J, Kim S, Kim S, Seo H. Utilizing building foundations as micro-scale compressed air energy storage vessel: Numerical study for mechanical feasibility. J Energy Storage 2020;28. https://doi.org/10.1016/j.est.2020.101225.
[31] King M, Jain A, Bhakar R, Mathur J, Wang J. Overview of current compressed air energy storage projects and analysis of the potential underground storage capacity in India and the UK. Renewable and Sustainable Energy Reviews 2021;139. https://doi.org/10.1016/j.rser.2021.110705.
[32] Crotogino F, Schneider GS, Evans DJ. Renewable energy storage in geological formations.

Proceedings of the Institution of Mechanical Engineers, Part A: Journal of Power and Energy 2018;232:100–14. https://doi.org/10.1177/0957650917731181.
[33] Bashiri Mousavi S, Adib M, Soltani M, Razmi AR, Nathwani J. Transient thermodynamic modeling and economic analysis of an adiabatic compressed air energy storage (A-CAES) based on cascade packed bed thermal energy storage with encapsulated phase change materials. Energy Convers Manag 2021;243:114379. https://doi.org/10.1016/j.enconman.2021.114379.
[34] Cheayb M, Marin Gallego M, Tazerout M, Poncet S. Modelling and experimental validation of a small-scale trigenerative compressed air energy storage system. Appl Energy 2019;239:1371–84. https://doi.org/10.1016/j.apenergy.2019.01.222.
[35] Briola S, di Marco P, Gabbrielli R, Riccardi J. A novel mathematical model for the performance assessment of diabatic compressed air energy storage systems including the turbomachinery characteristic curves. Appl Energy 2016;178:758–72. https://doi.org/10.1016/j.apenergy.2016.06.091.
[36] Denholm P, Kulcinski GL. Life cycle energy requirements and greenhouse gas emissions from large scale energy storage systems. Energy Convers Manag 2004;45:2153–72. https://doi.org/10.1016/j.enconman.2003.10.014.
[37] Wang J, Lu K, Ma L, Wang J, Dooner M, Miao S, et al. Overview of compressed air energy storage and technology development. Energies (Basel) 2017;10. https://doi.org/10.3390/en10070991.
[38] Budt M, Wolf D, Span R, Yan J. A review on compressed air energy storage: Basic principles, past milestones and recent developments. Appl Energy 2016;170:250–68. https://doi.org/10.1016/j.apenergy.2016.02.108.
[39] Zhao P, Lai Y, Xu W, Zhang S, Wang P, Wang J. Performance investigation of a novel near-isothermal compressed air energy storage system with stable power output. Int J Energy Res 2020;44:11135–51. https://doi.org/10.1002/er.5633.
[40] Chen H, Peng Y hang, Wang Y ling, Zhang J. Thermodynamic analysis of an open type isothermal compressed air energy storage system based on hydraulic pump/turbine and spray cooling. Energy Convers Manag 2020;204:112293. https://doi.org/10.1016/j.enconman.2019.112293.
[41] Xia T, Li Y, Zhang N, Kang C. Role of compressed air energy storage in urban integrated energy systems with increasing wind penetration. Renewable and Sustainable Energy Reviews 2022;160. https://doi.org/10.1016/j.rser.2022.112203.
[42] He W, Wang J. Optimal selection of air expansion machine in Compressed Air Energy Storage: A review. Renewable and Sustainable Energy Reviews 2018;87:77–95. https://doi.org/10.1016/j.rser.2018.01.013.
[43] Dooner M, Wang J. Compressed-air energy storage. Future Energy: Improved, Sustainable and Clean Options for Our Planet, Elsevier; 2020, p. 279–312. https://doi.org/10.1016/B978-0-08-102886-5.00014-1.
[44] Abbaspour M, Satkin M, Mohammadi-Ivatloo B, Hoseinzadeh Lotfi F, Noorollahi Y. Optimal operation scheduling of wind power integrated with compressed air energy storage (CAES). Renew Energy 2013;51:53–9. https://doi.org/10.1016/j.renene.2012.09.007.
[45] Robb D. The CAES for wind. Renewable Energy Focus 2011;12:18–9. https://doi.org/10.1016/S1755-0084(11)70014-X.
[46] Mason JE, Archer CL. Baseload electricity from wind via compressed air energy storage (CAES). Renewable and Sustainable Energy Reviews 2012;16:1099–109.

https://doi.org/10.1016/j.rser.2011.11.009.
[47] Raju M, Kumar Khaitan S. Modeling and simulation of compressed air storage in caverns: A case study of the Huntorf plant. Appl Energy 2012;89:474–81. https://doi.org/10.1016/j.apenergy.2011.08.019.
[48] Nakhamkin M, Andersson L, Swensen E, Howard J, Meyer R, Schainker R, et al. Aec 110 mw caes plant: Status of project. J Eng Gas Turbine Power 1992;114:695–700. https://doi.org/10.1115/1.2906644.
[49] Denholm P, Sioshansi R. The value of compressed air energy storage with wind in transmission-constrained electric power systems. Energy Policy 2009;37:3149–58. https://doi.org/10.1016/j.enpol.2009.04.002.
[50] Lessons from Iowa: Development of a 270 Megawatt Compressed Air Energy Storage Project in Midwest Independent System Operator | T&D World n.d. https://www.tdworld.com/grid-innovations/distribution/article/20961512/lessons-from-iowa-development-of-a-270-megawatt-compressed-air-energy-storage-project-in-midwest-independent-system-operator (accessed June 6, 2022).
[51] Crotogino F, Mohmeyer KU, Scharf R, On Kraftwerke E. Huntorf CAES: More than 20 Years Huntorf CAES: More than 20 Years of Successful Op of Successful Operation eration Huntorf CAES: More than 20 Years of Successful Operation. 2001.
[52] Guo C, Xu Y, Zhang X, Guo H, Zhou X, Liu C, et al. Performance Analysis of Compressed Air Energy Storage Systems Considering Dynamic Characteristics of Compressed Air Storage. Energy 2017. https://doi.org/10.1016/j.energy.2017.06.145.
[53] Satkin M, Noorollahi Y, Abbaspour M, Yousefi H. Multi criteria site selection model for wind-compressed air energy storage power plants in Iran. Renewable and Sustainable Energy Reviews 2014;32:579–90. https://doi.org/10.1016/j.rser.2014.01.054.
[54] He W, Dooner M, King M, Li D, Guo S, Wang J. Techno-economic analysis of bulk-scale compressed air energy storage in power system decarbonisation. Appl Energy 2021;282:116097. https://doi.org/10.1016/j.apenergy.2020.116097.
[55] Tong Z, Cheng Z, Tong S. A review on the development of compressed air energy storage in China: Technical and economic challenges to commercialization. Renewable and Sustainable Energy Reviews 2021;135:110178. https://doi.org/10.1016/j.rser.2020.110178.
[56] Aghahosseini A, Breyer C. Assessment of geological resource potential for compressed air energy storage in global electricity supply. Energy Convers Manag 2018;169:161–73. https://doi.org/10.1016/j.enconman.2018.05.058.
[57] Denholm P, Sioshansi R. The value of compressed air energy storage with wind in transmission-constrained electric power systems. Energy Policy 2009;37:3149–58. https://doi.org/10.1016/j.enpol.2009.04.002.
[58] Mauch B, Carvalho PMS, Apt J. Can a wind farm with CAES survive in the day-ahead market? Energy Policy 2012;48:584–93. https://doi.org/10.1016/j.enpol.2012.05.061.
[59] Fertig E, Apt J. Economics of compressed air energy storage to integrate wind power: A case study in ERCOT. Energy Policy 2011;39:2330–42. https://doi.org/10.1016/j.enpol.2011.01.049.
[60] Madlener R, Latz J. Economics of centralized and decentralized compressed air energy storage for enhanced grid integration of wind power. Appl Energy 2013;101:299–309. https://doi.org/10.1016/j.apenergy.2011.09.033.
[61] Cleary B, Duffy A, O'Connor A, Conlon M, Fthenakis V. Assessing the economic benefits of compressed air energy storage for mitigating wind curtailment. IEEE Trans Sustain Energy

2015;6:1021–8. https://doi.org/10.1109/TSTE.2014.2376698.
[62] Swider DJ. Compressed air energy storage in an electricity system with significant wind power generation. IEEE Transactions on Energy Conversion 2007;22:95–102. https://doi.org/10.1109/TEC.2006.889547.
[63] Safaei H, Keith DW. Compressed air energy storage with waste heat export: An Alberta case study. Energy Convers Manag 2014;78:114–24. https://doi.org/10.1016/j.enconman.2013.10.043.
[64] Luo X, Dooner M, He W, Wang J, Li Y, Li D, et al. Feasibility study of a simulation software tool development for dynamic modelling and transient control of adiabatic compressed air energy storage with its electrical power system applications. Appl Energy 2018;228:1198–219. https://doi.org/10.1016/j.apenergy.2018.06.068.
[65] Razmi A, Soltani M, Tayefeh M, Torabi M, Dusseault MB. Thermodynamic analysis of compressed air energy storage (CAES) hybridized with a multi-e ff ect desalination (MED) system. Energy Convers Manag 2019;199:112047. https://doi.org/10.1016/j.enconman.2019.112047.
[66] Kim YM, Shin DG, Favrat D. Operating characteristics of constant-pressure compressed air energy storage (CAES) system combined with pumped hydro storage based on energy and exergy analysis. Energy 2011;36:6220–33. https://doi.org/10.1016/j.energy.2011.07.040.
[67] Razmi A, Soltani M, Aghanajafi C, Torabi M. Thermodynamic and economic investigation of a novel integration of the absorption-recompression refrigeration system with compressed air energy storage (CAES). Energy Convers Manag 2019;187:262–73. https://doi.org/10.1016/j.enconman.2019.03.010.
[68] Najjar YSH, Zaamout MS. PERFORMANCE ANALYSIS OF COMPRESSED AIR ENERGY STORAGE (CAES) PLANT FOR DRY REGIONS 1998;39:1503–11.
[69] Sadreddini A, Fani M, Ashjari Aghdam M, Mohammadi A. Exergy analysis and optimization of a CCHP system composed of compressed air energy storage system and ORC cycle. Energy Convers Manag 2018;157:111–22. https://doi.org/10.1016/j.enconman.2017.11.055.
[70] Razmi A, Soltani M, Torabi M. Investigation of an e ffi cient and environmentally-friendly CCHP system based on CAES , ORC and compression-absorption refrigeration cycle : Energy and exergy analysis. Energy Convers Manag 2019;195:1199–211. https://doi.org/10.1016/j.enconman.2019.05.065.
[71] Gayathri Venkataramani and Velraj Ramalingam. Energy and Exergy analysis of Isothermal compressed air energy storage system. Encyclopaedia of Energy Storage 2022;1:215–31.
[72] Razmi AR, Soltani M, Ardehali A, Gharali K, Dusseault MB, Nathwani J. Design, thermodynamic, and wind assessments of a compressed air energy storage (CAES) integrated with two adjacent wind farms: A case study at Abhar and Kahak sites, Iran. Energy 2021;221:119902. https://doi.org/10.1016/j.energy.2021.119902.
[73] Ghorbani B, Mehrpooya M, Ardehali A. Energy and exergy analysis of wind farm integrated with compressed air energy storage using multi-stage phase change material. J Clean Prod 2020;259:120906. https://doi.org/10.1016/j.jclepro.2020.120906.
[74] Mohammadi A, Ahmadi MH, Bidi M, Joda F, Valero A, Uson S. Exergy analysis of a Combined Cooling, Heating and Power system integrated with wind turbine and compressed air energy storage system. Energy Convers Manag 2017;131:69–78. https://doi.org/10.1016/j.enconman.2016.11.003.
[75] Chen J, Liu W, Jiang D, Zhang J, Ren S, Li L, et al. Preliminary investigation on the feasibility of a clean CAES system coupled with wind and solar energy in China. Energy

2017;127:462–78. https://doi.org/10.1016/j.energy.2017.03.088.
[76] Yang Z, Wang Z, Ran P, Li Z, Ni W. Thermodynamic analysis of a hybrid thermal-compressed air energy storage system for the integration of wind power. Appl Therm Eng 2014;66:519–27. https://doi.org/10.1016/j.applthermaleng.2014.02.043.
[77] Li Y, Miao S, Luo X, Yin B, Han J, Wang J. Dynamic modelling and techno-economic analysis of adiabatic compressed air energy storage for emergency back-up power in supporting microgrid. Appl Energy 2020;261:114448. https://doi.org/10.1016/j.apenergy.2019.114448.
[78] Zhang X, Qin C (Chris) C, Xu Y, Li W, Zhou X, Li R, et al. Integration of small-scale compressed air energy storage with wind generation for flexible household power supply. J Energy Storage 2021;37. https://doi.org/10.1016/j.est.2021.102430.
[79] Jin H, Liu P, Li Z. Dynamic modeling and design of a hybrid compressed air energy storage and wind turbine system for wind power fluctuation reduction. Comput Chem Eng 2019;122:59–65. https://doi.org/10.1016/j.compchemeng.2018.05.023.
[80] Das T, Krishnan V, Gu Y, McCalley JD. Compressed air energy storage: State space modeling and performance analysis. IEEE Power and Energy Society General Meeting 2011:1–8. https://doi.org/10.1109/PES.2011.6039712.
[81] Marano V, Rizzo G, Antonio F. Application of dynamic programming to the optimal management of a hybrid power plant with wind turbines , photovoltaic panels and compressed air energy storage 2012;97:849–59. https://doi.org/10.1016/j.apenergy.2011.12.086.
[82] Wang SY, Yu JL. Optimal sizing of the CAES system in a power system with high wind power penetration. International Journal of Electrical Power and Energy Systems 2012;37:117–25. https://doi.org/10.1016/j.ijepes.2011.12.015.
[83] Zhang J, Li KJ, Wang M, Lee WJ, Gao H, Zhang C, et al. A Bi-Level Program for the Planning of an Islanded Microgrid Including CAES. IEEE Trans Ind Appl 2016;52:2768–77. https://doi.org/10.1109/TIA.2016.2539246.
[84] Xu X, Hu W, Cao D, Huang Q, Liu W, Liu Z, et al. Designing a standalone wind-diesel-CAES hybrid energy system by using a scenario-based bi-level programming method. Energy Convers Manag 2020;211:112759. https://doi.org/10.1016/j.enconman.2020.112759.
[85] Akbari E, Hooshmand RA, Gholipour M, Parastegari M. Stochastic programming-based optimal bidding of compressed air energy storage with wind and thermal generation units in energy and reserve markets. Energy 2019;171:535–46. https://doi.org/10.1016/j.energy.2019.01.014.
[86] Bai J, Wei W, Chen L, Mei S. Rolling-horizon dispatch of advanced adiabatic compressed air energy storage based energy hub via data-driven stochastic dynamic programming. Energy Convers Manag 2021;243:114322. https://doi.org/10.1016/j.enconman.2021.114322.
[87] Bai J, Wei W, Xue X, Mei S. Scheduling of AA-CAES Based Energy Hub with Wind Power Generation: A Multi-stage Robust Optimization Approach. Chinese Control Conference, CCC 2021;2021-July:1681–6. https://doi.org/10.23919/CCC52363.2021.9550739.
[88] Bracken J, McGill JT. Mathematical Programs with Optimization Problems in the Constraints. Https://DoiOrg/101287/Opre21137 1973;21:37–44. https://doi.org/10.1287/OPRE.21.1.37.
[89] Yin B, Li Y, Miao S, Lin Y, Zhao H. An economy and reliability co-optimization planning method of adiabatic compressed air energy storage for urban integrated energy system. J Energy Storage 2021;40:102691. https://doi.org/10.1016/j.est.2021.102691.
[90] Li K, Wei X, Yan Y, Zhang C. Bi-level optimization design strategy for compressed air

energy storage of a combined cooling, heating, and power system. J Energy Storage 2020;31. https://doi.org/10.1016/j.est.2020.101642.
[91] Tiwari S, Gupta N. Weibull parameter estimation for wind energy at different elevations using graphical method. International Journal of Scientific and Technology Research 2019;8:2921–5.
[92] Aghbalou N, Charki A, Elazzouzi SR, Reklaoui K. A probabilistic assessment approach for wind turbine-site matching. International Journal of Electrical Power and Energy Systems 2018;103:497–510. https://doi.org/10.1016/j.ijepes.2018.06.018.
[93] Borowy BS, Salameh ZM. Methodology for Optimally Sizing the Combination of a Battery Bank and PV Array in a Wind/PV Hybrid System. vol. 11. 1996.
[94] Design Considerations with Respect to Long-Term Diesel Saving in Wind/Diesel Plants Author(s): Øyvin Skarstein and Kjetil Uhlen Source: Wind Engineering. n.d.
[95] Tola V, Meloni V, Spadaccini F, Cau G. Performance assessment of Adiabatic Compressed Air Energy Storage (A-CAES) power plants integrated with packed-bed thermocline storage systems. Energy Convers Manag 2017;151:343–56. https://doi.org/10.1016/j.enconman.2017.08.051.
[96] Zhang X, Zeng R, Deng Q, Gu X, Liu H, He Y, et al. Energy, exergy and economic analysis of biomass and geothermal energy based CCHP system integrated with compressed air energy storage (CAES). Energy Convers Manag 2019;199:111953. https://doi.org/10.1016/j.enconman.2019.111953.
[97] Razmi A, Soltani M, Aghanaja C, Torabi M. Thermodynamic and economic investigation of a novel integration of the absorption-recompression refrigeration system with compressed air energy storage (CAES) 2019;187:262–73. https://doi.org/10.1016/j.enconman.2019.03.010.
[98] Zhao P, Wang J, Dai Y. Thermodynamic analysis of an integrated energy system based on compressed air energy storage (CAES) system and Kalina cycle. Energy Convers Manag 2015;98:161–72. https://doi.org/10.1016/j.enconman.2015.03.094.
[99] Meng H, Wang M, Olumayegun O, Luo X, Liu X. Process design, operation and economic evaluation of compressed air energy storage (CAES) for wind power through modelling and simulation. Renew Energy 2019;136:923–36. https://doi.org/10.1016/j.renene.2019.01.043.
[100] Soltani M, Nabat MH, Razmi AR, Dusseault MB, Nathwani J. A comparative study between ORC and Kalina based waste heat recovery cycles applied to a green compressed air energy storage (CAES) system. Energy Convers Manag 2020;222:113203. https://doi.org/10.1016/j.enconman.2020.113203.
[101] Nami H, Mahmoudi SMS, Nemati A. Exergy, economic and environmental impact assessment and optimization of a novel cogeneration system including a gas turbine, a supercritical CO2 and an organic Rankine cycle (GT-HRSG/SCO2). Appl Therm Eng 2017;110:1315–30. https://doi.org/10.1016/j.applthermaleng.2016.08.197.
[102] Mohammadi A, Ahmadi MH, Bidi M, Joda F, Valero A, Uson S. Exergy analysis of a Combined Cooling , Heating and Power system integrated with wind turbine and compressed air energy storage system. Energy Convers Manag 2016. https://doi.org/10.1016/j.enconman.2016.11.003.
[103] Daneshvar Garmroodi A, Nasiri F, Haghighat F. Optimal dispatch of an energy hub with compressed air energy storage: A safe reinforcement learning approach. J Energy Storage 2023;57. https://doi.org/10.1016/j.est.2022.106147.
[104] Yang K, Zhang Y, Li X, Xu J. Theoretical evaluation on the impact of heat exchanger in Advanced Adiabatic Compressed Air Energy Storage system. Energy Convers Manag

2014;86:1031–44. https://doi.org/10.1016/j.enconman.2014.06.062.
[105] Diyoke C, Wu C. Thermodynamic analysis of hybrid adiabatic compressed air energy storage system and biomass gasification storage (A-CAES + BMGS) power system. Fuel 2020;271:117572. https://doi.org/10.1016/j.fuel.2020.117572.
[106] Sadeghi S, Askari IB. Prefeasibility techno-economic assessment of a hybrid power plant with photovoltaic, fuel cell and Compressed Air Energy Storage (CAES). Energy 2018. https://doi.org/10.1016/j.energy.2018.11.108.
[107] Hossein M, Zeynalian M, Reza A, Arabkoohsar A, Soltani M. Energy , exergy , and economic analyses of an innovative energy storage system ; liquid air energy storage (LAES) combined with high-temperature thermal energy storage (HTES). Energy Convers Manag 2020;226:113486. https://doi.org/10.1016/j.enconman.2020.113486.
[108] Kim YM, Lee JH, Kim SJ, Favrat D. Potential and evolution of compressed air energy storage: Energy and exergy analyses. Entropy 2012;14:1501–21. https://doi.org/10.3390/e14081501.
[109] Kim YM, Favrat D. Energy and exergy analysis of a micro-compressed air energy storage and air cycle heating and cooling system. Energy 2010;35:213–20. https://doi.org/10.1016/j.energy.2009.09.011.
[110] Sadreddini A, Fani M, Ashjari Aghdam M, Mohammadi A. Exergy analysis and optimization of a CCHP system composed of compressed air energy storage system and ORC cycle. Energy Convers Manag 2018;157:111–22. https://doi.org/10.1016/j.enconman.2017.11.055.
[111] Han Z, Guo S. Investigation of operation strategy of combined cooling, heating and power(CCHP) system based on advanced adiabatic compressed air energy storage. Energy 2018;160:290–308. https://doi.org/10.1016/j.energy.2018.07.033.
[112] Karapekmez A, Dincer I, Javani N. Development of a new integrated energy system with compressed air and heat storage options. J Energy Storage 2020;32:101955. https://doi.org/10.1016/j.est.2020.101955.
[113] Wang Z, Xiong W, Ting DSK, Carriveau R, Wang Z. Conventional and advanced exergy analyses of an underwater compressed air energy storage system. Appl Energy 2016;180:810–22. https://doi.org/10.1016/j.apenergy.2016.08.014.
[114] Szablowski L, Krawczyk P, Badyda K, Karellas S, Kakaras E, Bujalski W. Energy and exergy analysis of adiabatic compressed air energy storage system. Energy 2017;138:12–8. https://doi.org/10.1016/j.energy.2017.07.055.
[115] Fournier M. Daily load profiles clustering: a powerful tool for demand side management in medium-sized industries. 2017.
[116] Zhang T, Zhang G, Lu J, Feng X, Yang W. A new index and classification approach for load pattern analysis of large electricity customers. IEEE Transactions on Power Systems 2012;27:153–60. https://doi.org/10.1109/TPWRS.2011.2167524.
[117] Azad SA, Ali ABMS, Wolfs P. Identification of typical load profiles using K-means clustering algorithm. Asia-Pacific World Congress on Computer Science and Engineering, APWC on CSE 2014, Institute of Electrical and Electronics Engineers Inc.; 2014. https://doi.org/10.1109/APWCCSE.2014.7053855.
[118] Wang D, Tan D, Liu L. Particle swarm optimization algorithm: an overview. Soft Comput 2018;22:387–408. https://doi.org/10.1007/s00500-016-2474-6.
[119] Du K-L, Swamy MNS. Search and Optimization by Metaheuristics Techniques and Algorithms Inspired by Nature. n.d.
[120] Su B, Xie N, Yang Y. Hybrid genetic algorithm based on bin packing strategy for the

unrelated parallel workgroup scheduling problem. J Intell Manuf 2021;32:957–69. https://doi.org/10.1007/s10845-020-01597-8.
[121] Eberhart RC, Shi Y. Tracking and optimizing dynamic systems with particle swarms. Proceedings of the IEEE Conference on Evolutionary Computation, ICEC, vol. 1, 2001, p. 94–100. https://doi.org/10.1109/cec.2001.934376.
[122] Electricity facts n.d. https://www.nrcan.gc.ca/science-and-data/data-and-analysis/energy-data-and-analysis/energy-facts/electricity-facts/20068 (accessed August 16, 2021).
[123] Nunavik wants to join Quebec power grid: Plan Nunavik | Nunatsiaq News n.d. https://nunatsiaq.com/stories/article/20889_nunavik_wants_to_join_quebecs_power_grid/ (accessed October 4, 2021).
[124] Status of Remote/Off-Grid Communities in Canada n.d. https://www.nrcan.gc.ca/energy/publications/sciences-technology/renewable/smart-grid/11916 (accessed August 16, 2021).
[125] Canada Invests in Wind Energy to Reduce Diesel in Northern Quebec n.d. https://www.newswire.ca/news-releases/canada-invests-in-wind-energy-to-reduce-diesel-in-northern-quebec-871089197.html (accessed August 16, 2021).
[126] Weather Dashboard for Kuujjuaq n.d. https://kuujjuaq.weatherstats.ca/ (accessed September 25, 2021).
[127] Hossain M, Mekhilef S, Olatomiwa L. Performance evaluation of a stand-alone PV-wind-diesel-battery hybrid system feasible for a large resort center in South China Sea, Malaysia. Sustain Cities Soc 2017;28:358–66. https://doi.org/10.1016/j.scs.2016.10.008.
[128] Wang H, Zhang C, Li K, Ma X. Game theory-based multi-agent capacity optimization for integrated energy systems with compressed air energy storage. Energy 2021;221. https://doi.org/10.1016/j.energy.2021.119777.
[129] Jiang R, Cai Z, Peng K, Yang M. Thermo-economic analysis and multi-objective optimization of polygeneration system based on advanced adiabatic compressed air energy storage system. Energy Convers Manag 2021;229. https://doi.org/10.1016/j.enconman.2020.113724.
[130] Giordano N, Kanzari I, Miranda MM, Dezayes C, Raymond J. Underground thermal energy storage in subarctic climates: a feasibility study conducted in Kuujjuaq (QC, Canada). n.d.

Appendix: Python codes

Wind turbine model:

In [4]:
```
def speed_limit(v):
    if (v<v_ci) or (v>v_co):
        return 0
    elif (v_r<=v<=v_co):
        return P_r_wt
    else:
        return ((v**3-v_ci**3)/(v_r**3-v_ci**3))*P_r_wt
```

CAES model:

In [9]:
```
class CAES(object):

    def eta_c (self,a):

        a1 =  4.6948804252492010e+001
        a2 =  5.9916135114652325e-001
        a3 = -2.3775603099293894e-003

        eta_c = a1 + a2 * (a) + a3 * (a**2)
        return (eta_c/100)

    def eta_t (self,a):
        a1 = 4.1390729581326283e+001
        a2 = 8.6154009677822008e-001
        a3 = -5.7158107778840558e-003
        a4 = 9.5398673887267854e-006

        eta_t = a1 + a2 * (a) + a3 * (a**2) + a4 * (a**3)
        return (eta_t/100)

    def __init__ (self,P_tank,V_tank,T_tank,p_min,p_max,P_ch_max,P_dch_max,N,M):

        self.T_tank = T_tank
        self.p_min = p_min
        self.p_max = p_max
        self.P_ch_max = P_ch_max
        self.P_dch_max = P_dch_max
        self.N = N
        self.M = M
        self.rc = self.p_max **(1/N)
        self.rt = self.p_min **(1/M)
        self.P_tank = P_tank
        self.V_tank = V_tank
        self.Density = (self.P_tank*100000)/((self.T_tank)*self.R)
        self.mass = self.Density * self.V_tank
        self.SOC = (self.P_tank-self.p_min)/(self.p_max - self.p_min)

    def Charge(self,P_ch):
        eff=0.85
        self.time_step = 3600
        partial_load = P_ch/self.P_ch_max * 100
        P_c = np.arange(2*self.N + 1, dtype=float) * 0
        P_c[0] = self.P0

        self.T_c = np.arange(2*self.N + 1, dtype=float) * 0
        self.T_c[0] = self.T0

        self.To_out_c = np.arange(self.N)*0

        for n in range(self.N):
            P_c[2*n+1] = P_c[2*n]*self.rc
            P_c[2*n+2] = P_c[2*n+1]

            self.T_c[2*n+1] = self.T_c[2*n]*(1+((self.rc**((self.k-1)/self.k)-1)/self.eta_c(partial_load)))
            self.T_c[2*n+2] = (1-eff)* self.T_c[2*n+1]+eff*self.T0

            self.To_out_c[n] = (self.T_c[2*n+1]-self.T_c[2*n+2])+self.T0

        sum_delta_T_c = 0
```

```
        sum_delta_T_c = 0
        for n in range(self.N):
            sum_delta_T_c += (self.T_c[2*n+1] - self.T_c[2*n])

        self.m_dot_charge = (P_ch*self.N) / (self.cp * sum_delta_T_c)
        self.Q_c=self.cp*self.m_dot_charge*(self.T_c[1]-self.T_c[2])
        self.A_c=self.Q_c/(self.To_out_c[0]-self.T0)
        self.mass += (self.m_dot_charge * self.time_step)
        self.Density = (self.mass/self.V_tank)
        self.P_tank = (self.Density * self.T_tank *287 /100000)
        self.SOC = (self.P_tank-self.p_min)/(self.p_max - self.p_min)

        return (self.m_dot_charge)

    def Discharge(self,P_dch):
        eff=0.85
        self.T_history = []
        self.P_history = []
        n = 2
        self.time_step = n*60
        partial_load = P_dch/self.P_dch_max * 100

        for i in range(int(60/n)):
            if i==0:
                self.P_t = np.arange(2*self.M + 4, dtype=float) * 0
                self.P_t[0] = self.P_tank
                self.P_t[1] = self.p_min
                self.P_t[2] = self.P_t[1]

                self.T_t = np.arange(2*self.M +4, dtype=float) * 0
                self.T_t[0] = self.T_tank
                self.T_t[1] = self.T_tank
                self.T_t[2] = self.T_t[1]

                self.To_out_t = np.arange(self.M)*0


                for m in range(self.M):
                    self.P_t[2*m+3] = self.P_t[2*m+2]
                    self.P_t[2*m+4] = self.P_t[2*m+3]/self.rt

                    self.T_t[2*m+3] = (1-eff)* self.T_t[2*m+2]+eff*self.T_hot
                    self.T_t[2*m+4] = self.T_t[2*m+3]*(1-(self.eta_t(partial_load)*(1 - self.rt**((self.k-1)/self.k))))

                    self.To_out_t[m] = +self.T_hot-(self.T_t[2*m+3]-self.T_t[2*m+2])

                self.sum_delta_T_t = 0
                self.T_rec_in = self.T_t[2*self.M + 2]
                self.T_t[2*self.M+3] = self.T_rec_in

                for m in range(self.M+1):
                    if m>=1:
                        self.sum_delta_T_t += (self.T_t[2*m+1] - self.T_t[2*m+2])


                self.m_dot_discharge = (P_dch*self.M)/ (self.cp * self.sum_delta_T_t)
                self.mass -= (self.m_dot_discharge * self.time_step)
                self.Density = (self.mass/self.V_tank)
                self.P_tank = (self.Density * self.T_tank *287 /100000)
                self.SOC = (self.P_tank-self.p_min)/(self.p_max - self.p_min)
```

```
                self.SOC = (self.P_tank-self.p_min)/(self.p_max - self.p_min)

                self.T_history.append(self.T_t)
                self.P_history.append(self.P_t)

            else:

                self.P_t = np.arange(2*self.M + 4, dtype=float) * 0
                self.P_t[0] = self.P_tank
                self.P_t[1] = self.p_min
                self.P_t[2] = self.P_t[1]

                self.T_t = np.arange(2*self.M +4, dtype=float) * 0
                self.T_t[0] = self.T_tank
                self.T_t[1] = self.T_tank
                self.T_t[2] = (1-self.eff)* self.T_t[1]+self.eff*self.T_rec_in


                for m in range(self.M):
                    self.P_t[2*m+3] = self.P_t[2*m+2]
                    self.P_t[2*m+4] = self.P_t[2*m+3]/self.rt

                    self.T_t[2*m+3] = (1-eff)* self.T_t[2*m+2]+eff*self.T_hot
                    self.T_t[2*m+4] = self.T_t[2*m+3]*(1-(self.eta_t(partial_load)*(1 - self.rt**((1-self.k)/self.k))))

                    self.To_out_t[m] = self.T_hot-(self.T_t[2*m+3]-self.T_t[2*m+2])

                self.delta_T_t = 0
                self.T_rec_in = self.T_t[2*self.M + 2]
                self.T_t[2*self.M+3] = (1-self.eff)* self.T_rec_in + self.eff*self.T_t[0]


                self.sum_delta_T_t = 0
                for m in range(self.M+1):
                    if m>=1:
                        self.sum_delta_T_t += (self.T_t[2*m+1] - self.T_t[2*m+2])


                self.m_dot_discharge = (P_dch*self.M)/ (self.cp * self.sum_delta_T_t)
                self.Q_t=self.cp*self.m_dot_discharge*(self.T_t[3]-self.T_t[2])
                self.A_t=self.Q_t/(self.T_hot-self.To_out_t[0])
                self.mass -= (self.m_dot_discharge * self.time_step)
                self.Density = (self.mass/self.V_tank)
                self.P_tank = (self.Density * self.T_tank *287 /100000)
                self.SOC = (self.P_tank-self.p_min)/(self.p_max - self.p_min)

                self.T_history.append(self.T_t)
                self.P_history.append(self.P_t)
```

Operation optimization (lower level):

In [11]:
```
def operational_cost_optimize(V_tank, p_min, p_max, P_ch_max, P_dch_max, N, M,N_dg,N_wt,day):

    #----------------- Input DATA ----------------#

    demand = data["Demande (KW)"][day*24:(day+1)*24].values
    wind_power = data["Wind Power 50m (kW)"][day*24:(day+1)*24].values * N_wt
    caes = CAES(50,V_tank,267,p_min,p_max,P_ch_max,P_dch_max,N,M)

    #-----------------------------#
    #print("---------------------------------------\n Linearizing CAES Operation \n-----------------------------------------
    x = np.arange(0.1*P_dch_max,P_dch_max+5,5)
    y1 = list()
    for i in x:
        y1.append(caes.Discharge(i))

    from sklearn.preprocessing import PolynomialFeatures
    poly = PolynomialFeatures(degree=1, include_bias=False)
    poly_features = poly.fit_transform(x.reshape(-1, 1))
    from sklearn.linear_model import LinearRegression
    poly_reg_model = LinearRegression()
    poly_reg_model.fit(poly_features, y1)
    poly_reg_y_predicted_lin = poly_reg_model.predict(poly_features)
    from sklearn.metrics import mean_squared_error
    poly_reg_rmse_lin = np.sqrt(mean_squared_error(y1, poly_reg_y_predicted_lin))

    discharge_coeff = poly_reg_model.coef_
    discharge_intercept = poly_reg_model.intercept_

    #--------------------------#
```

```
x = np.arange(0.1*P_ch_max,P_ch_max+5,5)
y1 = list()
for i in x:
    y1.append(caes.Charge(i))

from sklearn.preprocessing import PolynomialFeatures
poly = PolynomialFeatures(degree=1, include_bias=False)
poly_features = poly.fit_transform(x.reshape(-1, 1))
from sklearn.linear_model import LinearRegression
poly_reg_model = LinearRegression()
poly_reg_model.fit(poly_features, y1)
poly_reg_y_predicted_lin = poly_reg_model.predict(poly_features)
from sklearn.metrics import mean_squared_error
poly_reg_rmse_lin = np.sqrt(mean_squared_error(y1, poly_reg_y_predicted_lin))

charge_coeff = poly_reg_model.coef_
charge_intercept = poly_reg_model.intercept_
#print("----------------------------------------\n Linearizing CAES Operation (Done) \n----------------------------------------
#print("----------------------------------------\n Optimal Cost (start) \n----------------------------------------------")

#------------ Operation for year-------------#

#------------CAES Linear-------------#

def discharging_mfr(P_discharge):
    term2 = discharge_coeff * P_discharge + discharge_intercept

    return term2

def new_pressure(P_charge,P_discharge,P_tank,bin_charge,bin_discharge):
    timestep = 3600
    T_tank = 262
    old_density = P_tank * 100000 / (287 * T_tank)
    new_density = (old_density * V_tank + (charging_mfr(P_charge)*bin_charge-
                                           discharging_mfr(P_discharge)*bin_discharge)*timestep)/V_tank

    new_pressure = new_density * (T_tank)*287 /100000

    return new_pressure

#---------------- Optimization --------------#

t= range(24)
t2 = range(25)

model = pyo.ConcreteModel()
model.time = pyo.Set(initialize=(i for i in t))
model.timestep = pyo.Param(model.time,initialize=3600)
model.time_soc = pyo.Set(initialize=(i for i in t2))
```

```
P_ch_min = 0.1 * P_ch_max
P_dch_min = 0.1 * P_dch_max
model.P_CAES_ch = pyo.Var(model.time,bounds = (P_ch_min,P_ch_max))
model.P_CAES_dch = pyo.Var(model.time,bounds = (P_dch_min,P_dch_max))
model.P_dg = pyo.Var(model.time,bounds = (0,P_max_dg))
model.Pressure_CAES = pyo.Var(model.time_soc, bounds=(p_min,p_max))
model.Wind_cur = pyo.Var(model.time,bounds = (0,max(wind_power)))
model.demand_cur = pyo.Var(model.time,bounds = (0,max(demand)))
model.bin_CAES_ch = pyo.Var(model.time, bounds=(0,1), domain=Binary)
model.bin_CAES_dch = pyo.Var(model.time, bounds=(0,1), domain=Binary)
model.bin_P_dg = pyo.Var(model.time, bounds=(0,1), domain=Binary)
model.bin_wc = pyo.Var(model.time, bounds=(0,1), domain=Binary)
model.bin_dc = pyo.Var(model.time, bounds=(0,1), domain=Binary)

P_CAES_ch =model.P_CAES_ch
P_CAES_dch=model.P_CAES_dch
Pressure_CAES=model.Pressure_CAES
bin_CAES_ch=model.bin_CAES_ch
bin_CAES_dch=model.bin_CAES_dch
P_dg = model.P_dg
bin_P_dg = model.bin_P_dg
bin_wc = model.bin_wc
bin_dc =  model.bin_dc
wind_cur = model.Wind_cur
demand_cur = model.demand_cur
```

```
def CAES_charge_lower(model,i):
    return model.bin_CAES_ch[i]*P_ch_min <= model.P_CAES_ch[i]
model.CAES_charge_limit_lower = Constraint(model.time, rule=CAES_charge_lower)

def CAES_charge_upper(model,i):
    return model.P_CAES_ch[i] <= model.bin_CAES_ch[i]*P_ch_max
model.CAES_charge_limit_upper = Constraint(model.time, rule=CAES_charge_upper)

def CAES_discharge_lower(model,i):
    return model.bin_CAES_dch[i]*P_dch_min <= model.P_CAES_dch[i]
model.CAES_discharge_limit_lower = Constraint(model.time, rule=CAES_discharge_lower)

def CAES_discharge_upper(model,i):
    return model.P_CAES_dch[i] <= model.bin_CAES_dch[i]*P_dch_max
model.CAES_discharge_limit_upper = Constraint(model.time, rule=CAES_discharge_upper)

def CAES_operation_mode(model,i):
    return bin_CAES_ch[i]+bin_CAES_dch[i]<=1
model.CAES_operation_mode_limit = Constraint(model.time, rule=CAES_operation_mode)

def CAES_charge_wind_only(model,i):
    return model.P_CAES_ch[i]*N <= wind_power[i]
model.CAES_charge_wind_only = Constraint(model.time, rule=CAES_charge_wind_only)

def Wind_cur_limit(model,i):
    return bin_wc[i] * wind_cur[i] <= wind_power[i]
model.Wind_cur_limit = Constraint(model.time, rule=Wind_cur_limit)
```

```
def Demand_cur_limit(model,i):
    return bin_dc[i] * demand_cur[i] <= demand[i]
model.Demand_cur_limit = Constraint(model.time, rule=Demand_cur_limit)

def curtailment_mode (model,i):
    return bin_dc[i] + bin_wc[i] <= 1
model.curtailment_mode = Constraint(model.time, rule=curtailment_mode)

def SOC_initial(model):
    return Pressure_CAES[0] == p_min + (p_max - p_min)/2
model.Pressure_CAES_initial = Constraint(rule= SOC_initial)

def SOC_final(model):
    return Pressure_CAES[24] == Pressure_CAES[0]
model.Pressure_CAES_final = Constraint(rule= SOC_final)


model.Pressure_CAES_new = pyo.ConstraintList()
for i in range(24):
    model.Pressure_CAES_new.add(expr = Pressure_CAES[i+1] ==
                                new_pressure(P_CAES_ch[i],P_CAES_dch[i],Pressure_CAES[i],bin_CAES_ch[i],bin_CAES_dch[i]))

def DG_limit_upper(model,i):
    return P_dg[i] <= bin_P_dg[i]*P_max_dg
model.DG_limit_upper = Constraint(model.time, rule=DG_limit_upper)

def DG_limit_lower(model,i):
    return P_dg[i] >= bin_P_dg[i]*P_min_dg
model.DG_limit_lower = Constraint(model.time, rule=DG_limit_lower)

def elec_balance(model,i):
    return  demand[i] + P_CAES_ch[i]*N + wind_cur[i] == wind_power[i] + P_dg[i]*N_dg + P_CAES_dch[i]*M + demand_cur[i]
model.elec_balance = pyo.Constraint(model.time, rule = elec_balance)


def objective_function(model):
    return sum((N_dg * (2.5*(a * P_dg[i] + b * bin_P_dg[i] * P_max_dg))+ (N_dg*(2.6333 * 0.1 * (a * P_dg[i] + b * bin_P_dg[i]
                *(demand_cur[i])+ 0.1 *(wind_cur[i]) + c_w_op * wind_power[i]) for i in model.time)
model.objective_function = pyo.Objective(rule = objective_function, sense=pyo.minimize)

opt = SolverFactory("gurobi")
results = opt.solve(model)
operation_cost = results.Problem._list[0].lower_bound

#print("----------------------------------------\n Optimal Cost (Done) \n----------------------------------------")
```

Sizing optimization (upper-layer)

In [14]:

```
def func1(x):

    N_wt = int((x[0]))
    N_dg = int((x[1]))
    P_ch_max = (x[2])
    P_dch_max = (x[3])
    V_tank = (x[4])
    N = int((x[5]))
    M = int((x[6]))
    p_min = (x[7])
    p_max = (x[8])



    penalty1 = 0
    penalty2 = 0
    P_tankk = p_min + (p_min+p_max)/2
    caes_oil_check_c = CAES(P_tankk, V_tank, 267, p_min, p_max, P_ch_max, P_dch_max, N, M)
    caes_oil_check_c.Charge(P_ch_max)
    A_cc=caes_oil_check_c.A_c

    for i in caes_oil_check_c.To_out_c:
        if i>600:
            penalty1 = 100000

    caes_oil_check_t = CAES(P_tankk, V_tank, 267, p_min, p_max, P_ch_max, P_dch_max, N, M)
    caes_oil_check_t.Discharge(P_dch_max)
    A_tt=caes_oil_check_t.A_t

    for j in caes_oil_check_t.To_out_t:
        if j<263:
            penalty2 = 100000


    step=1
    op_cost=0
    for i in range(0,5,step):
        op_cost += operational_cost_optimize(V_tank,p_min,p_max,P_ch_max,P_dch_max,N,M,N_dg,N_wt,i)

    CRF = ((r*((1+r)**y))/(((1+r)**y)-1))

    C_invst =(CRF*((c_wt*N_wt) + (c_dg*N_dg) + (N*c_c*P_ch_max) + (M*c_t*P_dch_max) +(c_v* V_tank)))/365

    obj_function = C_invst + penalty1+ penalty2 + op_cost/5
    return obj_function

#--- PSO ----------------------------------------------------------------------+

class Particle:
    def __init__(self,num_dimensions):
        self.position_i=[]          # particle position
        self.velocity_i=[]          # particle velocity
        self.pos_best_i=[]          # best position individual
        self.err_best_i=-1          # best error individual
        self.err_i=-1               # error individual
```

```
        self.velocity_i.append(random.uniform(-1,1)) #wind
        self.velocity_i.append(random.uniform(-1,1)) #disel
        self.velocity_i.append(random.uniform(-1,1)) #charge
        self.velocity_i.append(random.uniform(-1,1)) #discharge
        self.velocity_i.append(random.uniform(-1,1)) #tank
        self.velocity_i.append(random.uniform(-1,1)) #comp
        self.velocity_i.append(random.uniform(-1,1)) #turbine
        self.velocity_i.append(random.uniform(-1,1)) #pmin
        self.velocity_i.append(random.uniform(-1,1)) #pmax




        self.position_i.append(random.uniform(1,100)) #wind
        self.position_i.append(random.uniform(1,100)) #disel
        self.position_i.append(random.uniform(1,2000)) #charge
        self.position_i.append(random.uniform(1,2000)) #discharge
        self.position_i.append(random.uniform(1,3000)) #tank
        self.position_i.append(random.uniform(1,5)) #comp
        self.position_i.append(random.uniform(1,5)) #turbine
        self.position_i.append(random.uniform(30,55)) #pmin
        self.position_i.append(random.uniform(60,100)) #pmax
```

```
    # evaluate current fitness
    def evaluate(self,costFunc):
        self.err_i=costFunc(self.position_i)

        # check to see if the current position is an individual best
        if self.err_i < self.err_best_i or self.err_best_i==-1:
            self.pos_best_i=self.position_i
            self.err_best_i=self.err_i

    def cost_function(self,costFunc):
        return costFunc(self.position_i)

    # update new particle velocity
    def update_velocity(self,pos_best_g):
        w=0.8       #interia
        wmin=0.2
        wmax=0.9
        c1=2        # cognative constant
        c2=2        # social constant

        for i in range(0,num_dimensions):
            r1=random.random()
            r2=random.random()

            vel_cognitive=c1*r1*(self.pos_best_i[i]-self.position_i[i])
            vel_social=c2*r2*(pos_best_g[i]-self.position_i[i])
            self.velocity_i[i]=w*self.velocity_i[i]+vel_cognitive+vel_social
```

```
    # update the particle position based off new velocity updates
    def update_position(self,bounds):
        for i in range(0,num_dimensions):
            self.position_i[i]=self.position_i[i]+self.velocity_i[i]

            # adjust maximum position if necessary
            if self.position_i[i]>bounds[i][1]:
                self.position_i[i]=bounds[i][1]

            # adjust minimum position if neseccary
            if self.position_i[i] < bounds[i][0]:
                self.position_i[i]=bounds[i][0]


if __name__ == "__PSO__":
    main()
```

```
#--- RUN ----------------------------------------------------------------------+

costFunc,x0,bounds,num_particles,maxiter = func1, initial, bounds, 30, 50

global num_dimensions

num_dimensions=len(x0)
err_best_g=-1                   # best error for group
pos_best_g=[]                   # best position for group2

# establish the swarm
swarm=[]
for i in range(0,num_particles):
    swarm.append(Particle(num_dimensions))

# begin optimization loop
i=0
gbest=[]
while i < maxiter:
    #print i,err_best_g
    # cycle through particles in swarm and evaluate fitness
    wmin=0.2
    wmax=0.9
    w = wmax - i * ( (wmax - wmin) / maxiter)
    for j in range(0,num_particles):
        swarm[j].evaluate(func1)

        # determine if current particle is the best (globally)
        if swarm[j].err_i < err_best_g or err_best_g == -1:
            pos_best_g=list(swarm[j].position_i)
            err_best_g=float(swarm[j].err_i)

    # cycle through swarm and update velocities and position
    for j in range(0,num_particles):
        swarm[j].update_velocity(pos_best_g)
        swarm[j].update_position(bounds)
    i+=1
```